NR 356
Proj. 10-29, Appx A-C

APPENDIX A

LITERATURE REVIEW

INTRODUCTION

Considerable previous work has been done in the area of post-tensioned anchorage zones. Information about the design and behavior of anchorage zones can be found from three literature sources:

1) Technical literature,

2) Product literature, and

3) Current codes and commentaries.

Each one of these sources will be outlined in the following sections. The objective of this Appendix is to show the current status of post-tensioning anchorage zone design.

TECHNICAL LITERATURE

This section will give a basic overview of the available technical literature for the design and analysis of post-tensioned anchorage zones. Much of the literature dates back to the 1950's and 1960's, but there have been many significant works since then. The technical literature can be divided into six main approaches:

1) Analysis utilizing the theory of elasticity,

2) Equilibrium methods of analysis,

3) Photoelastic investigations,

4) Finite element studies,

5) Strut-and-tie models, and

6) Experimental investigations.

In some cases, studies have incorporated more than one of these approaches (e.g. finite element analysis with an experimental investigation). When this occurs and one approach is more prevalent than the other, the study is mentioned under the prevalent approach.

Analysis Utilizing the Theory of Elasticity.

If a reinforced concrete anchorage zone can be assumed to be a homogeneous, isotropic, and linearly elastic body, then the anchorage zone analysis can be treated as that for the effects of concentrated loads on an elastic body. Such an approach has been shown *(66)(67)* to be valid until the onset of visible cracking. Since the elastic analysis will satisfy equilibrium, the distribution of elastic stresses will indicate a possible load carrying mechanism. If an appropriate criteria is chosen for the tensile and compressive stress limits, the elastic analysis results can be useful in determining the crushing and allowable loads. Such analyses usually do not consider the effect or distribution of anchorage zone reinforcement.

Several authors including Guyon *(6)* have used a two-dimensional elasticity approach. Guyon's approach to the determination of stresses in the anchorage zone has been widely utilized in design. The classic theory of elasticity solution for the stresses is very complicated and time consuming unless approximated by finite element solutions. Guyon was able to model the spreading of forces in the anchorage zones and then quantify them as bursting stresses and spalling stresses. Bursting stresses are the stresses normal to the axis of loading caused by the lateral spreading of the concentrated load. Spalling stresses are stresses acting normal to the axis of load but along the loaded surface. Guyon determined that the most important variable in determining the magnitude of the stresses and forces in the anchorage zone was the ratio of the plate width to the section depth (a/h). Guyon developed a number of design aids for some of the most common situations to assist the engineer.

In Fig. A.1a, the general anchorage zone of a rectangular beam is shown subjected to a concentrated load. The depth of the section is equal to "h" with the horizontal load being applied along the line of symmetry. The longitudinal stresses are assumed to be uniformly distributed at a distance of "h" from the anchor. The other dimension shown is the anchor plate width, "a". Based on a classic theory of elasticity solution, Guyon developed the design aid shown in Fig. A.1b. Once the ratio a/h is determined, Fig. A.1b is used to determine the bursting tensile stress distribution beneath the load point. Figure A.2 shows additional design aids, for bursting force (Fig. A.2a), for maximum bursting stress (Fig. A.2b), and for the location of the maximum and zero bursting stresses (Fig. A.2c).

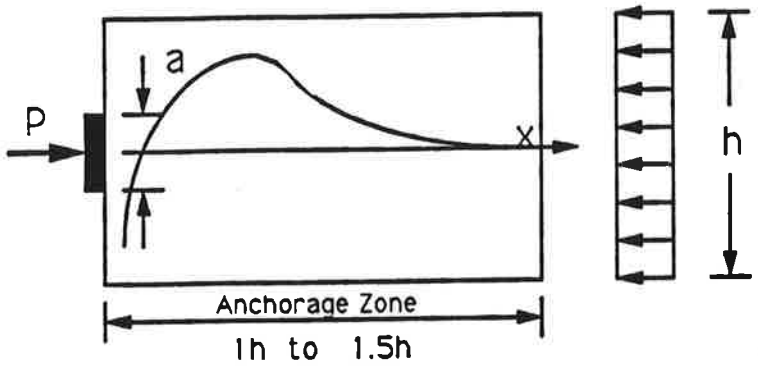

Figure A.1a Anchorage zone for a concentric anchorage.

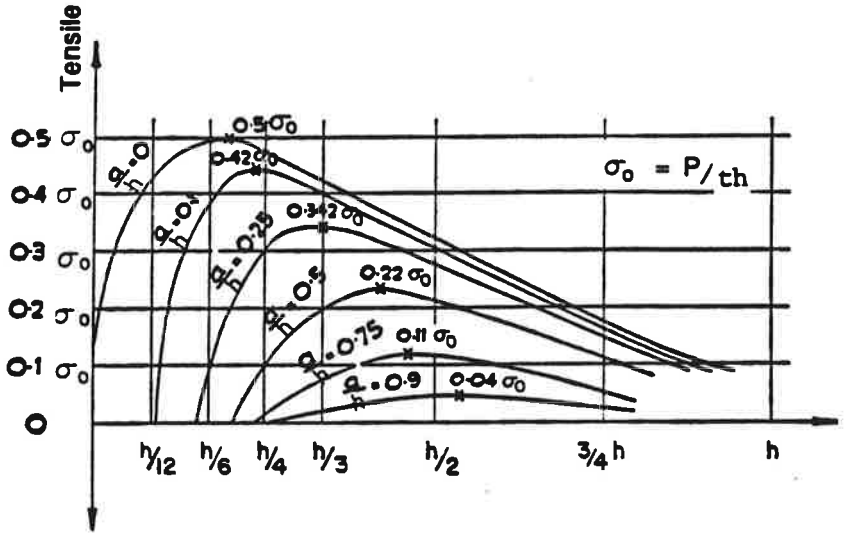

Figure A.1b Bursting stress distribution for concentric anchorages *(6)*.

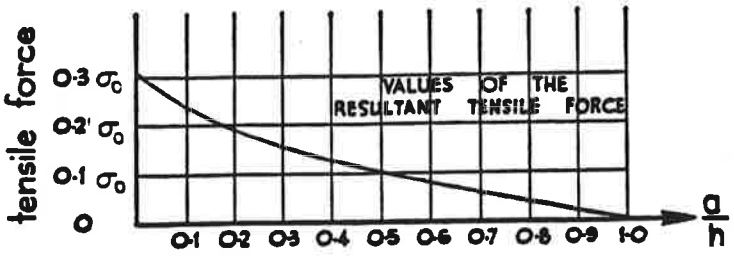

a) Magnitude of bursting force

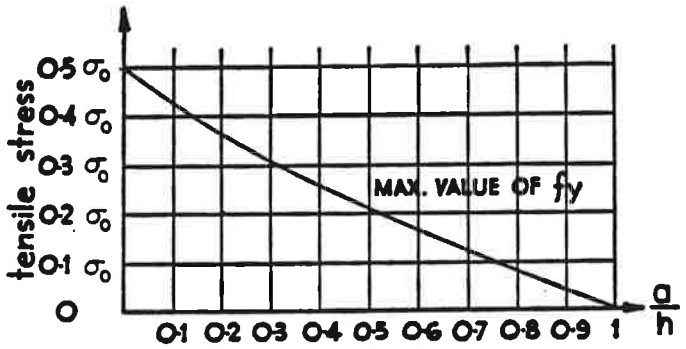

b) Maximum bursting stress

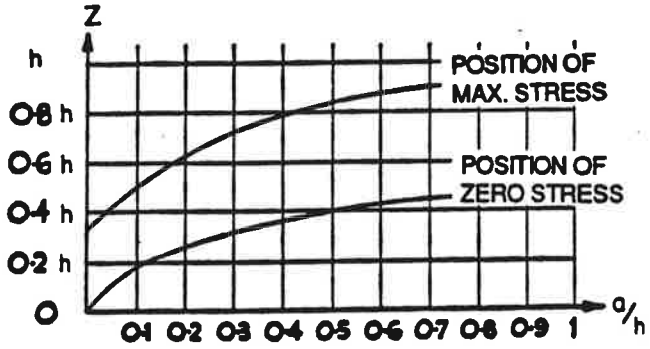

c) Location of maximum and zero stress

Figure A.2 Bursting zone data for a concentric anchorage zone.

When the applied load is eccentric, Guyon proposed that the symmetric prism be used to determine the ratio a/h' (see Fig. A.3a). The premise behind the symmetric prism is that the distribution of bursting stresses calculated for the prism would be equivalent to those in the beam. The width of the prism (h') is equal to twice the minimum distance from the centerline of the tendon to the concrete edge. He also proposed the symmetric prism for use with multiple loads that are closely spaced (see Fig. A.3b). In this case, the width of the symmetric prism is taken as the smaller of the spacing between the anchors or two times the distance from the concrete edge to the tendon centerline. The a/h' ratio is used in place of a/h in Figs. A.1 and A.2 to determine the maximum bursting stress, the magnitude of the bursting force and/or the location of the maximum stress.

Guyon also determined that spalling tensile stresses existed. Utilizing photoelastic work by Tesar, Guyon calculated the following spalling force magnitudes for various a/h' or a/h ratios.

a/h', a/h	0	0.1	0.25	0.5
Spalling Force	0.04P	0.03P	0.025P	0.02P

Douglas and Trahair *(73)* also used an elasticity approach. They investigated the stress distribution for a variety of bearing surface areas and the effect of including the tendon duct in the analysis. Their investigation consisted of a series of tests and elastic analyses with 6 x 12 inch concrete cylinders. Good agreement was found with Guyon's theory except they did not find evidence to support spalling stresses. The presence of the tendon duct reduced the ultimate load by nine percent.

Gergely et al. *(66) (67)* conducted an extensive study that included elasticity principles, equilibrium concepts, and experimental tests. Each approach will be discussed in its related section. Gergely determined the stress contours for a rectangular section with an eccentrically applied distributed load. The solution was developed using two Airy stress functions and finite differences. The results were very close to the levels found by Guyon. Analytical tests were run with several different Poisson's ratios (0.1 to 0.2). When the ratio was changed from 0.1 to 0.15, the bursting stress changed by 20 percent. The change in the ratio also had a considerable influence on bursting strains but only close to the load where the longitudinal stresses were high.

Gerstner and Zienkiewicz *(68)* solved the problem of a concentrated load at an eccentricity of 0 and 3/8 of the depth of the section. The problem was divided into a particular solution and a corrective solution. The particular solution was the elasticity solution for stress distribution in a semi-infinite medium, while the corrective solution adjusts the stresses to conform to the boundary conditions and can be solved using finite differences. The solutions were extremely close to those of Guyon. Therefore, Gerstner stopped after only two cases.

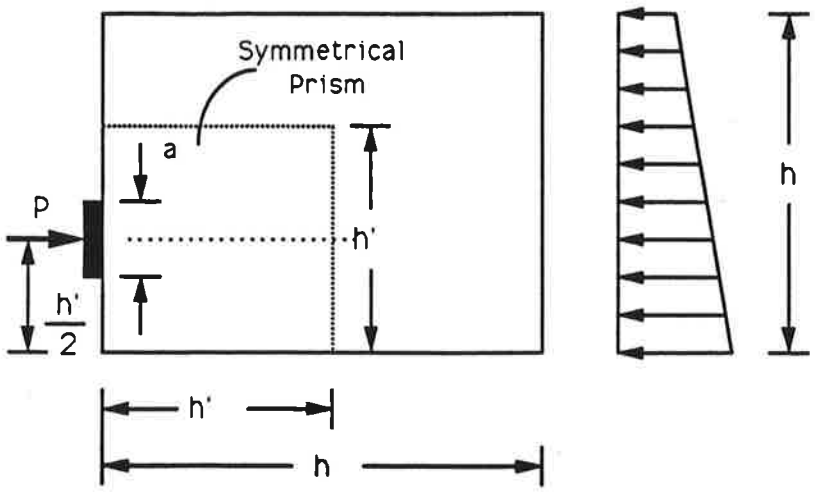

Figure A.3a Guyon's symmetrical prism.

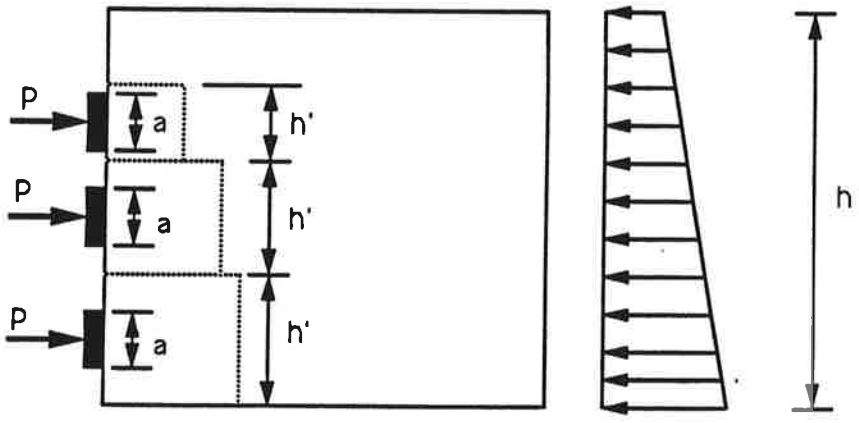

Figure A.3b Symmetrical prism for closely spaced anchors.

Iyengar continued the work on the effect of boundary conditions of the elastic solution. Iyengar *(69)* did an extensive comparison of the existing analytical models of Guyon *(6)*, Sievers *(70)*, Bleich *(71)* and Morsch *(5)*. Iyengar's results agree with Guyon's solution for the bursting stresses. He found that the symmetric prism is a good technique for modeling the zone but believed that the solution was not accurate near the boundaries or for longitudinal and shear stress distributions. Iyengar also conducted a three-dimensional elastic analysis *(72)* which detected the spalling stresses that were discussed by Guyon. The peak stresses of Guyon's elasticity solution are about 12 percent smaller than those determined by Iyengar. Iyengar detected the development of spalling stresses. He theorized that Douglas and Trahair *(73)* did not detect the spalling stresses because they focused on hoop stresses. Spalling stresses are determined from the radial stress component.

Som and Ghosh *(74)* developed expressions for bursting stresses for concentric, eccentric, and multiple anchors using Airy stress functions. For the concentric case, the calculated bursting stresses are very close to Guyon but differ greatly from Magnel *(75)*. Magnel *(75)* and Som *(74)* showed for concentric multiple anchors a reduction in the maximum bursting stress level from that of the concentric single anchor case while Guyon showed the same value for constant dimensions of the symmetric prism. The maximum bursting stress predicted by Magnel and Som for eccentric anchors are approximately the same while Guyon is higher.

Equilibrium Methods of Analysis.

The distribution of reinforcement to control crack widths in a cracked anchorage zone has been studied based on equilibrium models. Gergely et al. *(66) (67)* developed the following technique to design the spalling reinforcement along the loaded face in addition to the elasticity solution. The equilibrium conditions that are used to determine the spalling force are shown in Fig. A.4. The first step is to establish a crack length and then determine the moment and shear along plane AB that are necessary for equilibrium. The cracking will usually occur at the position of maximum moment. Reinforcement requirements are determined from the force T which is related to the moment and the crack length. For design purposes they suggested that the crack length can be assumed to be equal to the height of the member.

Lenschow and Sozen *(53)* introduced an approximate method of analysis for anchorage zone cracking based on the analogy of a beam on an elastic foundation (see Fig. A.5). A reference plane is selected parallel to the longitudinal axis. The reference plane is where the bursting stresses will be calculated; therefore, it is usually parallel to but offset from the load. The beam is divided into three beams that are symmetric about the centroid of the beam. Fictitious springs, representing the concrete, are added and the loads are adjusted so that the beams have the same curvature. Since the beams have the same curvature, the springs will no longer come into effect. The method then uses equilibrium and compatibility relations to analyze the beam below the reference plane as a beam on an elastic foundation. The forces in the spring are equal to the bursting forces.

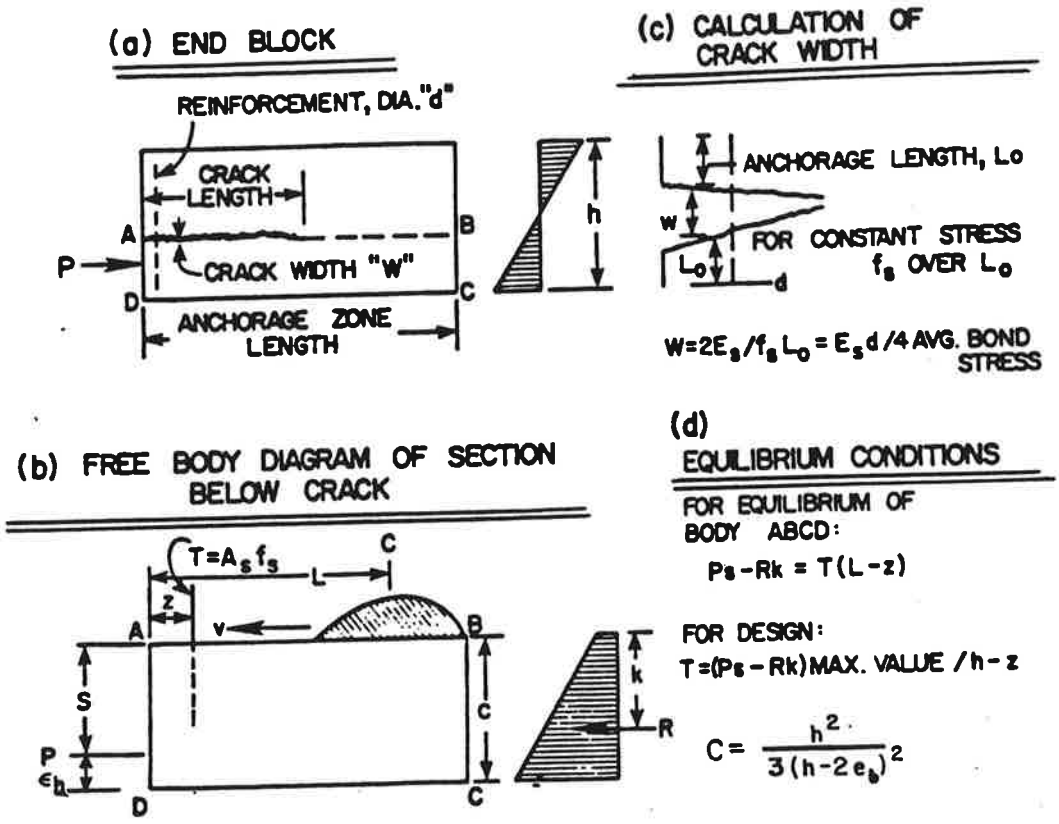

Figure A.4 Gergely's beam analysis *(66) (67)*.

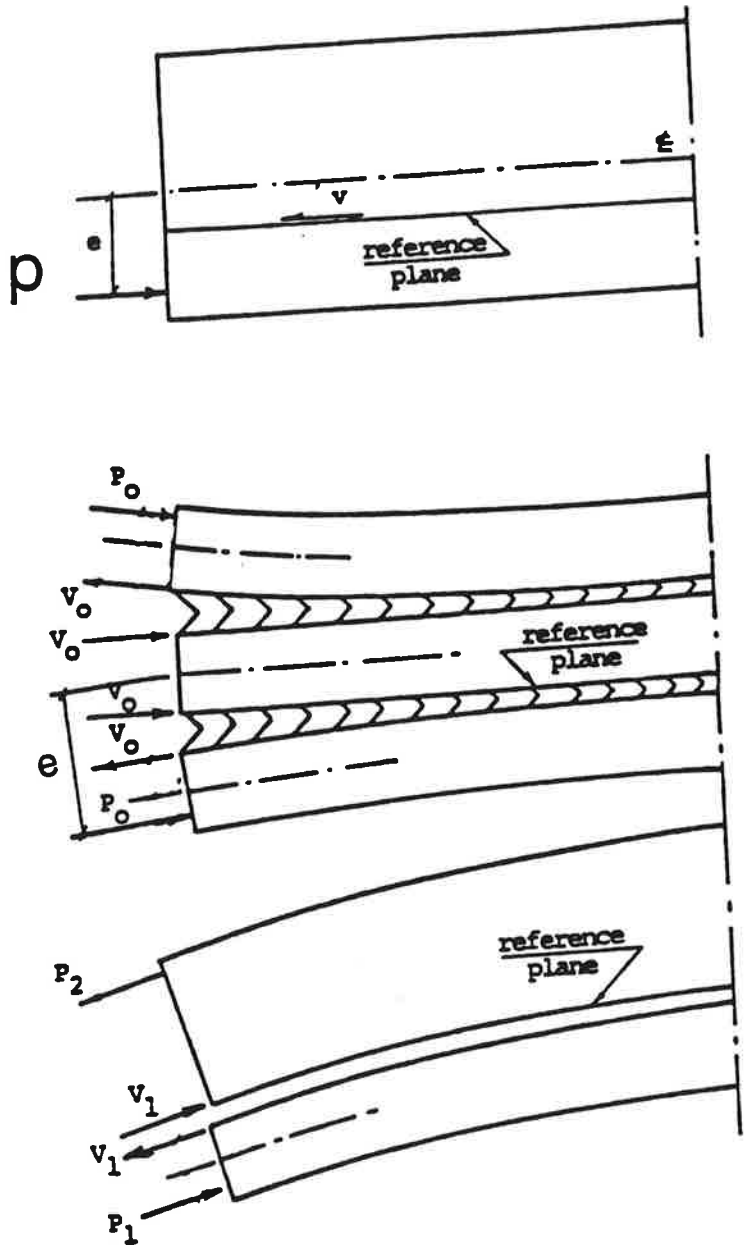

Figure A.5 Beam on an elastic foundation analogy by Lenschow and Sozen *(53)*.

The results of this analysis compare well with the results of Guyon for both concentric and eccentric loads (see Fig. A.6). The primary difficulty with this method comes with defining the value of the spring stiffness. The advantage of the method occurs in that, once a problem is solved, it is easy to proportion the reinforcement since the engineer knows the force distribution directly.

Magnel *(75)* developed an approximate method based on equilibrium. Magnel assumed that the stresses became linear at a distance equal to the depth of the member and that the bursting stress distribution along any reference line parallel to the longitudinal axis of the beam had a parabolic distribution. From equilibrium, Magnel determined the moment and the shear on the reference plane then solved the resulting parabolic function. Magnel carried out tests on two unreinforced blocks to show that his results were conservative.

Photoelastic Investigations.

Christodoulides *(76) (77) (78) (79)* performed two-dimensional photoelastic tests to explore the distribution of stresses in a rectangular block with two anchors symmetrically arranged about the centerline of the section. Christodoulides also conducted a three-dimensional photoelastic test on a concrete crane gantry to compare the photoelastic results with strain data. From his tests, he concluded that maximum stresses occur directly in front of the load. He determined that Poisson's ratio had no effect on stresses because his plastic model answers agreed with the results from the concrete gantry beam test. According to the results of Christodoulides, both the Magnel and Guyon theories underestimated the maximum stresses on the concrete surface.

Leonhardt *(80)* relied heavily on the symmetrical prism theory of Guyon and on extensive photoelastic studies by *(81)* to generalize design theories for reinforcing anchorage zones. While a major proponent of strut-and-tie models for reinforcement proportioning, it is notable that his 1964 English edition did not mention this latter approach in its chapter on anchorage zones.

Rasheeduzzafar and Al-Saadoum *(82)* conducted a three-dimensional photoelastic investigation on anchorage bearing stresses in rectangular blocks. The study looked at embedded anchors versus external anchors and also treated both multiple anchors and edge spacing. The following trends were determined from the program. Embedded anchors allow part of the force to be transferred by shear and part by bearing. The study concluded that one-third of the force can by transferred by shear traction. Embedded anchors have smaller maximum tensions than external plates. Forces become essentially uniform after a longitudinal distance of two-thirds the depth of the block. The stresses that develop on the unloaded faces are very dependent on the location of the anchor; therefore, they predicted that a design formula that does not incorporate the proximity of the anchor to the unloaded faces will not be entirely successful in predicting stresses. In the tests, the geometry of the single and multiple anchorages were not exactly the same but the stress data obtained suggested that, apart from an increase in the bursting tension on the loaded face, there is no significant interaction between

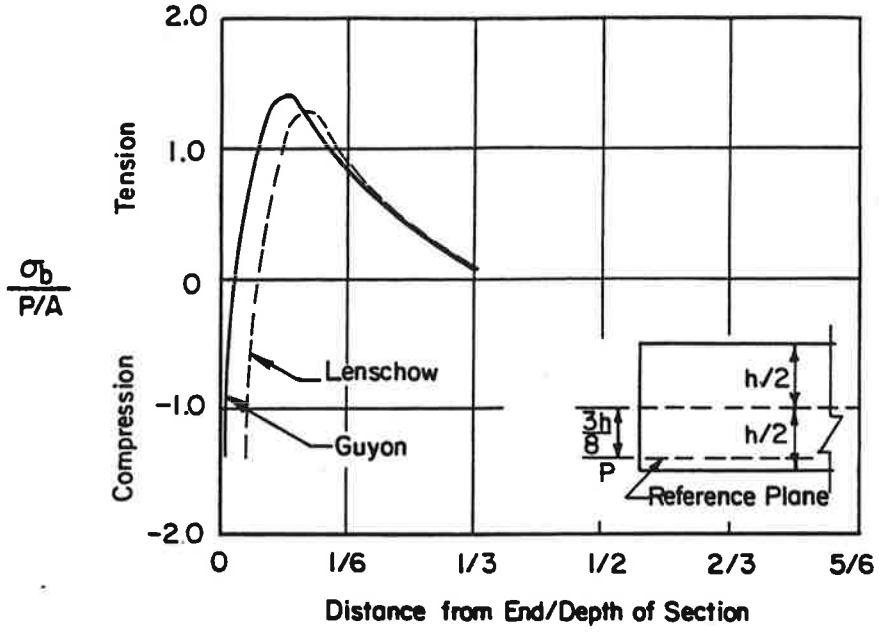

Figure A.6a Bursting stress under an eccentric load.

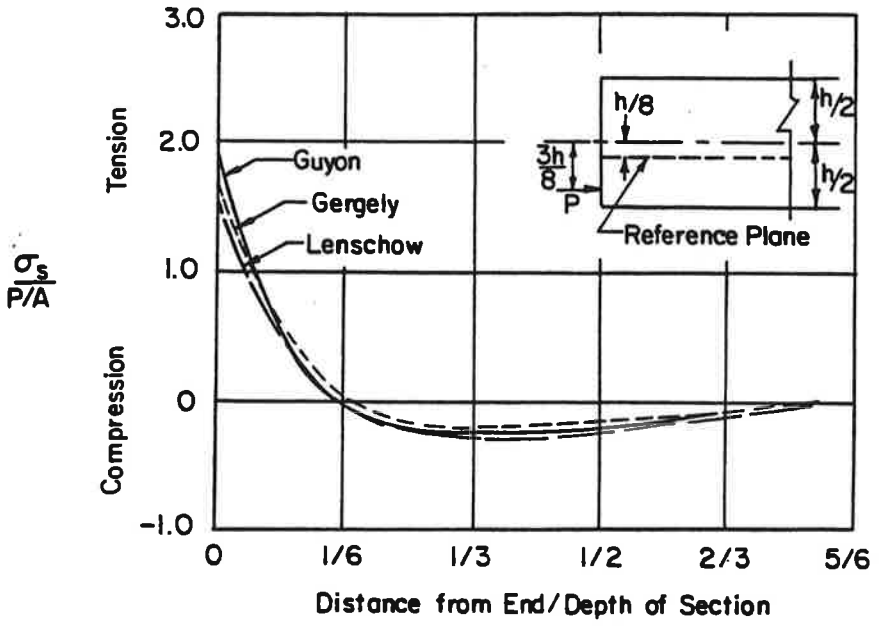

Figure A.6b Spalling Stresses.

adjacent anchor units spaced apart at least a distance equal to twice the largest anchor dimension. They concluded that, in the absence of more comprehensive design criteria, the symmetric prism approach provides the most reasonable model for evaluating the bursting force.

Vaughn *(83)* investigated two-dimensional photoelastic techniques to model multiple tendons, eccentricity, and inclination. Vaughn discovered that a conical shaped anchor produced principal tensile stresses approximately 150 percent greater than those for flat bearing anchors and produced maximum shearing stresses approximately 250 percent greater. The spalling stresses increased significantly for increasing eccentricity and for an increasing angle of inclination. Large spalling stresses were also created between multiple anchors along the loaded face.

Finite Element Studies.

The development of comprehensive finite element analysis models has opened the way for powerful analytical studies. While results depend on the mesh and the solution techniques used, the linear finite element analysis has great promise for determining uncracked-state stresses. Nonlinear finite element studies can model the cracked anchorage zone state.

Adeghe and Collins *(7)* used a nonlinear finite element analysis to study the effect of reinforcement distribution in the bursting region on the strain distribution. The specimens investigated had an a/h of 0.1 and a total length of 1220 mm (48.0 in.). Figure A.7 shows the results of the three reinforcement distributions. The strain distribution changes significantly for the three reinforcement patterns after the cracking load (95 kN or 21.4 kips). Adeghe and Collins determined that placing all the reinforcement in the high stress region (see Fig. A.7a) would result in brittle behavior. Spreading the reinforcement along the entire bursting region (see Fig. A.7c) would make much better use of the reinforcement. Figure A.8 shows the principal compressive stress trajectories for an elastic analysis and a nonlinear analysis. The dispersion angle of the compression from the bearing surface is steeper in the elastic analysis than in the nonlinear analysis. This indicates that more reinforcement would be required from the elastic analysis because the centroid of the bursting force is closer to the bearing surface. Therefore, the elastic analysis would be conservative.

In conjunction with the test results reported by Sanders (*1*) in this dissertation, Burdet *(47)* conducted an analytical investigation of the anchorage zone problems. His analytical approaches

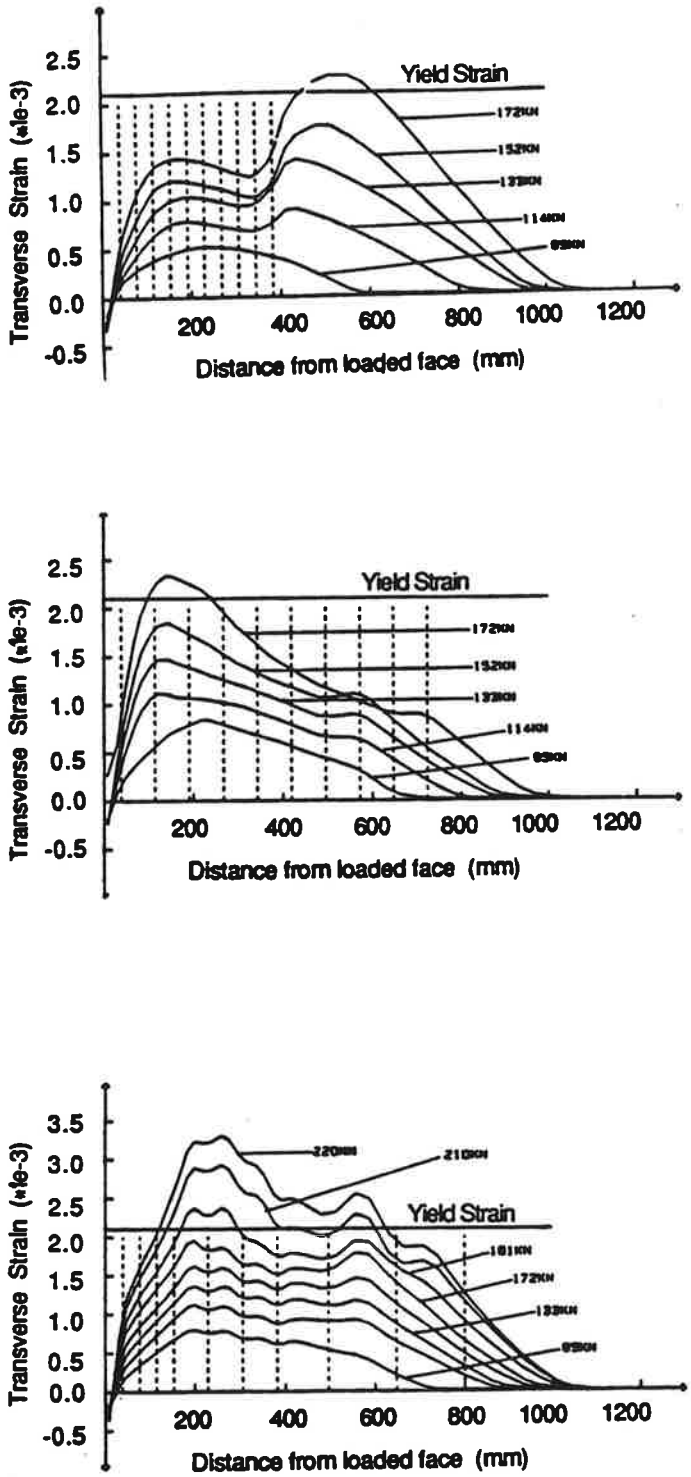

Figure A.7 Transverse tensile strain distribution for three stirrup arrangements *(7)*.

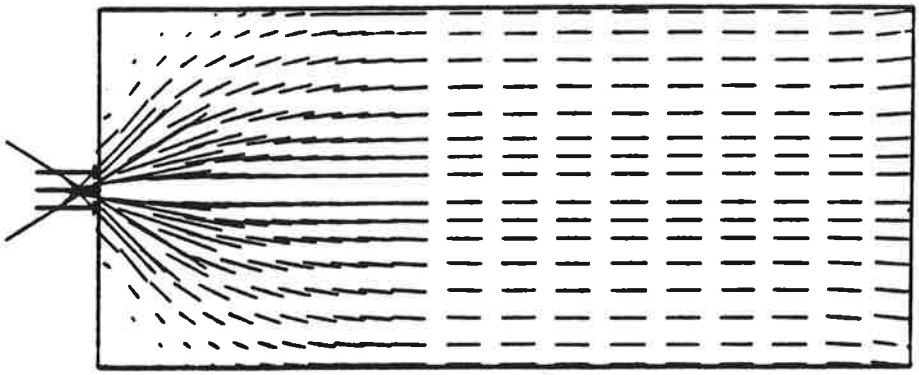

a) Compressive stress flow, linear elastic analysis

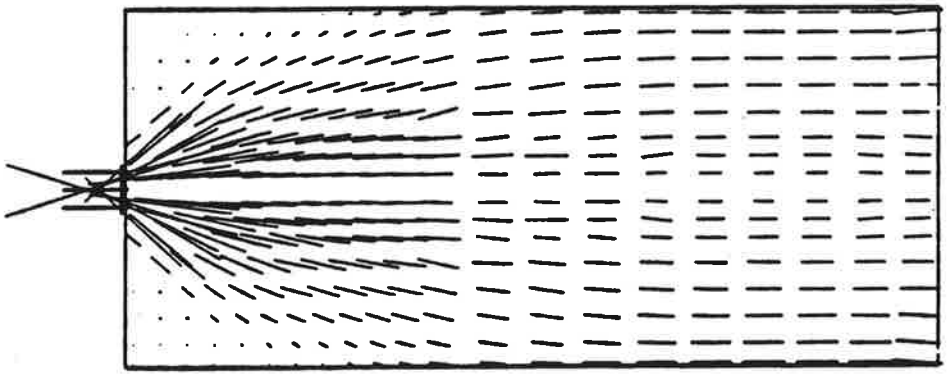

b) Compressive stress flow, nonlinear analysis

Figure A.8 Comparison of linear elastic and nonlinear compressive stress flow *(8)*.

included extensive parameter studies based both on linear elastic finite element analyses and on strut-and-tie models. He examined different variables influencing the design of post-tensioned anchorage zones. He determined that the failure of the anchorage zone could be due to a local zone bearing failure, a tension tie failure, or a compression failure in the general zone. For the local zone bearing criteria, Burdet refers to the work of Roberts *(4)* and did not include explicit consideration of the local zone. For tensile tie limitations, Burdet used the strut-and-tie model as well as integration of tensile stresses from the finite element analyses. His parametric studies show generally good agreement between the two approaches except for higher spalling stresses computed by finite element analyses which consider continuity effects omitted in the equilibrium based strut-and-tie models. Burdet found that the maximum compressive strength of the anchorage zone could be found by matching the peak compressive stress as determined from the finite element analysis to $0.75f_c'$ at a distance from the loading surface equal to the lateral dimension of the anchorage device.

From the parametric studies, Burdet developed the following formulas to estimate the bursting force and the location of the bursting force. These equations are valid for initial anchorage inclinations of -5 degrees (extrapolated) to 20 degrees.

$$T_{burst} = 0.25P\,(1 - a/h) + 0.5\,P\sin(\theta)$$

$$d_{centroid} = 0.5\,(h - 2e) + 5\,e\sin(\theta)$$

Where

P is the total factored tendon load for the stressing arrangement considered;

a is the lateral dimension of the anchorage device or group of devices in the direction considered;

e is the eccentricity (always taken as positive) of the anchorage device or group of devices;

h is the transverse dimension of the cross section in the direction considered; and

θ is the angle of inclination of the resultant of the tendon or tendons with respect to the centerline of the member, positive for concentric tendons or if the anchor force point towards the centerline of the member, but negative if the anchor force points away from the centroid of the section.

Burdet also formulated procedures to develop strut-and-tie models and correlated the resulting models with his finite element analysis and existing experimental results including those reported in this dissertation. He found that using the strut-and-tie model based on an assumed

dispersion angle (α, see Fig. A.9) of 26 degrees for the compression struts correlated well with the test results for most anchorage zone configurations. Designing with the strut-and-tie model must include checks of the tension tie capacity and compression capacity at the local zone-general zone interface. He concluded that, for a very complex configuration, it is difficult to determine critical strut patterns and strength so that it appears desirable to use a finite element analysis to determine compressive strength limits.

Egeberg *(84)* conducted two-dimensional linear finite element studies with concentric and eccentric single tendon anchorage blocks. Cases were run for uncracked, cracked, and reinforced sections. He found very close agreement with Guyon's theories and close agreement with Magnel. The maximum bursting stress level was the same as Guyon's, but the spalling stresses were significantly less. Egeberg determined that the bursting stresses were almost exactly the same for eccentric and concentric cases with the distributions simply shifted to a different location. The introduction of a crack at a predescribed stress level caused the raising of stresses ahead of the crack, propagating the crack. The addition of reinforcement significantly dropped the stress level in the concrete because the force was transferred to steel.

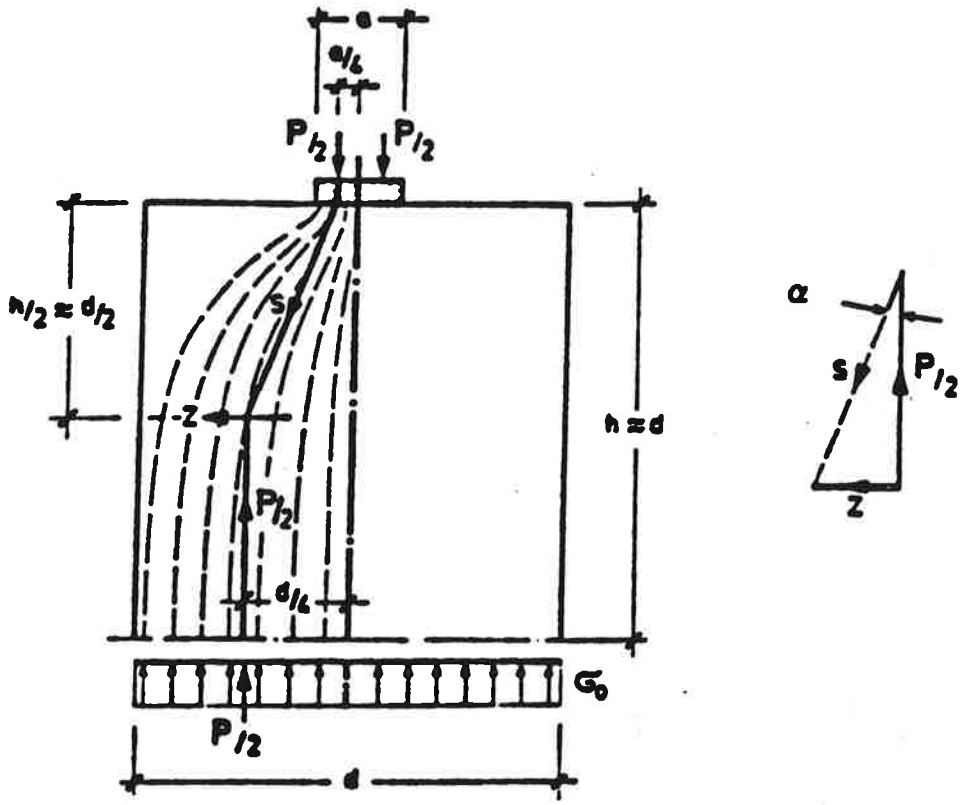

Figure A.9 Strut-and-tie model by Morsch.

Stone and Breen *(9)(10)* used a combination of finite element analysis and experimental testing to study single anchorage zones in thin web members. This study is discussed in detail in the experimental investigation section. Stone and Breen found good correlation between experimental and analytical results.

A broad investigation using finite elements was conducted by Yettram and Robbins *(40) (85) (86)*. The research was presented in a series of three articles with the first addressing the simplest case of concentric anchorage zone stresses in a rectangular section. In the first study, both two- and three-dimensional cases were reported with the following conclusions.

1) The distance to form a uniform normal stress field is 1.25 times the height of the prism.

2) A variation of Poisson's ratio between 0.125 and 0.2 has little effect upon the stress distribution.

3) Iyengar's and Guyon's two-dimensional elastic analysis results give good values for the average stress when compared with Yettram, although they cannot indicate the transverse variations in the stress distribution.

4) The experimental results of Zielinski and Rowe were based on surface measurements and significantly over-estimated the maximum bursting stress for all ratios of bearing surface area to cross section area; therefore, Yettram's results were not close to those of Zielinski.

In the second paper, Yettram and Robbins addressed the problem of eccentric and multiple anchorages in rectangular and non-rectangular sections. From the cases studied, it was determined that the symmetric prism method of Guyon gave a satisfactory representation of the bursting stresses for design purposes. They suggested that, if the symmetric prism extends into either or both of the flanges with non-rectangular sections, then the influence of the bursting stresses will extend a further distance in front of the loaded face than the depth of the rectangular symmetric prism. They found that in non-rectangular sections, the effect of flanges was generally to reduce the importance of spalling stresses.

In their third paper, Yettram and Robbins studied anchorage zone stresses in I section members with end blocks. In the study, the length of the end block was the major variable. They concluded that, in very short end blocks, the lateral (out of plane) bursting stresses should be considered. A longitudinal taper between the block and the web is advantageous. The maximum bending stress is greater than the maximum bursting stress except in very long blocks. Short end blocks (length/depth less than 0.75) are of little advantage because bending stresses overshadow the bursting stress, and this causes an increase in the transverse reinforcement and greater congestion.

Strut-and-Tie Model.

The strut-and-tie model is a concept in which elasticity stress trajectory fields or a basic understanding of the flow of forces in the member are used to formulate an equilibrium based model consisting of struts and ties. In these models, the applied loads such as post-tensioning forces are transferred through the structure with the use of compression members (struts) and tension members (ties). The strut-and-tie models stem from the pioneering work of Ritter in 1899 who used such a model to develop the truss analogy to explain the shear-diagonal tension resistance in reinforced concrete beams. It has been developed by many engineers such as Morsch, Leonhardt, Thürlimann and Schlaich. The most comprehensive treatment in English is the recent paper by Schlaich et al. *(2)* which shows many applications of the strut and tie model including the modeling of an anchorage zone. Figure A.9 shows a strut-and-tie model that was used by Morsch *(5)* in 1924. Even though the model is based on very simplified assumed force trajectories, the analysis of the tie force Z gives an equation for the bursting force that is very close to what many current codes use. An example for an eccentric anchorage is shown in Fig. A.10. Figures A.10a and A.10b show the elastic stress distribution, as determined by theory of elasticity analysis. Figure A.10c is the representative strut-and-tie model which is the simplified depiction of the elastic stress fields. The elastic stress fields can be used to determine where the struts and ties should be placed. The strut-and-tie model is gaining popularity because a designer can readily formulate general anchorage zone reinforcement from such a model. Even though very little previous research has been conducted into the direct application of the strut-and-tie model to the ultimate strength design of the anchorage zone, the technique holds much promise.

Schlaich divides a member into two types of regions, "B" and "D". "B" regions are zones with linear strain distributions where beam theories apply. The stress states in these regions are easily derived from the sectional forces. "D" regions are zones in which the strain distributions are significantly nonlinear such as near concentrated loads, corners, openings and other discontinuities. The anchorage zone is a "D" region. Saint Vénant's principle can be used to find the approximate length of the disturbed anchorage zone. Therefore, for most applications the length of the anchorage zone can be taken to be the depth of the section. The following steps are necessary to use the strut-and-tie procedure:

1) Develop the strut-and-tie model where the struts and ties model the actual stress trajectories by lines of action and concentrate their curvature in nodes;

2) Calculate the strut and tie forces;

3) Dimension the struts, ties and nodes; and

4) Check stresses and forces.

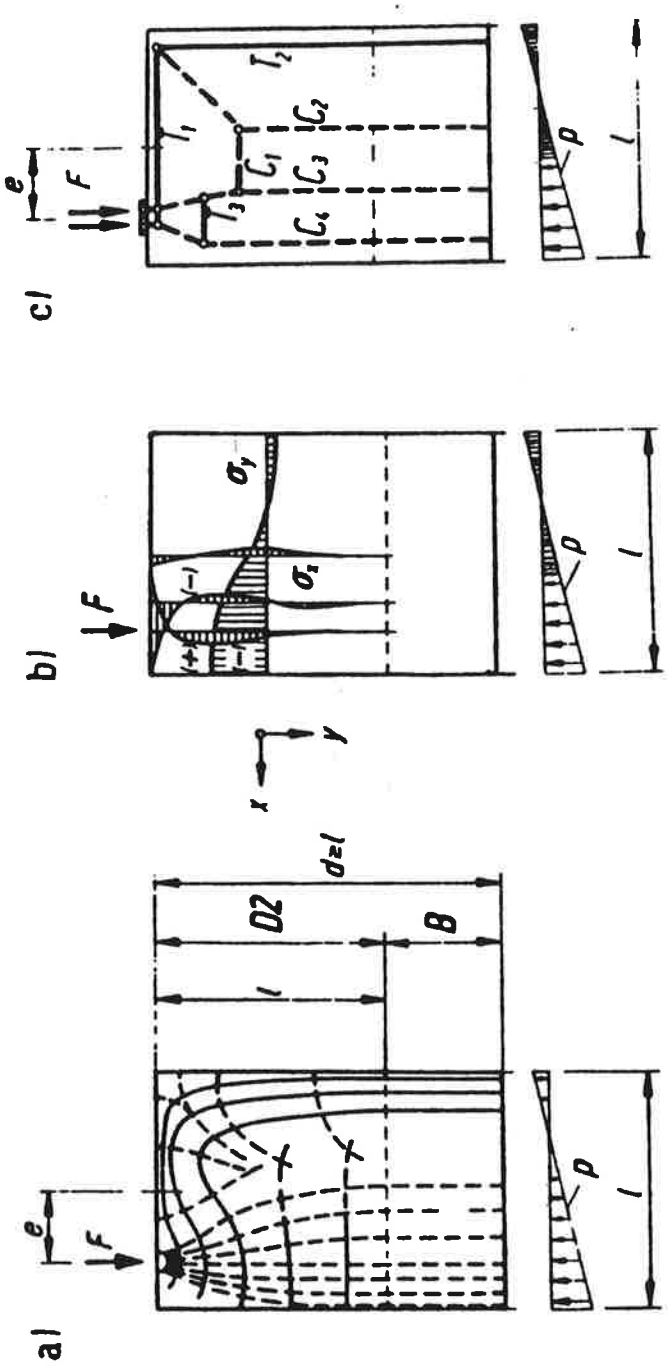

Figure A.10 Strut-and-tie development from an elastic stress distribution *(2)*.

The strut-and-tie model is a lower bound plasticity theory. The lower bound theory of plasticity assumes that both internal and external equilibrium are satisfied, and that stresses do not exceed the material yield conditions. The theory also assumes that the system has sufficient ductility to develop the yield conditions. Since concrete has limited plastic rotation capabilities, it is important to choose a strut-and-tie model that does not require large rotation in order to mobilize the struts and ties. Struts and ties oriented along the elastic trajectories neglect some potential gain from plastic behavior but also ensure reasonable rotations. If the assumptions of the lower bound theory are met, then the predicted capacity will be smaller than or equal to the collapse load.

Schlaich details the dimensioning of struts, ties, and nodes and their stress limitations. Tension ties carried by reinforcement are essentially linear or one-dimensional elements between two nodes. Compression struts or tension ties carried by concrete between nodes tend to spread or bulge out. This spreading can induce additional tension (see Fig. A.11). Schlaich defines nodes as simplified idealizations of reality that are defined at the intersection points of three or more straight struts or ties. A node is a sudden change in the direction of the strut that would not occur in the actual structure. Schlaich classifies nodes as either singular or smeared. Singular nodes are caused when a strut or tie is representing a concentrated stress field. If the stress field is wide or when the tension ties consist of many closely spaced bars, the deviation of the forces may be smeared over some length. If a node is smeared, there is typically not a stress problem at the node, since the forces are spread out over a larger area. Figure A.11 shows the locations of the smeared and singular nodes.

The concrete compression strength is dependent on the stress state in the concrete. Transverse compression is favorable because it acts as confinement. Transverse tension is very detrimental especially if cracks form parallel to the principal direction of the struts. Schlaich proposes the following strength values for concrete in compression.

$f_c = 1.0f_{cd}$	for undisturbed and uniaxial compression;
$f_c = 0.8f_{cd}$	if cracks parallel to the direction of the strut may form or in node regions where a tension tie is anchored;
$f_c = 0.6f_{cd}$	where there may be skewed cracking;
$f_c = 0.4f_{cd}$	where there is extensive cracking such as what is necessary for large plastic rotations; and
f_{cd}	is the effective design strength of compression concrete.

According to the CEB Code *(56)* $f_{cd} = 0.85f'_c/\gamma_c$ where γ_c is a factor of safety and the coefficient of 0.85 accounts for sustained loading. In the CEB Code, $\phi = 1.0$ and the load factors for dead loads and live loads are 1.35 and 1.5 respectively.

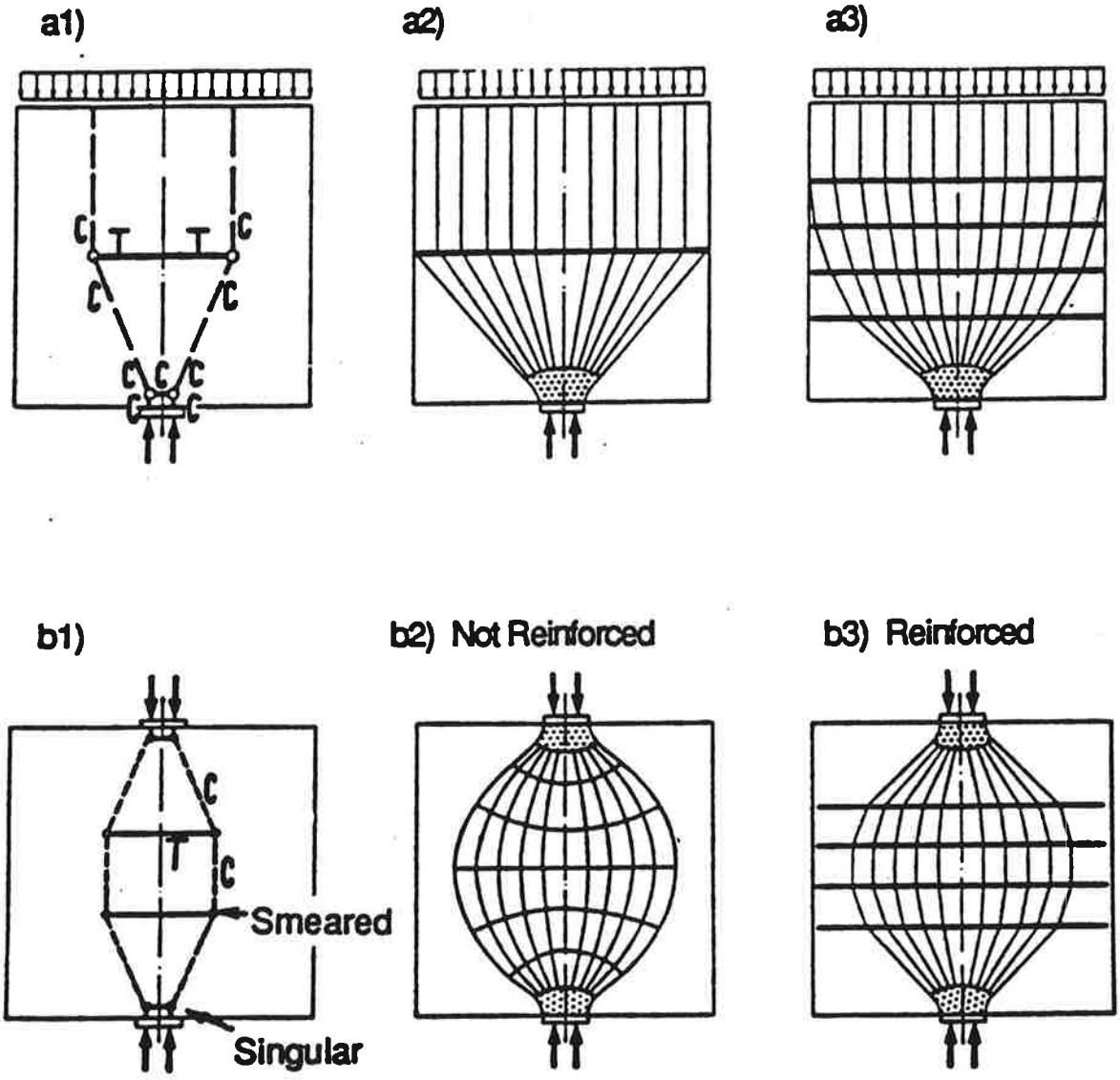

Figure A.11 Stress fields for concentric strut-and-tie models *(2)*.

Marti *(87) (88)* recommended an average effective compressive strength of $0.6f'_c$. He stressed the importance of visualizing the force flow consistent with the equilibrium assumptions and providing the necessary detailing to develop the required forces.

Collins and Mitchell *(65)* proposed the following equations for the compressive strength of concrete based on longitudinal (ϵ_l) and transverse strains (ϵ_t).

$$f_c = 5.5f'_c/(4 + \gamma_d/\epsilon_d)$$

where $\gamma_d = 2\epsilon_d + \epsilon_l + \epsilon_t$

and ϵ_d at failure can be taken as 0.002.

Experimental Investigations.

Experimental work can be placed into two groups: those focusing on studying the general zone behavior and those focusing on the study of the local zone behavior. Investigations have been placed in one of these two classifications, even though most studies are not mutually exclusive. The general zone is usually assumed to extend for a length about equal to the overall depth of the member. The local zone extends for a length about equal to the largest dimension of the anchorage device.

General Zone. Bain et al. *(89)* conducted both an experimental and analytical study. The analytical study consisted of two and three-dimensional elastic investigations, while the experimental study consisted of 36 block tests. The main variables in the study were the amount of spiral reinforcement, the size of the anchor plate and the concrete strength. Strain gages were used to measure surface strains on the concrete. The results from the study were then compared with existing theories.

The research had five major conclusions.

1) The arrangement of a proper amount of transverse reinforcement is effective in increasing the cracking and ultimate loads of the end block.

2) When the bearing surface of the anchor is increased, a slight increase in the ultimate load may occur.

3) Linear relationships can be developed to relate both the concrete strength and thickness of the anchorage plate to the cracking load and to the ultimate load.

4) In comparing two-dimensional solutions to experimental results, Bleich's solution compared very well while those of Guyon deviated considerably.

5) Siever's three-dimensional analysis approximated the experimental distributions.

Breen, Cooper and Galloway *(22)* tested fifteen "I" section specimens to examine the effects of the anchorage geometry, concrete strength, local reinforcement patterns, length of spirals, lateral post-tensioning, tendon curvature, and percentage of web reinforcement. They concluded the following.

1) Formation of cracks along the tendon axis can be accelerated by anchorages with stiff transitional cones and radial forces due to tendon curvatures.

2) The cracking load is not affected by increasing the percentage of web reinforcement and is only slightly affected by concrete compressive strength.

3) The cracking load is not greatly affected by the size of the bearing plate.

4) Very long spirals are effective in delaying the first cracking load.

5) Transverse post-tensioning is very effective in controlling and preventing tendon path cracks.

Fenwick and Lee *(8) (90)* loaded a series of 18 rectangular and "I" section anchorage zones. In addition to the shape of the section, other test variables included the bearing surface area and the tie spacing. The researchers concluded that most of the past research has ignored force redistribution after cracking and that most designs are based on the force being sustained in an uncracked member. Consequently, bursting forces are overestimated. In the tests, the bursting force in "I" sections was much higher than in rectangular sections of the same depth and web thickness. Based on the results of the project, a design procedure was developed. The design is based on an average stress to peak stress ratio of 0.76 in uniformly distributed reinforcing ties. This factor would be increased if the reinforcement is placed according to the stress distribution. The procedure was developed for only concentric single anchorages.

Area of Steel $= 1.32F_{bursting}/f_{steel}$

$F_{bursting} = 1.20m_f M_a/l_a$

$m_f = 1.25 - 0.25(R)^{0.5}$

$l_a = 1.73r(2.9 - 1.9(R)^{0.25})$

Where R equals the stiffness ratio, the ratio of the transverse stiffness after cracking to that existing before cracking (R for one test equaled 0.033); M_a is the maximum anchorage zone bending moment; and r equals the radius of gyration of the section or the equivalent prism.

Gergely et al. *(66) (67)* conducted 25 tests on anchorage zones in end blocks. The specimens consisted of rectangular and "I" beam sections with different reinforcement patterns. A parallel analytical study was conducted using finite differences. The research was very productive and derived the following conclusions:

1) In members with low eccentricities, bursting stresses beneath the load are the highest stresses; while, with high eccentricities the spalling stresses at the mid height of the section are highest. The tensile zone is larger for concentric loaded sections, but the stress peaks are higher for eccentric loaded sections.

2) In "I" beams, the performance is better if the force goes through the flange.

3) Reinforcement cannot be utilized before cracking, therefore, elastic analysis is invalid in a cracked section.

4) Bursting stresses are not affected by the behavior of the spalling zone; therefore, the symmetric prism of Guyon is valid.

Higashida and Nakajima tested eight rectangular blocks each with 18 prestressing bars anchored at the end sections in six rows of three anchors. The specimens were loaded by stressing the bars by rows, starting in the middle and moving to the ends. The specimens varied by altering the reinforcement amount and the stressing level of the bars. Higashida and Nakajima concluded that, for design purposes, the amount of reinforcement for multiple anchorages can be calculated by using the theory for single anchorage systems.

Huang *(91)* tested one "I" beam and did an accompanying finite difference solution. The "I" beam had end block sections with different lengths (depth of the beam and 1.5 times depth of the beam). Stress results agreed with those of Magnel and Guyon. Huang discovered that it is not good to make end blocks too long because they develop high vertical tensile stresses. However, they need to be long enough to distribute the stresses. Huang suggested using a length equal to the depth of the member.

Stone and Breen *(54) (58)* conducted an experimental and analytical study of single anchorage zones in thin web members. The experimental program investigated the following primary variables: tendon eccentricity and inclination, section height and width, concrete tensile splitting strength, anchor width and geometry, and the effect of supplementary anchorage zone reinforcement, both active (lateral post-tensioning) and passive. The experimental study consisted of three phases. Two phases

tested a total of forty one-quarter scale specimens; and, in a third phase, ten tests were performed on five full-scale specimens, one test at each end. The analytical study utilized a three-dimensional linear finite element computer analysis to generalize the experimental results.

The conclusions of the investigation were:

1) For increasing eccentricity and inclination, the cracking load decreased. (This contradicts theories which base cracking on critical bursting stresses since both Guyon's symmetrical prism results and finite element analyses indicate that bursting stresses decrease with increasing eccentricity.)

2) Bearing stresses as high as 2.5 times the compressive concrete strength were routinely achieved before the ultimate load. The cracking strength raised with the increasing of the ratio of the bearing area to the surrounding concrete surface area.

3) Tendon path cracks can occur at locations well outside the general anchorage zone in sections where the tendon profile has significant curvature and multiple strands are used, because of the tendency for the tendon bundle to flatten out and create lateral forces.

4) Tests on unreinforced sections using plate-, bell-, and cone-type anchors showed that anchor geometry can affect the cracking load. (A cone anchor has stiff bearing walls in the conical section. Many times plate anchors are equipped with a conical trumpet, but it is flexible.) The cracking load of the bell anchor is equal to 1.08 times that of the plate anchor, and the cracking load of the cone anchor was equal to 0.61 times that of the plate anchor. The ultimate loads for the plate and cone anchors are only slightly above cracking load, while bell anchors could reach loads up to approximately 25 percent above cracking.

5) Spiral passive reinforcement exhibits much better performance than standard orthogonal reinforcement both for increasing cracking and ultimate loads and for controlling crack widths. The ultimate load for anchorages with spiral reinforcement is as much as 45 to 60 percent higher than those with orthogonal reinforcement having a reinforcement ratio ten times that of the spiral. Spirals were more effective when smaller wires were used with as short a pitch as possible. In addition, long spirals ($2b$ to $2.5b$ in length, where b is the web width) performed no better than short spirals.

6) Lateral post-tensioning reinforcement was the most effective method for controlling cracking in the anchorage zone. The best location for active reinforcement was as close to the loaded face as possible.

7) The tensile strengths of micro-concrete used in one-quarter scale models were found to be substantially higher than those of normal concrete. Therefore, cracking and ultimate loads should be normalized with respect to the tensile strength.

8) Crack patterns observed in the full-scale specimens could be accurately reproduced in the one-quarter scale models; but crack widths, even after scaling, were 40 percent smaller on the average.

From their conclusions, Stone and Breen developed an empirical design procedure based on the cracking load of the concrete. While applicable to sections similar to those tested, the empirical procedure can give misleading results for extreme values of variables such as eccentricity, section dimensions, etc.

Taylor *(92)* tested seven anchorages to develop a failure criterion for plain concrete. His values for the bursting stresses were between those of Guyon and those of Zielinski and Rowe. Taylor found that these values could be reduced by applying a compressive load perpendicular to the axis of the post-tensioning force. He also noted the formation of a cone of concrete ahead of the bearing plate. This cone of concrete is formed due to the stiffness provided by the bearing plate. Once the shear forces along the surface of the cone loosen, the cone acts as a wedge in the concrete. This causes bursting forces perpendicular to the axis of the load.

Trinh *(93)* tested 24 specimens to investigate lightweight concrete in anchorage zones. He determined that lightweight concrete was less resistant. To adjust for the lower strength he recommends using larger bearing plates or increasing the thickness of the section. He also noted that plate flexibility was important when determining the strength of a specimen. Trinh determined that the best equation for the effective width of the plate was the width of the wedge plate plus two times the bearing plate thickness. A safe lower bound equation was 0.886 times the wedge plate width plus two times the bearing plate thickness. When lightweight concrete was used the effective width was best found by adding three times the thickness instead of two. These equations correlated well when rectangular plates were used but not as well for circular plates. Trinh also developed an equation for the bearing capacity of the local zone.

Virlogeux *(94)* tested three large specimens that examined the effects of lightweight concrete. The specimens had anchorages that were inclined and had tendons with curvature. He also did an initial study on small blocks of concrete which showed that: the post-tensioning duct reduces the ultimate strength; the bearing capacity of lightweight concrete is less than that of normal weight concrete; and the more rigid a bearing plate, the better the performance of the specimen. In the large specimens, one was cast monolithically while the other two used a precast plug for the anchorage device. This precast plug used normal weight concrete and contained the bearing plate and the confining reinforcement. The two specimens with plugs had different strengths of lightweight concrete

in the general zone. The specimen without the plug failed in the local zone, while failure of those with the plugs occurred along the tendon path.

Welsch and Sozen *(95)* did an extensive number of tests which focused on spalling cracking in both rectangular and "I" sections. The beam tests were either unreinforced or lightly reinforced near the anchorages. Welsh and Sozen found that spalling cracks did not lead to failure as long as the cracks were small. Since their beams were unreinforced in the bursting region, failure of the specimen was almost simultaneous with the formation of cracks in the bursting region. Welsh and Sozen also did sustained load tests and found that more than one-half of the total crack growth for their specimens occurred in the first week of the eight month tests. Their results correlated well with the basic method of Lenschow.

Zielinski and Rowe *(42) (96)* conducted one of the most extensive experimental programs. The program was divided into two parts: single axial symmetric anchorages and multiple anchorages. The following variables were studied: the ratio of the size of the loading plate to the area of the cross section (A_b/A), the duct size of the post-tensioning cable, the position (external or embedded) of the anchorage device, the shape of the bearing plate (square or circular), and type, position and amount of reinforcement. Stresses were measured using strain gages on the concrete surface. The study investigated both bursting stresses and forces, but only in small specimens. Therefore, their study was a combination of a local zone and general zone study. The study had the following conclusions:

1) The distribution of bursting stresses and the ultimate load of an end block are not significantly affected by the anchorage being embedded or external.

2) The dominant factor in the distribution of bursting stresses and the ultimate load is the ratio of the loaded area to the cross sectional area of the prism (A_b/A), while the positions at which the maximum and zero bursting stresses occur are not significantly affected by the ratio.

3) The maximum bursting stress, which always occurs in the central axis of the prism, is considerably greater than that predicted by any of the existing theories.

4) The percent of reinforcement has a significant effect on the bearing capacity of end blocks, and spirals were found to be more efficient than orthogonal reinforcement.

5) When two anchors are set apart in an anchorage zone, the deep-beam effect sets up tensile forces between the anchors.

6) For a group of anchors, the individual symmetric prism may be used to design reinforcement under each anchor.

7) The size of the duct did not seem to be a major factor affecting the bursting stress distribution.

Yong et al. *(97)* utilized a combination of finite element solutions and 15 experimental tests to investigate how shear forces affect anchorage zone stresses. The specimens were "I" sections with end blocks. The 15 tests included three beams with concentric anchors and end block lengths of 12 inch, 18 inch and 24 inch and 12 tests with eccentric anchors with the same set of three end block lengths. From these tests, it was concluded that a lateral shear force on a beam causes a significant reduction in the value of the lateral tensile strains but has relatively little effect on the transverse tensile strains. If lateral active reinforcement is used to control lateral bursting strains, special attention needs to be paid to potentially high transverse strains in thin web members. Peak lateral bursting strains do not occur at the same location as peak lateral bursting stresses.

Local Zone. A major concern in American anchorage zone specifications has been the limitation of anchorage bearing stresses. Much of the research regarding bearing stresses has been originated by concern over bearing capacity.

Hawkins *(13) (14) (15)* has done extensive research into the bearing capacity of concrete under both rigid and flexible loading plates as well as with strip loadings. One series *(13)* addressed loading through rigid plates. The test program consisted of 230 tests in which the loading geometry (R), the size of the specimen, and the type and strength of the concrete were varied. R is a confinement factor equal to the effective unloaded area divided by the loaded area (for an unconfined plate of the same dimension as the concrete, $R = 0$). The effective unloaded area takes into account the edge distance around the loaded surface and is geometrically similar to the loaded surface. From the tests with R less than 40, the following conservative estimate of the ultimate bearing strength was developed.

$$q = f_c' + K (R f_c' - f_c')^{0.5}$$

K is equal to a function of the angle of internal friction that can be conservatively taken to be 50. Hawkins also concluded that any increase in bearing capacity above the compressive strength of the concrete is directly dependent upon the angle of internal friction and that it is essential for the concrete to be densely compacted and for the air voids and shrinkage cracks to be kept to a minimum.

In another research program *(14)*, Hawkins investigated the relationship between flexible, semi-flexible, and rigid plates with 33 tests. From the tests, it was determined that the load capacity versus the thickness of the plate is linear when the plate is flexible. In the semi-flexible range, the capacity rises exponentially until a maximum value is reached, corresponding to the capacity for a rigid

plate. In a flexible plate, increasing the bearing area does little to increase the ultimate bearing load. However, increasing the area is very effective in increasing bearing capacity for rigid plates.

Hawkins *(15)* also reports the results of 39 tests on rigid plates extending across the full width of the block. From the tests, two modes of failure were observed: the corners of the block including the strip plate can shear off, or the crack which develops on the axis of the load can propagate spontaneously and cause the bearing plate to punch down into it. The bearing capacity for design purposes can be predicted by the following equation developed by Kriz and Raths: $q = 5.91 f_c'^{0.5} (D/W)^{1/3}$ where D is the distance from the edge of the block to the centerline of the bearing plate, W is the width of the bearing plate, f_c' is the compressive strength of the concrete in psi.

Middendorf *(12) (98)* conducted 48 tests with f_c' between 4000 and 6000 psi to investigate the validity of the then current code of practice, "Criteria for Prestressed Concrete Bridges" by the Bureau of Public Roads. The code of practice used the following equation:

$$q = 0.5 f_{ci}' (A/A_b)^{1/3} \leq f_{ci}'$$

A is the effective concrete area and A_b is the bearing area. Middendorf concluded that the cube root formula for design should be replaced with a square root formula, and that the maximum bearing stress should be limited to three times the compressive strength. He also determined that the relationship between effective concrete area and bearing area is valid except in the case of grouped plates where the overall plate area should be used, and that tilting the plate up to five degrees does not affect its bearing ability. Middendorf limited his theories to applications after the concrete is three days old.

Niyogi *(34) (35)* tested 154 reinforced concrete blocks to investigate the problem of bearing stress capacity. He developed three equations to determine the ultimate concentric bearing capacity, ultimate eccentric bearing capacity, and the effect of adding a spiral. He determined that the eccentricity of the load tended to decrease the ultimate bearing strength and that spiral reinforcement increased the bearing strength by increasing the lateral confinement. He also determined that large diameter spirals appeared to be the most effective against cracking, and that large bearing plate performance was enhanced less by additional reinforcement than by smaller plates. In his tests, visible cracking loads were increased by the addition of reinforcement and grid steel increased bearing strength but not as effectively as spiral reinforcement.

Most of the current standards include anchorage bearing stress criteria. A majority of the codes and guidelines, as shown in Section A.5, utilize a bearing capacity based on the equation $f_c' \sqrt{A/A_b}$.

Roberts *(4)* examined a wide range of variables that affect the performance of the local zone including concrete strength, plate size, confinement and edge distance. Roberts made the following observations:

1) The first cracking load is primarily affected by the ratio a/h and the tensile strength of the concrete. It is not affected by the presence of reinforcement.

2) Auxiliary reinforcement can be used to reduce crack size.

3) The ultimate load can be raised by increasing the diameter or increasing the pitch of the spiral reinforcement. By increasing the edge distance or including auxiliary reinforcement, the ultimate load is increased.

4) An equation was determined for the design of the local zone confinement.

The equation which best fit the data for the bearing capacity was Equation (1). Equation (2) was the recommended design equation.

$$P_b = 0.8 f_c' \sqrt{A/A_b}\, A_b + k f_{lat} (1 - s/d_c)^2 A_{core} \le 3 f_c' A_b \quad (1)$$

$$P_b = 0.7 f_c' \sqrt{A/A_b}\, A_b + k f_{lat} (1 - s/d_c)^2 A_{core} \le 3 f_c' A_b \quad (2)$$

Where $f_{lat} = k_2 A_s f_y/(d_c s)$

And

A is the supporting area defined as the maximum area geometrically similar to the loaded area and concentric with it;

A_b is the full net area of the bearing plate;

A_{core} is the area of the confined portion of concrete;

A_s is the cross sectional area of the confining reinforcement;

d_c is the outside dimension of the confining reinforcement;

f_c' is the compressive strength of concrete;

f_y is the yield stress of the confining reinforcement;

k is 2 for spiral reinforcement and 1 for tie reinforcement; and

s is the center to center spacing of the confining reinforcement.

For f'_c above 8000 psi, the 0.8 in Equation (1) and the 0.7 in Equation (2) should be reduced 0.05 for every 2000 psi increase in f'_c above 8000 psi but should not be taken as less than 0.65. Equation (1) which best fit the data has a standard deviation of 20 percent.

5) To fully use the net bearing area of an anchor, the anchor must meet the slenderness requirement of Equations (3) and (4).

$$n/t \leq 0.07 \sqrt[3]{E_b / f_b} \tag{3}$$

and

$$f_s \leq 3 f_b n^2 / t^2 \tag{4}$$

where t is the thickness of the bearing plate;

n is the distance from the edge of the stiff wedge plate or outer perimeter of wedge holes for plate with integral wedge plates;

E_b is the Modulus of Elasticity for the bearing plate material; and

f_b is F_{pu}/A_b, F_{pu} is the guaranteed ultimate load of the tendon.

6) When local zone details were tested in the small prism and then tested in a large specimen, the details were always found to be conservative.

7) The study recommends test data be furnished by manufacturers on standardized specimens in order to verify reinforcing details and edge distances.

Wurm and Daschner *(37) (38)* conducted an extensive study with 130 specimens. Their study investigated 1) the effects of the A/A_b ratio, 2) the type of confining reinforcement, 3) the amount of reinforcement, 4) sustained loading , 5) post-tensioning duct effects, 6) placing the anchorage at an eccentricity and 7) concrete age. Their major conclusions were that:

1) Spiral is the most efficient form of reinforcement;

2) If confining reinforcement is too short, a crushing of the concrete will occur at the base of the confinement;

3) The post-tensioning duct reduces the ultimate load; and

4) Ultimate loads for specimens with sustained loading were 20 percent lower than those loaded short term.

Slab Edge Anchors. A very special situation exists with multiple anchors typically found on slab edges. These anchors are small and the local zone is often unconfined. Burgess et al. *(108)* performed an experimental study on the behavior of closely spaced edge anchors (monostrand an four-strand) in heavily reinforced bridge decks. They concluded that interaction between closely-spaced anchors was favorable and spiral anchorage reinforcement was only moderately beneficial in heavily reinforced bridge decks. Furthermore, they emphasized that exterior anchors with small edge distances could be weaker because the width of the anchorage zone affects its strength.

Experiments on closely-spaced monostrand edge anchors performed by Sanders, Breen and Duncan *(62)* varied the anchorage zone reinforcement and rotated the anchors from horizontal orientation to vertical. They concluded that the addition of back-up bars and hairpin reinforcement increased the strength of the anchorage zone, that closely-spaced anchors cracked and failed at lower levels per anchor than single anchors, and that horizontal multiple anchors were able to withstand higher loads than vertical multiple anchors because the horizontal anchors utilized the surrounding concrete more efficiently.

Research has concentrated on the failure from jacking forces on the anchorage zone, but in 1985 a post-tensioned roof slab failed after the anchor load had been sustained for five years *(26)*. A crack had crept through the anchorage zones at a corner of the slab. There was no vertical reinforcement in the anchorage zones along the slab's edge, and when the crack extended far enough ahead of the anchor, the slab split apart. Anchorage zone reinforcement could have been used to provide general structural integrity rather than just for strength for initial jacking forces.

The Post Tensioning Institute suggests the use of one of two details for the edges of post-tensioned slabs (Figures A.12 and A.13) *(19)*. Both details incorporate vertical anchorage zone reinforcement, but the reinforcement is spread uniformly along the edge instead of being concentrated in individual anchorage zones.

PRODUCT LITERATURE

An additional source of information about anchorage zone and anchorage devices is from the product literature of anchorage device suppliers. For the scope of the this study, the type of anchorage

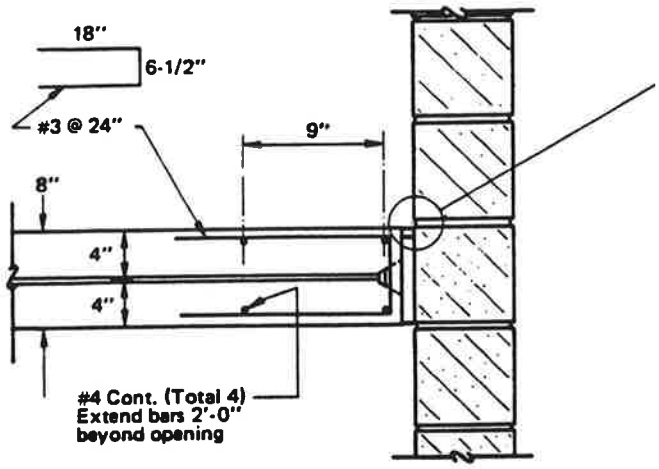

Figure A.12 Detail of post-tensioned anchorage zone in slab which is separated from the wall *(19)*.

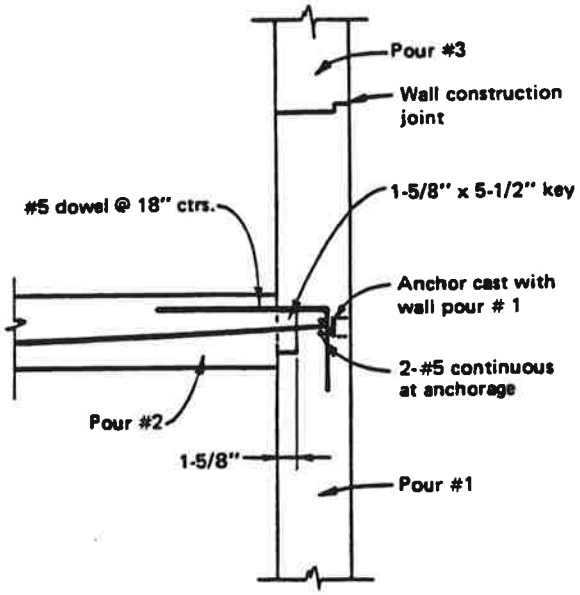

Figure A.13 Detail of post-tensioned anchorage zone in slab which is cast monolithically with wall *(19)*.

that is the focus is multiple strand anchorages. There are many post-tensioning anchorage suppliers in the United States that furnish the multistrand type of anchors predominant in bridge girder construction. Few applications are envisioned in bridge girder construction for the monostrand type of anchors; while they could be used in transverse deck post-tensioning, the difficulty in developing adequate long term corrosion protection and the large number of closely spaced strands required makes the use of monostrands less desirable.

In the initial stages of this program, information was solicited on bridge anchorages from the producer membership of the Post-Tensioning Institute, which represents the majority of suppliers in the United States. Product information was obtained from:

1) CCL Division of Nicholson Construction Company,

2) CEC Systems, Inc.,

3) Continental Concrete Structures,

4) Dywidag Systems International,

5) Genstar Structures Limited,

6) Linden Post-Tensioning Corporation,

7) Prescon Corporation,

8) Stresstek Division of Conner Corporation, and

9) VSL Corporation.

In spite of the large number of hardware suppliers, an examination of their catalog and typical application examples indicated that most of the manufacturers had three basic multistrand anchors: 1) a square flat bearing anchor, 2) a rectangular flat bearing anchor, and 3) a multiple plane anchor (see Fig. A.14). The square flat bearing anchor comes in various sizes with capacities from three to 55 strands, while the multiple plane anchor is produced in sizes and capacities ranging from three to 61 strands. The rectangular flat bearing anchor is only available with a four strand capacity and is widely used for deck slab stressing. Most anchors were available for use with either 0.5 inch strand or 0.6 inch strand.

Some of the anchor devices are equipped with confining spirals. In the copious product data received, only three companies gave information on the local zone confinement reinforcement size or

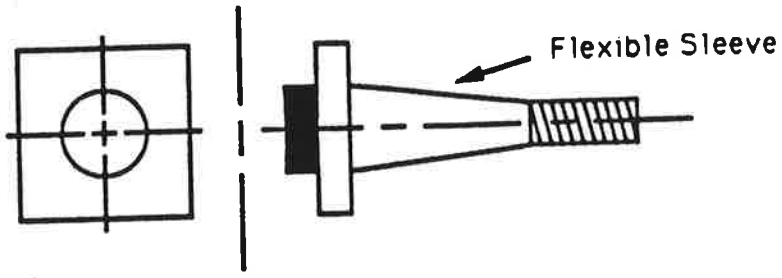

a) Square Flat Bearing Anchor

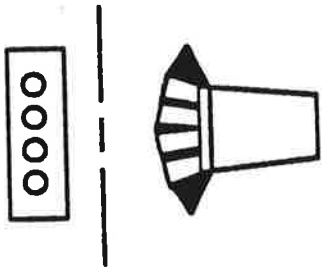

b) Rectangular Flat Bearing Anchor

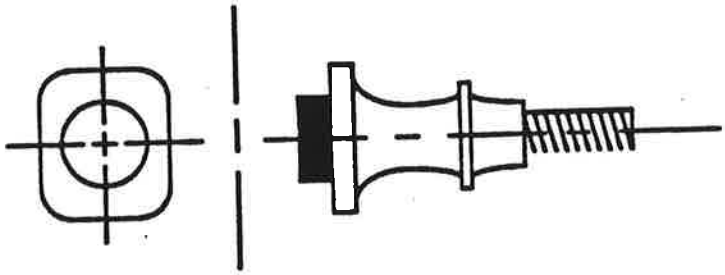

c) Multiple Plane Anchor

Figure A.14 Anchor types.

spacing required to ensure satisfactory anchor performance up to the design load. There is a major discrepancy between the local zone information supplied to the engineer in Europe versus that supplied in the United States. Figure A.15 shows the information provided for one anchor. Figure A.15a is from a supplier here in the United States while Fig. A.15b is from the same supplier in West Germany. Figure A.15a has only the basic anchorage geometry and some minimum guidance. Figure A.15b has extensive information on the reinforcing details to be used to confine the local zone. This is not completely the fault of the supplier because the governing codes in the United States have no requirements that such guidance be provided while it is mandatory under the West German system. In the survey of practitioners discussed in detail in Appendix B, it was frequently reported that the local zone reinforcement immediately around the anchorage device is designed by the post-tensioning supplier and not by the engineer of record. When the division of responsibility envisioned in this study was described to suppliers, all said they were in favor of the design engineer of record taking control of the general zone which would allow the suppliers to concentrate on specifying the required confining reinforcement and concrete cover of the local zone. For anchorage device applications where high stresses are expected or where auxiliary local zone confinement is necessary, a standard test method should be developed so that third party test agencies could certify special anchorage assemblies as acceptable in specified concretes and with specified minimum edge covers, minimum center-to-center spacings, and minimum auxiliary reinforcement. This acceptance procedure is currently used in Europe and would provide the engineer with much needed information.

CURRENT CODES AND COMMENTARIES

In a post-tensioned anchorage system, very large highly concentrated forces must be transferred to a continuous distribution of stresses at a distance approximately equal to the depth of the member. The anchorage zone consists of two distinct parts: 1) the region immediately surrounding the anchorage device [*the local zone*] and 2) a second region [*the general zone*] where the major transition from highly localized to distributed stresses occurs. The state-of-the-art for design of these zones will be detailed in this section. There are a number of current codes and published guidelines used to design post-tensioned anchorages. Generally, current design techniques do not specifically distinguish between the local and general zones. Therefore, most of the discussion of current design techniques deals with general zone design. The following major codes and guides are reviewed in this study.

AASHTO Bridge Code '89 *(16)*

ACI 318-89 *(63)*

Austrian Code '79 *(99)*

CEB-FIP Model Code '78 *(56)*

Anchor Type		6812	6815	6819
Ultimate Load	(kN)	3180	3975	5035
Recess Form	Øa(mm)	300	300	360
Multi-Surface Anchor	Øb	220	205	280
	c	190	200	220
	Ød	160	180	200
	e	43	50	55
Transition Tube	Øg	120	130	145
	L	350	400	450
Min. Concrete Strength	B45 (5000 psi)			
Anchorage Spacing				
Center Distance		300	340	400
Edge Distance		170	190	220
Cracking Tensile Reinforcement	Depends on National Spec.			

(a) United States

Anchorage Type 6812

Concrete Strength (psi)	B25 (3600)	B35 (5000)	B45 (6500)	B45 (6500)	B45 (6500)	B45 (6500)
Anchor Distances (mm)						
Center Distance	380	350	320	370	430	480
If reduced center distance is	350	320	290	340	400	450
then opposite direction must be	410	380	350	400	460	510
Edge Distance	210	195	180	205	235	260
Stirrups						
Number	5	5	5	4	5	4
Bar Diameter	10	10	10	10	8	8
Stirrup Width	350	320	290	340	400	450
Initial Distance from Anchor	70	65	60	75	75	110
Spacing	35	35	35	50	50	50
Spiral						
Number of Turns	5	5	5	4	4	4
Bar Diameter	14	14	12	12	8	8
Spiral Diameter	340	310	280	275	400	400
Initial Distance from Anchor	40	40	40	75	100	100
Spacing	55	50	50	70	70	70

(b) West Germany

Figure A.15 Product information

CIRIA Anchorage Design '76 *(100)*

FIP Recommendations '81 *(3)*

Florida DOT Design Criteria *(101)*

German Code, DIN 1045 *(102)*

North Carolina DOT Design Criteria *(103)*

Ontario Bridge Code '83 *(104)*

PTI Design and Construction Specification for Segmental Bridges *(17)*

Switzerland Code, SIA 162 *(105)*

VSL End Block Design '75 *(106)*

Most of the standards use different notation. In order to permit comparison, this report uses the notation shown in Table A.1 and Fig. A.16.

Local Zone Criteria.

The local zone of a particular anchorage is greatly influenced by the anchor force and is relatively insensitive to surrounding anchors, section geometry, or other applied forces. Tests have shown *(14)* that this zone is very critical to the behavior of the anchorage zone. In order to properly distribute the forces in the general zone, most anchor devices require local zone confinement. Several of the codes and standards do require tests to determine if the anchor is properly reinforced. This would be classified as a local zone test. Such tests are normally sponsored by the device manufacturers and do not usually need to be conducted for each individual application. Four publications that give guidelines for tests on the local zone are the PTI Design and Construction Specification (17), the Austrian Code *(100)*, the FIP Recommendations *(3)* and the German Code *(103)*. A typical local zone test specimen is shown in Fig. A.17. In the PTI Segmental Bridge Specification *(17)*, the test block has a width that is twice the minimum edge distance from the centerline of the anchor to the face of the concrete or the minimum spacing between anchors plus 3 inches. The length should be three times the largest cross section dimension. The concrete strength at testing shall not exceed 85 percent of concrete strength at the time of the post-tensioning in the actual structure. Three tests should be conducted. The anchorage should not have more than 0.01 inches of permanent distortion after being loaded to 95 percent of the ultimate tendon strength. At a load of 40 percent of the ultimate tendon strength, there should be no concrete cracks. At 70 percent, the width of concrete cracks should not

Table A.1 Notation for Specification Comparison

a	=	lateral width of anchor bearing surface (see Fig. A.16)
A	=	effective bearing area
A_b	=	anchor bearing area
A_r	=	reinforcement area
A_s	=	area of hoop reinforcement
A_2	=	area of concrete within hoop
b	=	transverse width of anchor bearing surface (see Fig. A.16)
d	=	effective depth of anchorage zone, determined as depth from anchor where stresses become linear, assumed usually to be equal to height of section.
d_1	=	distance from centerline of tendon to edge of concentric symmetrical prism used for calculation of spalling stresses in CIRIA guide (see Fig. A.16), where .
f_b	=	bursting stress
f_c	=	stress in concrete
	=	concrete strength at 28 days
f_{ci}	=	concrete strength at stressing
f_{ck}	=	characteristic concrete cube strength at stressing
f_{cu}	=	concrete cube strength at stressing
f_{pu}	=	specified tensile strength of prestressing tendons
f_{py}	=	specified yield strength of prestressing tendons
f_t	=	tensile strength
f_y	=	steel yield strength
F_b	=	bursting force
h	=	height of section
	=	effective lateral width of bearing surface determined by boundaries of area which is geometrically similar to the anchor bearing area
M	=	maximum moment in hoop reinforcement zone
M^H_{sp}	-=	maximum difference between the moment caused by the linear stress distribution at h/2 from the anchor and the distribution at the anchor
N	=	maximum axial force in hoop reinforcement zone
P^H	=	jacking force
s	=	hoop spacing
t	=	thickness of the section
	=	effective transverse width of bearing surface determined by boundaries of area which is geometrically similar to the anchor bearing area.
u	=	perimeter of hoop

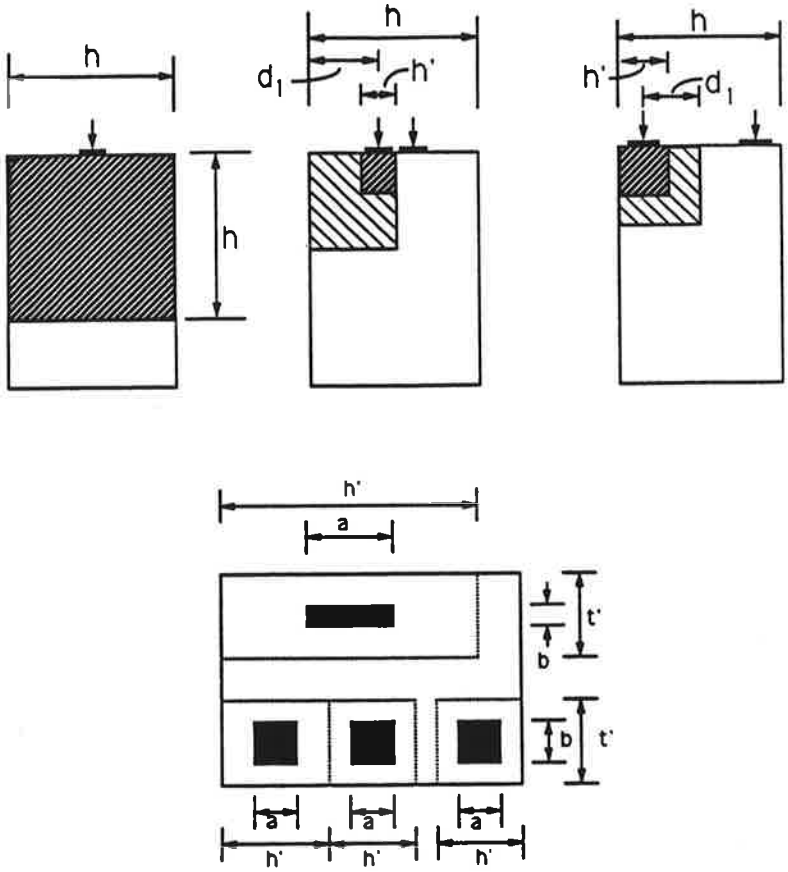

Figure A.16 Parameter Description for Specification Comparison

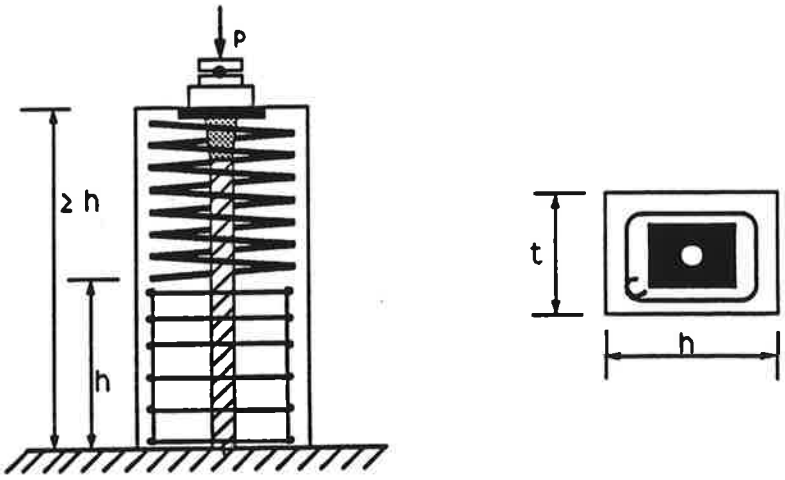

Figure A.17 Local zone test specimen.

exceed 0.005 inches. After loading to 95 percent, the width of concrete cracks should not exceed 0.015 inches.

In the Austrian Code *(100)*, the test specimen is a rectangular section with a height at least two times the width. The width is twice the shortest distance to the concrete face or is the distance between anchors. All anchors are tested with a spiral and confining reinforcement around the edge of the specimen. Four specimens should be tested with three loaded cyclically and then loaded to failure. The fourth specimen is loaded monotonically until failure. For the cyclic tests, the concrete strength should be 80 percent of the field strength; while, for the static test, the strength should be equal to the field strength. The cyclic test consists of ten cycles between six percent and 60 percent of the guaranteed minimum strand strength (F_n), ten cycles between six percent and 72 percent of F_n, and then increasing of the load until failure of the specimen at 0.2 to 0.3 N/mm^2/sec (29 to 44 psi/sec). For the static test, the specimen is loaded at the same rate as the cyclic test (0.2 to 0.3 N/mm^2/sec) until failure. At $0.06F_n$, cracks are limited to 0.05 mm (0.002 inches); and, at $0.72F_n$, cracks are limited to 0.12 mm (0.005 inches). Crack limits apply only to cracks that start in the upper or anchor portion of the specimen. The maximum required load is $0.90F_n$ for cyclic loading, F_n for static tests, and $1.2F_n$ if no spiral is ordinarily included with the anchorage device.

In the FIP Recommendation *(3)*, the specimen is a rectangular section in which the dimensions are taken to be twice the permissible minimum distance of the anchorage to the concrete edges of the structure in the corresponding directions. The height is taken to be two times the maximum section width (see Fig. A.17). In the upper part of the specimen, bursting reinforcement shall be provided as specified by the manufacturer for the proper use of the particular system. The remaining lower portion of the specimen should be reinforced to prevent premature failure; this portion should have at least a height equal to the maximum section width. The concrete strength at the start of testing shall not be greater than 85 percent of the specified application concrete characteristic value, which is defined as a statistical value that 95 percent of the concrete test specimens will exceed. During testing, the concrete strength shall not exceed the characteristic strength. Two testing procedures may be used: the static load transfer test and the slow cycle load transfer test. The static load transfer test is illustrated in Fig. A.18a. The load is applied in steps of 0.20 of the maximum load until a load of 80 percent of the tendon characteristic tensile strength is achieved. Crack measurements and deflections are taken at 20 percent, 40 percent, 60 percent, and 80 percent of the characteristic value of the tendon. The load is maintained at 80 percent of the characteristic value for 48 hours and then increased to failure. The slow cycle load transfer test is shown in Fig. A.18b. The test starts the same way as the static test; but, once the load of 80 percent is reached, the specimen is cycled between 80 percent and 15 percent for at least ten cycles or until the crack widths have stabilized. Once the crack widths are stable, the specimen is loaded to failure.

The German Code *(103)* and the FIP Recommendations have the same specimen guidelines but slightly different loading patterns. As with the FIP, the German Code specifies two different

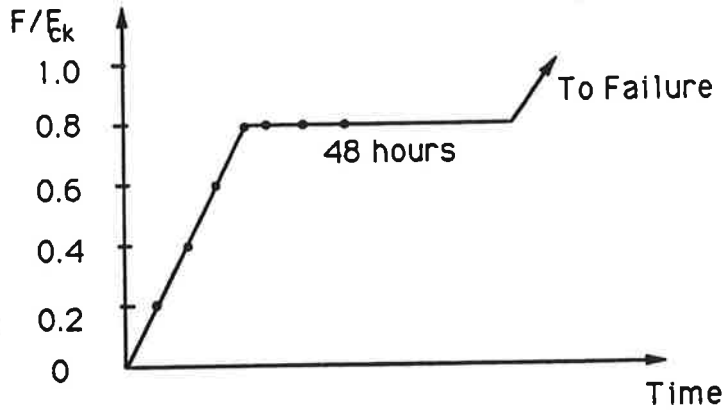

a) Static load test

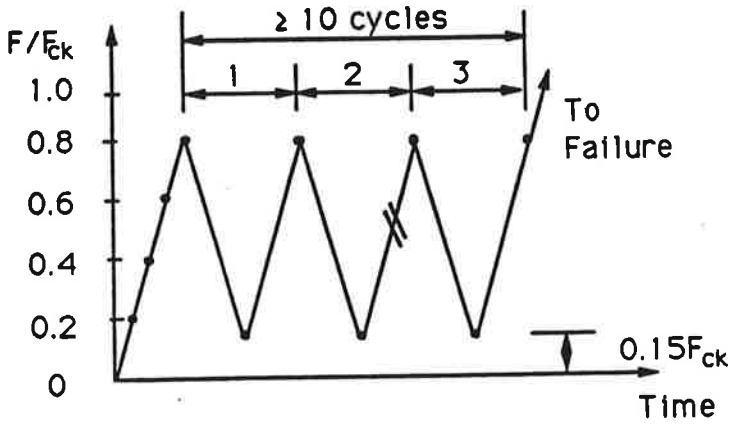

b) Cyclic load test

Figure A.18 Loading patterns for local zone test.

loading tests: static load transfer test and slow cycle load transfer test. The only difference in the slow cycle test is the maximum and minimum load level during cycling. The maximum German value is 70 percent of the nominal tendon strength, and the minimum is 10 percent. For the static load transfer test, two sustained load periods are specified. The specimen is first loaded to 55 percent of the nominal tendon strength and held there for 48 hours. It is then loaded to 70 percent and held for another 48 hours. At the conclusion of the time, the specimen is then loaded to failure.

Specific criteria for the testing of anchorages for unsatisfactory performance in the local zone have generally not been used in the United States. The widely utilized bearing stress limitations (the compression stress exerted by the anchor on the concrete) on anchorage devices contained in AASHTO *(16)* Section 9.15.2.4, ACI Code and Commentary *(63)* Section 10.15, and Section 4.2 of the PTI Segmental Bridge Construction Specification *(17)* are indirect local zone criteria. The most widely reported bearing stress formulas are listed in Table A.2. Most are related to the effective bearing area divided by the anchor force bearing area. The maximum bearing stress allowed is $2.2f_c$ in the CEB-FIP Code. In the United States, AASHTO limits the design to $0.9f_c$ but not more than 3000 psi, while the criteria of Florida and North Carolina *(102) (104)* and the PTI Specification limit it to $1.25f_c$, but not more than 6875 psi. The arbitrary maximum upper limits penalize high strength concrete.

General Zone Criteria.

The resistance to tensile forces becomes a major concern in the general zone. Tensile forces are induced by the lateral diffusion of forces in the member (bursting stresses) or by moments due to the eccentricity of the anchor force and/or multiple anchors(spalling stresses). The codes and guidelines listed previously address the problems in the general zone in a variety of ways. The methods have been grouped into the following: bursting force estimates, spalling force estimates, and restrictions on concrete stresses, reinforcement stresses, anchorage stresses, and prestress steel stresses.

Most guidelines check the bursting force (see Table A.3). The bursting force is the tensile force perpendicular to the axis of the tendon. Most use a formula of the form $kP(1 - a/h')$. The German code utilizes two bursting zones when the eccentricity of the anchor is outside the kern ($e/h > 1/6$). Zone 1 occurs directly ahead of the anchor within depth h', while Zone 2 is centered on the axis of the section at a depth of $2/3h$. In addition to the bursting force, many of the publications limit the bursting stress (see Table A.3). The VSL Guide [105] uses the stress distribution curves shown in Fig. A.1 to determine the bursting stress level. A loaded face tensile force (spalling force) also develops near the concrete surface next to the anchor for eccentric anchors (see Table A.4).

Several of the codes give explicit restrictions on concrete tensile stress levels. Such stresses may be computed by comprehensive linear analyses of the anchorage zone such as with application of finite element analysis. The analyses should consider all applied forces and are essentially based on a limiting principal tensile stress. Tensile stresses are limited in AASHTO *(16)* Section 9.15.2.2

Table A.2 Bearing Stress Estimates

AASHTO Bridge Code '89	At SL
PTI Segmental PT Guideline Proposal	At PT At SL
CIRIA Guide	At PT If bearing area is not well defined At PT If bearing area is well defined
Design Criteria for F1 & NC	At PT At SL
CEB-FIP Model Code '78	where K = 1.5 for normal conditions and K = 1.3 for overload
Austrian Code	where for 0 0.20 0.40 0.60 0.80 1.0 K 1.60 1.23 0.93 0.69 0.51 0.40
German Code	where and and no overlapping of A_2 at depth d in the case of multiple loads for 25 35 45 55 0.70 23 27 30
Swiss Code	or 1.8 limits of and

At S.L. = Service Load
At P.T. = At Stressing

Table A.3 Bursting Force Estimates

ACI 358-86	F_b = 0.70P
PTI Segmental PT Guideline Proposal	F_b = 0.35P
CIRIA Guide	F_b = cP/K where K = 1 for isolated anchors and anchors on the perimeter of the block, K = 1.5 for anchor distributed in one direction, and K = 2.0 for anchors distributed in two directions and for ≤0.3 0.4 0.5 0.6 ≥0.7 c 0.23 0.20 0.17 0.14 0.11
Design Criteria for FL & NC	F_b = f_b =
VSL End Block Design Guide	F_b = f_b = See Figure A.1b
Ontario Bridge Code '83	F_b = f_b =
CEB-FIP Model Code '78	F_b =
Austrian Code	
German Code	F_{b1} = F_{b2} =

to $7.5\sqrt{f_c'}$ while the PTI *(17)* Section 13.2.1 limits stresses to $6.\sqrt{f_c'}$ The Florida guide *(102)* is based on research with Florida limestone and limits tensile stresses to 0.8 times the split cylinder test or $5.\sqrt{f_c'}$

In addition to force and stress calculations, many codes have restrictions on the maximum stress levels for at least one of the following: concrete (see Table A.5), reinforcement (see Table A.6), anchorages (see Table A.7), and prestressing steel (see Table A.8).

Anchorage zone supplemental reinforcement is the last major area specified in several of the criteria for the design of the anchorage zone. AASHTO requires that a grid of #3 bars at 3 inches be placed not more than 1-1/2 inches from the inside face of the anchor bearing plate, if a recommended reinforcement is not given by the manufacturer. In the guide used by Florida and North Carolina, individual anchors must use spirals and anchor groups must use spirals in combination with links or prestressing to contain bursting stresses; grids may not be used. In the Ontario Bridge Code, the bursting reinforcement must extend from $0.28 1h'(1 - e^{3a/h'})$ to h'; but in the CEB-FIP Model Code, bursting reinforcement must extend from $0.1h'$ to h' and the allowable load may be increased as hoop reinforcement is added according to: $1.3u/A_s f_y - (A_b - A)f_{ck}(1 - M_s/(uNx/\text{pi}))$. In the Austrian Code, reinforcement behind a blister must take $P/4$ in tension, while the VSL guide says $P/2$ must be taken in tension.

Table 4. Spalling Force Estimates

CIRIA Guide	$F_{sp} = 0.2P\left[(h'/2 - d_1) / (h'/2 + d_1)\right]^3$
VSL End Block Design Guide	$F_{sp} = 2M_{sp} / h$ $f_{sp} = 6M_{sp} / th^2 \leq 0.6F_t$
Ontario Bridge Code '83	$F_{sp} = 0.04P$
Germand Code	$F_{sp} = P(e/d - 1/6) \geq 0$

Table A.5 Concrete Stress Restrictions

AASHTO Bridge Code '89	Unless otherwise stated in plans, at transfer f_{ci} must be $\geq$ 3500 psi
Design Criteria for FL & NC	In precast concrete for transverse PT, f_{ci} must be $\geq$ 4000 psi and for longitudinal PT must be $\geq f_c'$ 28 days. In cast-in-place concrete before partial PT f_{ci}' must be $\geq$ 2500 psi and for full PT $\geq$ 4000 psi
Swiss Code	Cannot use greater than f_{cu}' at 28 days for design calculations

Table A.6 Reinforcement Stress Restrictions

AASHTO Bridge Code '89	Anchorages of unbonded tendons shall develop at least 95% of the minimum specified ultimate tendon strength of the pre-stressing steel without exceeding anticipated set.
ACI 318-89	Anchorages of unbonded tendons shall develop the minimum specified ultimate tendon strength of the prestressing steel without exceeding anticipated set. The anchorage zone develop the ultimate tendon strength of the prestressing tendon using a strength reduction factor of 0.9 for concrete
CEB-FIP Model Code '78	Anchorages required to handle 1.2 times the maximum force in the prestress tendons

Table A.7 Anchorage Stress Restrictions

AASHTO Bridge Code '89	Anchorages of unbonded tendons shall develop at least 95% of the minimum specified ultimate tendon strength of the pre-stressing steel without exceeding anticipated set.
ACI 318-89	Anchorages of unbonded tendons shall develop the minimum specified ultimate tendon strength of the prestressing steel without exceeding anticipated set. The anchorage zone develop the ultimate tendon strength of the prestressing tendon using a strength reduction factor of 0.9 for concrete
CEB-FIP Model Code '78	Anchorages required to handle 1.2 times the maximum force in the prestress tendons

Table A.8 Prestressing Steel Stress Restrictions

AASHTO Bridge Code '89	Temporary stress before losses due to creep and shrinkage must be $\geq 0.7f_{pu}$ with allowances for temporary overstressing at seating up to $0.9f_{py}$.
ACI 318-89	Temporary stress due to tendon jacking force must be less than $0.94f_{py}$, $0.8f_{pu}$ or the maximum value recommended by the manufacturer of the prestressing tendon or anchorages.
Design Criteria for FL & NC	Maximum jacking stress is 0.76 f_{pu} for stress relieved strand (SRS) and $0.81f_{pu}$ for low relaxation strand (LRS)

APPENDIX B

USER SURVEY AND ASSESSMENT

INTRODUCTION

Design techniques, application details, and problems encountered with anchorage zones vary widely throughout the United States and worldwide. To help in formulating the research program, a survey concerning current practices and problems was developed and sent in 1987 to all the bridge division members of AASHTO (state highway departments and province highway departments), a number of firms that design post-tensioned structures, and to active research contributors in the area of anchorage zones. One-hundred forty four surveys were sent out and 66 responses were received.

SURVEY DESCRIPTION

The amount of knowledge and experience regarding post-tensioning varies greatly from agency to agency. Therefore, the survey had to be flexible enough so that information could be obtained from different levels of experience. The survey document had the following objectives:

1) To determine what procedures and criteria are currently being used to analyze, design, and evaluate anchorage zones,

2) To determine incidents of failure or severe distress which have occurred in anchorage zones,

3) To determine the most commonly used anchorage zone configurations, and

4) To determine typical reinforcing patterns.

It was decided that, instead of developing a very detailed series of questions, the format would consist of a set of general requests and a classification system for anchorage zones to help direct the answers to areas of interest. The following information was requested.

1) Problems encountered in design, checking or inspection of post-tensioned anchorage zones;

2) Analysis procedures, evaluation criteria, or references used in the design or checking anchorage zones;

3) Criteria used to judge when special attention had to be paid to the post-tensioning system;

4) Knowledge of specific failures or severe distress in post-tensioned anchorage zones including photos or crack pattern sketches; and

5) Sample plans or details of typical and special anchorage applications.

The classification system was divided into eight major areas: anchorage zone, location, geometry, loads, concrete, reinforcement, hardware, and design criteria. A copy of the survey document is included at the end of this Appendix as Exhibit B.1.

SURVEY RESULTS

The response to the survey was very good. Surveys were sent to 64 bridge engineer members of AASHTO, and 38 responded. Of the 38 responses, 23 (60 percent) use post-tensioning. Eighteen of the responses (80 percent of those who use post-tensioning) were highly informative and included either example plans, design guidelines, or written answers to the questions. Eighty surveys were sent to consulting engineers or researchers. The response was not as good as from the AASHTO members. Only 28 responses were received from consultants or researchers; but, as with AASHTO members, 17 (60 percent) used post-tensioning in design or had research experience with it. Sixteen (95 percent of those who use post-tensioning) gave informative responses.

The most common information included in responses was anchorage zone plans. The responses received included hundreds of pages of plans with reinforcement details. A sampling of various details is included in Figs. B.1 to B.11 and is subsequently referred to in order to illustrate terminology. The plans were examined, and it was apparent that there is a broad variety of applications and details being used. However, after further study, it became obvious that there seemed to be some general overall patterns that predominated. While of no statistical significance in strict mathematical terms, the incidence of type of anchorage application furnished by respondents was felt to be a good indication of the diversity of the problem and the general nature of the interests and concerns of the respondents. An examination of the plans and details submitted indicated that the anchorage applications could be classified by:

a) Location,

1. Beam or Slab - End surface (Figs. B.1, B.2), transverse tendon (Figs. B.3, B.4a) or interior anchors

2. Blister - End surface or interior anchors (Figs. B.5, B.6, B.10)

3. Recess Pocket (Fig. B.7)

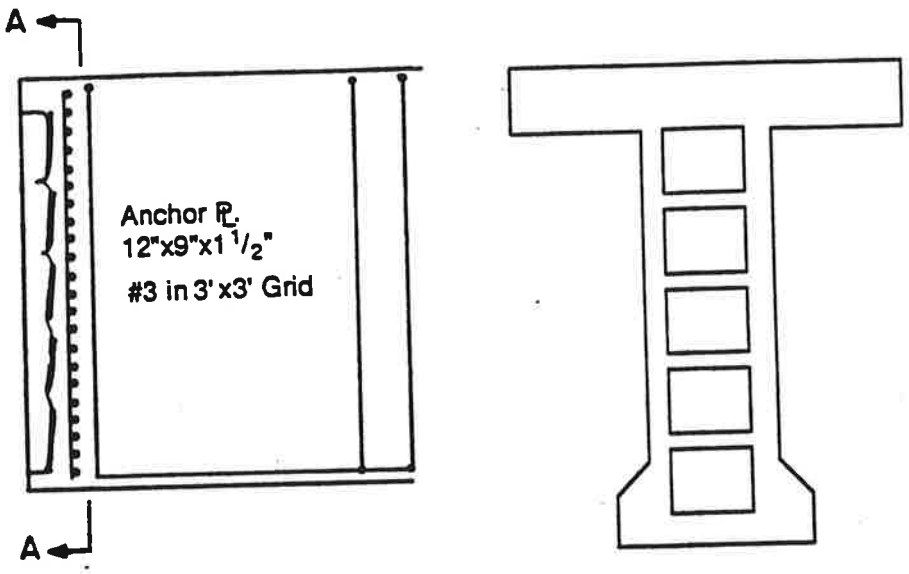

Figure B.1 Concentric end anchorage.

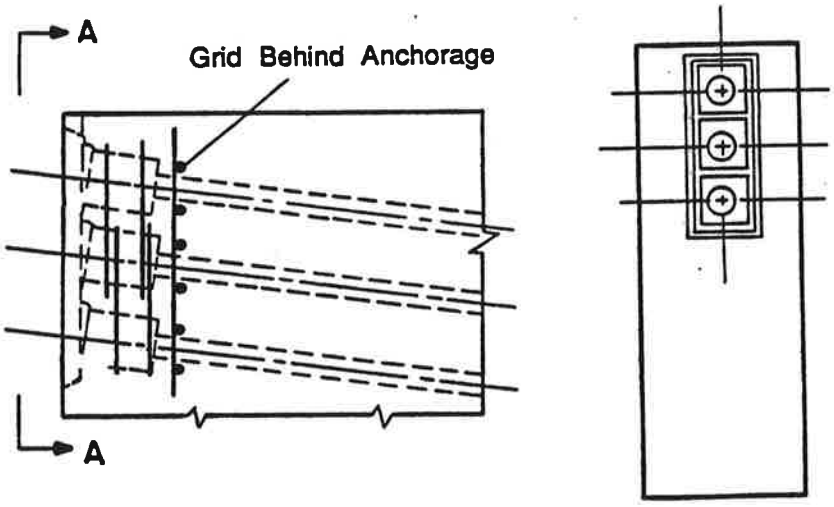

Figure B.2 Eccentric end anchorage.

Figure B.3 Transverse slab anchorage

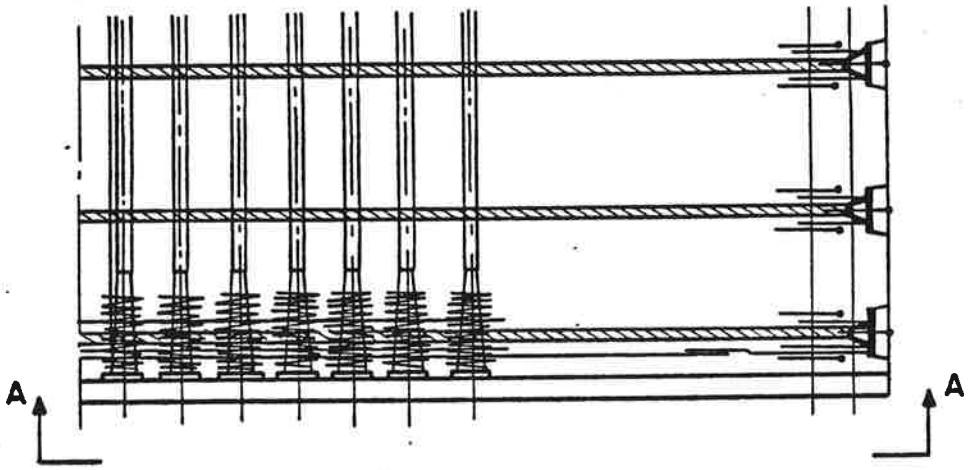

Figure B.4a Longitudinal and transverse deck tendons.

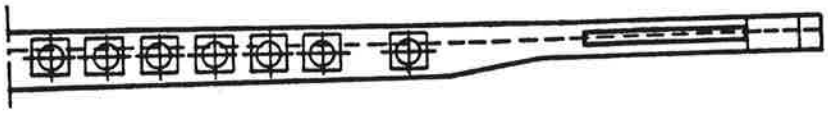

Figure B.4b Section A-A longitudinal deck tendons.

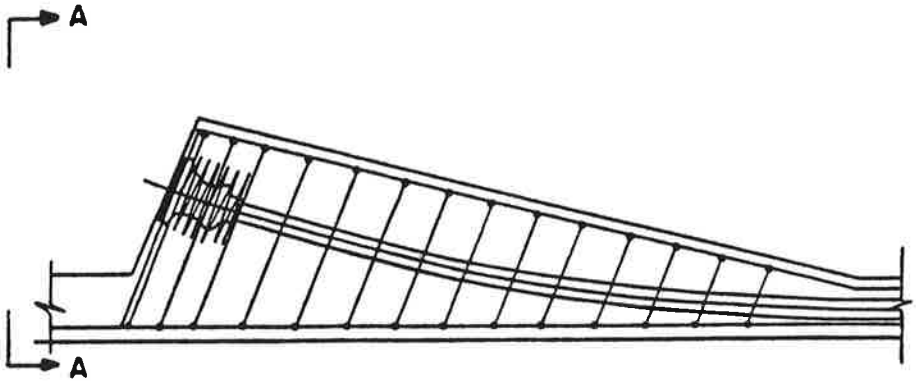

Figure B.5a Corner blister.

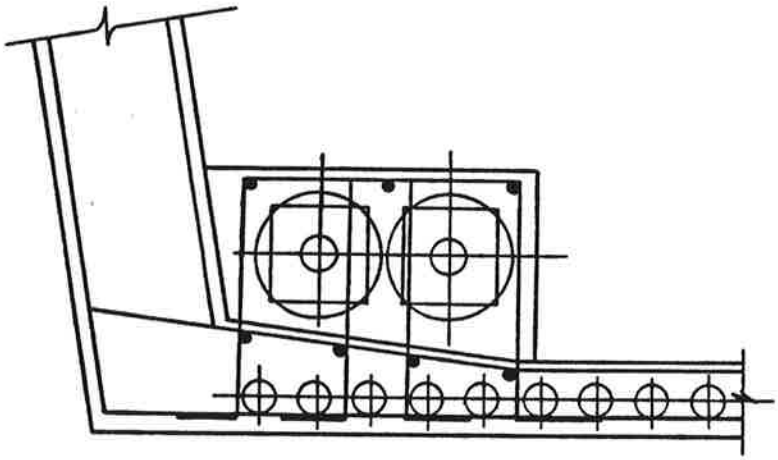

Figure B.5b Section A-A corner blister.

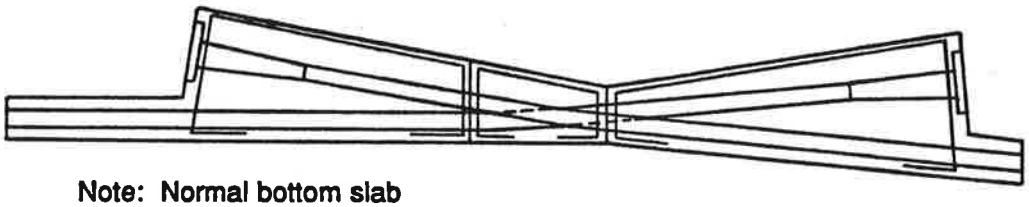

Note: Normal bottom slab
reinforcing not shown

Figure B.6 Double direction blister.

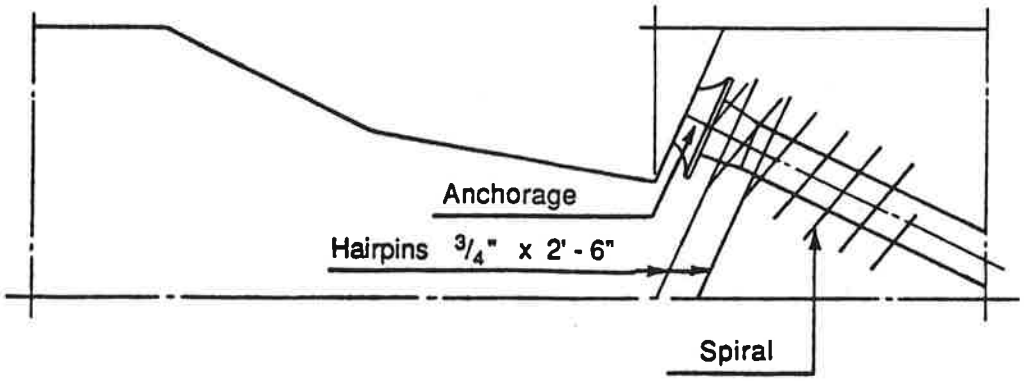

Figure B.7 Recessed deck pocket.

4. Diaphragm - End or transverse anchors (Figs. B.8 and B.9)

5. Rib - End or interior anchors (Fig. B.10 and B.11)

b) Number,

1. Single anchor

2. Multiple anchors

c) Supplemental Reinforcement, or

1. Orthogonal (Figs. B.1, B.2)

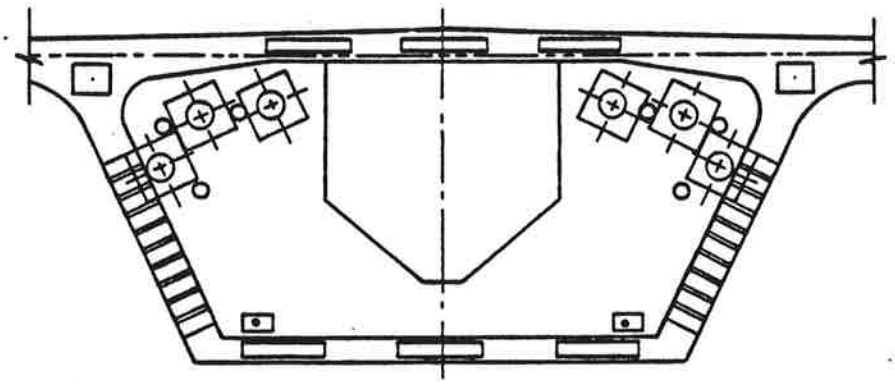

Figure B.8 Longitudinal anchorages in diaphragm.

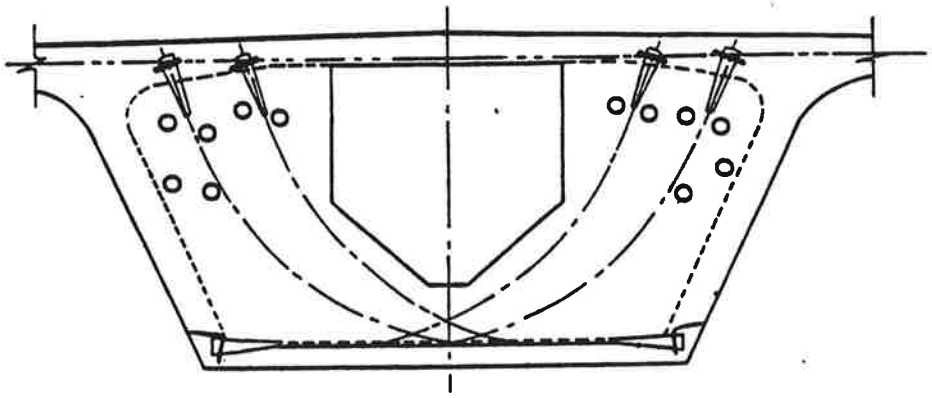

Figure B.9 Transverse post-tensioned diaphragm.

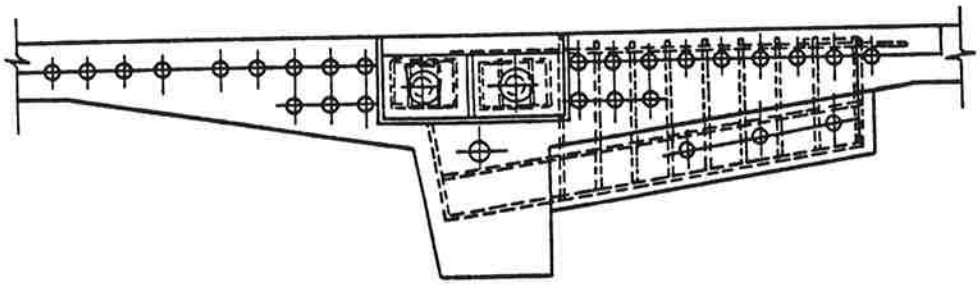

Figure B.10 End blister and deck anchorages.

2. Spiral (Fig. B.4a)

3. Mixture of orthogonal and spiral (Fig. B.5a)

4. No reinforcement specified

d) Type of Tendon Layout.

1. Concentric (Fig. B.1)

2. Eccentric (Fig. B.2)

3. Straight (Fig. B.4)

4. Curved (Fig. B.5)

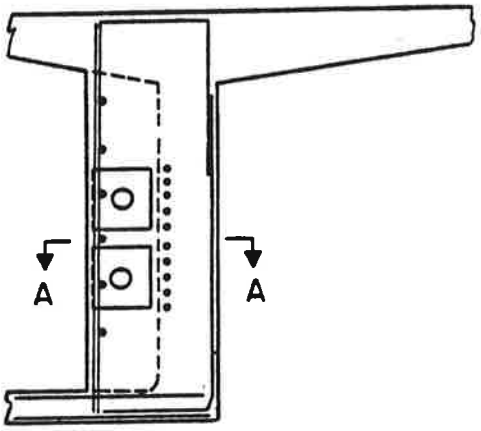

Figure B.11a Multiple rib anchorage

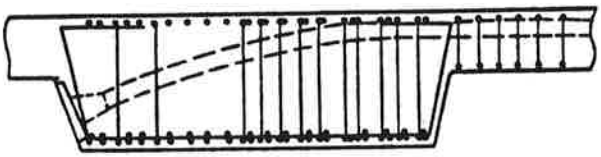

Figure B.11b Section A-A multiple rib anchorage.

5. Deviation: Horizontal (Fig. B.11) and Vertical (Fig. B.1)Each response was critically examined and the general applications classified using this system. Since respondents had submitted only sample details, the occurrence in a project was counted as a single unit whether the project used that anchorage application once or one hundred times in multiple girders and spans. The detailed tabulations according to these categories are given in Tables B.1 and B.2.

The plans that were sent were dominated by multiple end anchors (Figs. B.1 and B.2) and multiple anchor blisters (Fig. B.5), with very few anchorage zones having just single anchors. Since the plans that were sent were only small portions of all the plans of a bridge, single anchorages could still be in extensive use. However, the respondents' concern was clearly with multiple anchorages. Besides the different applications, locations, and number of anchorages, there were many other variables. Table B.1 also shows the number of anchors that utilize either orthogonal, spiral, or mixed supplemental reinforcement. The number of plans showing mixed supplemental reinforcement was very small, and the rest of the plans were divided evenly between orthogonal and spiral reinforcement. Another major variable was the angle of inclination of the anchor. For end anchors, the range in deviation from the vertical was 6 to 25 degrees; while the angular deviation of the blisters ranged from 3 to 22 degrees. Table B.2 shows that, in most cases, the anchor has an initial inclination and that, in many cases, the tendon is not curved in the anchorage zone.

Table B.1 Frequency of anchorage applications submitted by respondents.

Application Type	Number of Terminating Tendons in Anchorage Zone		Supplemental Reinforcement			
	Single	Multiple	Orthogonal	Spiral	Mixed	None Specified
Beam or Slab						
End	0	19	6	6	4	3
Transverse	0	8	3	3	0	2
Interior	0	0	0	0	0	0
Blister						
End	1	3	2	2	0	0
Interior	4	15*	7	10	0	2
Recess Pocket	2	0	0	2	0	0
Diaphragm						
End	0	17	9	8	0	0
Transverse	0	5	0	2	1	2
Rib						
End	0	1	1	0	0	0
Interior	0	2	2	0	0	0

*Two of these applications were double direction blisters.

Table B.2 Frequency of tendon characteristic submitted by respondents.

Application Type	Anchorage Zone Location		Anchorage Zone Profile		Initial Deviation		
	Concentric	Eccentric	Straight	Curved	Horiz.	Vert.	None
Beam or Slab							
End	6	13	12	7	0	14	5
Transverse	8	0	8	0	1	0	7
Blister							
End	–	–	2	2	1	2	1
Interior	–	–	7	12	4	13	2
Recess Pocket	–	–	2	0	0	2	0
Diaphragm							
End	6	11	8	3*	3	7	7
Transverse	1	4	2	3	1	4	0
Rib							
End	0	1	0	1	1	0	0
Interior	1	1	1	1	1	1	0

*Some drawings did not give enough detail to determine.

In addition to the geometry of the anchor and the reinforcement, most plans also include stressing instructions. The majority of the stressing instructions came in the form of a minimum concrete strength at the time of stressing, maximum tendon stress levels, and a minimum age of concrete at the time of stressing. Also, instructions were often given to indicate if a specific stressing sequence was assumed in the design and was to be followed in construction. Instructions were frequently given regarding the maximum eccentricity of prestress forces during the various stages of intermediate stressing of multiple tendons, the relation between stressing sequences on adjacent girders, and the necessity of jacking from both ends to minimize friction losses and equalize stress levels.

Besides submitting example plans, many respondents provided thoughtful and informative answers to the questions. Many respondents stated that they had no problems designing anchorage zones but added that, in most cases, they used guidelines in addition to AASHTO. In the case of foreign respondents, they used their more effective national codes. One response said, "The AASHTO post-tensioning anchorage specifications are completely out of date. We design based on CEB/FIP and/or PTI published recommendations and anchorage stresses based on Guyon's theories." Many utilize the classical theories developed by Guyon and Leonhardt. Several did not feel that the use of only orthogonal reinforcement was adequate and regularly require the use of spirals. One response stated that they used spiral confining reinforcement unless there was insufficient room, then they used layers of mat reinforcement. Several respondents said that they order full-scale tests of the anchorage zone if there was any question in the design of the reinforcement.

One question asked whether there is any situation where no special consideration had to be given to the post-tensioning design. One respondent said that the only anchorage not requiring special consideration are anchors in large diaphragms. Another said, "Post-tensioning details are given the utmost care and attention, perhaps more than any other portion of the structure." A quote that may represent the thoughts of many respondents is that, "Previous experience from jobs that worked well is certainly the best but is not worth a damn in court..."

Several responses mentioned failures but most were attributed to poor concrete or misplaced reinforcement. One response attributed excessive cracking to an incorrect stressing sequence in which large moments were developed. A few failures were caused by the lack of proper containment reinforcement around the anchorage zone.

Some additional comments concerned the limit state guidelines. A question that is very important is what type of safety factor should be used in design. One response said that a safety factor of at least three should be used against crushing and at least 2 1/2 for all other anchorage zone design procedures. Most responses indicated relatively little thought as to the proper safety level regarding strength or cracking. Another major limit state concern is the question of what amount of cracking should be allowed at service loads, if any. The range for allowable crack widths given in the responses was 0.004 inches to 0.01 inches.

Besides providing information on typical details being used in post-tensioned bridge anchorage zones, the survey clarified and dramatized the types of application problems that designers are encountering. It was apparent that American design criteria are fragmented, limited, and not well understood. Studies in the technical literature are primarily directed towards single anchorages, whereas applications are almost always of multiple anchorages. Actual tendons are frequently eccentric and inclined, although neither application is treated explicitly in present criteria.

EXHIBIT B1

SURVEY LETTER

Dear Mr.

The University of Texas at Austin is currently working under National Cooperative Highway Research Program sponsorship on Project 10-29, "Anchorage Zone Reinforcement for Post-Tensioned Concrete Girders," which is a direct response to an AASHTO-submitted problem statement reflecting concerns with the present AASHTO criteria (see Enclosure 1). The project's basic objectives project are:

(1) Evaluation of the state-of-the-art for bridge tendon anchorage zone reinforcement techniques.

(2) Exploration of typical applications through physical tests.

(3) Development of improved analytical procedures.

(4) Development of a generalized approach for anchorage zone analysis and proportioning of required reinforcement for both the serviceability (cracking) and strength limit states.

(5) Development of a draft AASHTO Specification revision

For the project to be of the most use to AASHTO, we need early input to make sure that major user concerns are addressed. We hope your organization can inform us of what is being done in design and approval of working drawings for anchorage zones.

We are enclosing a general guideline to define some terms and to point out possible areas of concern regarding post-tensioned anchorage zones. We are interested in your specific concerns and difficulties, as well as your evaluation of items which are of no concern or are really not problems.

You will note that we have subdivided the anchorage zone behavior into two areas, which reflect some difference in responsibilities. The first or local zone is that region that closely surrounds the specific hardware device. In this region the manufacturer or supplier often has a proprietary product and is basically interested in the local behavior. Such questions as effective bearing area and very local confinement immediately around the anchor fall into this classification. While the manufacturer or supplier has the prime responsibility, there may be a need for AASHTO criteria to establish performance requirements or provide checking procedures even for this local problem. The second or general region is the protion of the anchorage zone more remote from the immediate

anchorage hardware device. These are the areas subject to spalling or bursting stresses, where the designer and the constructor must ensure that proper confinement or reinforcment are provided to prevent premature failure or unwanted cracking. There obviously needs to be better AASHTO criteria for these general cases.

Could you send us, at your earliest convenience, at least the following:

(1) A brief statement of problems your organization has encountered in design, checking or inspection of post-tensioned anchorage zones.

(2) A description of any analysis procedures, evaluation criteria or references you use in design or checking anchorage zones.

(3) Any criteria that you may use to judge when no special attention has to be paid to the post-tensioning system.

(4) Any knowledge of specific failures or severe distress in post-tensioned anchorage zones (please include photos or crack pattern sketches).

(5) Sample plans or details of both commonly used and special anchorage applications.

If you indicate, we will be happy to share the results of the project.

We hope that your organization can provide this highly needed input into the AASHTO specification process. The final result will depend to a large extent on the scope and accuracy of the information submitted.

Sincerely yours,

John E. Breen Gregory L Fenves

Project Supervisors

Return all replies to:

David H. Sanders
Ferguson Structural Engineering Laboratory
10100 Burnet Road #24
Austin, TX 78758

AASHTO Post-Tensioning

Anchorage Provisions

Section 8

REINFORCED CONCRETE

(For information only - Section 8 does

not apply to prestressed concrete.)

8.1 APPLICATION

8.1.2 Notations

A_1 = loaded area (Articles 8.15.2.1.3 and 8.16.7.2)

A_2 = maximum area of the portion of the supporting surface that is geometrically similar to and concentric with the loaded area (Articles 8.15-.2.1.3 and 8.16.7.2).

8.15 SERVICE LOAD DESIGN METHOD

(Allowable Stress Design)

8.15.2 Allowable Stress

8.15.2.1 Concrete

Stresses in concrete shall not exceed the following.

8.15.2.1.3 Bearing Stress

The bearing stress, f_b, on loaded area shall not exceed 0.30 f'_c

When the supporting surface is wider on all sides than the loaded area, the allowable bearing stress on the loaded area may be increased by $\sqrt{A_2 / A_1}$, but not by more than 2.

When the supporting surface is sloped or stepped, A_2 may be taken as the area of the lower base of the largest frustrum of the right pyramid or cone contained wholly within the support and having for its upper base the loaded area, and having side slopes of 1 vertical to 2 horizontal.

When the loaded area is subjected to high edge stresse due to deflection or eccentric loading, the allowable bearing stress on the loaded area, including any increase due to the supporting surface being larger than the loaded area, shall be multiplied by a factor of 0.75.

8.31 MECHANICAL ANCHORAGE

8.31.1 Any mechanical device shown by tests to be capable of developing the strength of reinforcement without damage to concrete may be used as anchorage.

8.31.2 Development of reinforcement may consist of a combination of mechanical anchorage plus additional embedment length of reinforcement between point of maximum bar stress and the mechanical anchorage.

Section 9

PRESTRESSED CONCRETE

9.1 APPLICATION

9.1.3 Definitions

End Anchorages – Length of reinforcement, or mechanical anchor, or hook, or combination thereof, beyond point of zero stress in reinforcement; mechanical devices to transmit pre-stressing force to concrete in a post-tensioned member.

End Block – Enlarged end section of member designed to reduce anchorage stresses.

9.15 ALLOWABLE STRESSES

9.15.2 Concrete

9.15.2.4 Anchorage Bearing Stress

Post-tensioned anchorage

at service load ..... 3.000 psi

(but not to exceed 0.9 f'_c)

9.21 ANCHORAGE ZONES

9.21.1 For beams with post-tensioning tendons, end blocks shall be used to distribute the concentrated prestressing forces at the anchorage. where all tendons are pretensioned wires or 7-wire strand, the use of end blocks will not be required. End blocks shall have sufficient area to allow the spacing of the prestressing steel as specified in Article 9.25. Preferably, they shall be as wide as the narrower flange of the beam. They shall have a length at least equal to three-fourths of the depth of the beam and in any case 24 inches. In post-Tensioned members, a closely spaced grid of both vertically and hortzontal bars shall be placed near the face of the end block to resist bursting stresses. Amounts of steel in the end grid should follow recommendations of the supplier of the anchorage. Where such recommendations are not available the amount of steel in the grid shall be designed and shall consist of at least No. 3 bars on 3-inch centers in each direction placed not more than 1 1/2 inches from the inside face of the anchor bearing plate.

9.21.2 Closely spaced reinforcement shall be placed both vertically and horizontally throughout the length of the end block in accordance with accepted methods of end block stress analysis.

9.21.3 In pretensioned beams, vertical stirrups acting at a unit stress of 20,000 psi to resist at least 4 percent of the total prestressing force shall be placed within the distance of d/4 of the end of the beam, the end stirrups to be as close to the end of the beam as practicable. For at least the distance d from the end of the beam, nominal reinforcement shall be placed to enclose the prestressing steel in the bottom flange. For box girders, transverse reinforcement shall be provided and anchored by extending the leg into the web of the girder.

9.26 POST-TENSIONING ANCHORAGES AND COUPLES

9.26.1 Anchorages, couplers, and splices for bonded post-tensioned reinforcement shall develop at lest 95 percent of the minimum specified ultimate strength of the prestressing steel, tested in an unbonded state without exceeding anticipated set. Bond transfer lengths between anchorages and the zone where full prestressing force is required under service and ultimate loads shall normally be sufficient to develop the minimum specified ultimate strength of the prestressing steel. Couplers and splices shall be placed in areas approved by the Engineer and enclosed in a housing long enough to permit the necessary movements.

When anchorages or couplers are located at critical sections under ultimate load, the ultimate strength required of the bonded tendons shall not exceed the ultimate capacity of the tendon assembly, including the anchorage or coupler, tested in an unbonded state.

9.26.2 The anchorages of unbonded tendons shall develop at least 95 percent of the minimum specified ultimate strength of the prestressing steel without exceeding anticipated set. The total elongation under ultimate load of the tendon shall not be less than 2 percent measured in a minimum gauge length of 10 feet.

9.26.3 For unbonded tendons, a dynamic test shall be performed on a representative specimen and the tendon shall withstand, without failure, 500,000 cycles from 60 percent to 66 percent of its minimum specified ultimate strength, and also 50-cycles from 40 percent to 80 percent of its minimum specified ultimate strength. The period of each cycle involves the change from the lower stress level to the upper stress level and back to the lower. The specimen used for the second dynamic tests need not be the same used for the first dynamic test. Systems utilizing multiple strands, wires, or bars may be tested utilizing a test tendon of smaller capacity than the full size tendon. The test tendon shall duplicate the behavior of the full size tendon and generally shall not have less than 10 percent of the capacity of the full size tendon. Dynamic tests are not required on bonded tendons, unless the anchorage is located or used in such manner that repeated load applications can be expected on the anchorage.

9.26.4 Couplings of unbonded tendons shall be used only at locations specifically indicated and/or approved by the Engineer. Couplings shall not be used at points of sharp tendon curvature. All couplings shall develop at least 95 percent of the minimum specified ultimate strength of the prestressing steel without exceeding anticipated set. The coupling of tendons shall not reduce the elongation at rupture below the requirements of the tendon itself. Couplings and/or couplings components shall be enclosed in housings long enough to permit the necessary movements. All the coupling components shall be completely protected with a coating material prior to final encasement in concrete.

9.26.5 Anchorages, end fittings, couplers, and exposed tendons shall be permanently protected against corrosion.

BRIDGE POST-TENSIONING ANCHORAGE ZONE CLASSIFICATION SYSTEM

A) Anchorage Zone

1) Local
2) General
3) Outside

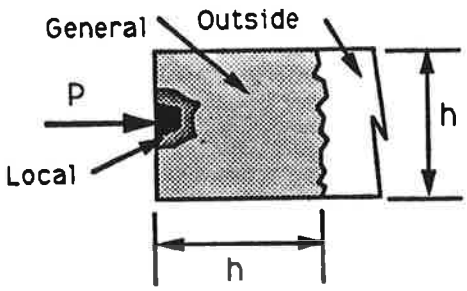

B) Location

1) Direction
   a) Longitudinal
   b) Transverse
   c) Vertical or Inclined

2) Position
   a) Web
   b) Flange
   c) Diaphragm
   d) Deck

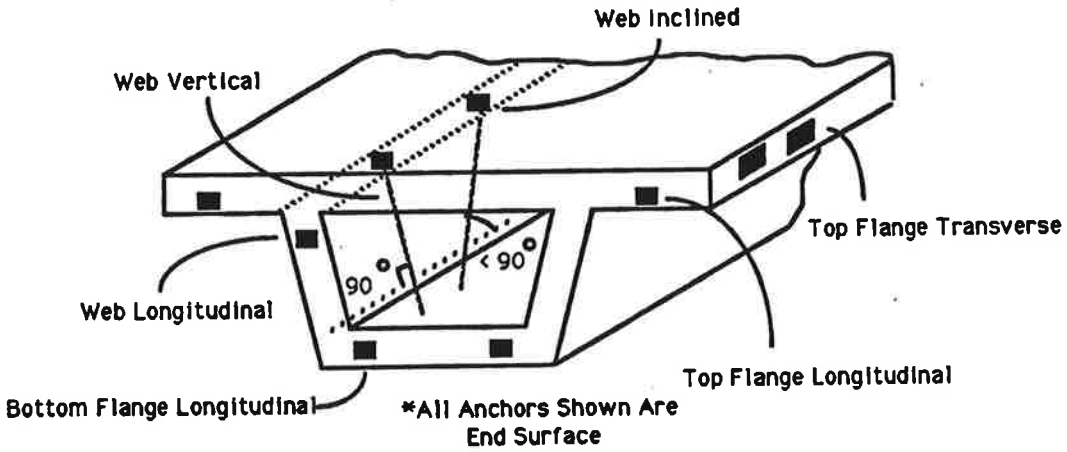

3) Entry
   a) Intermediate or Interior
   b) Blister or Rib
   c) End Surface

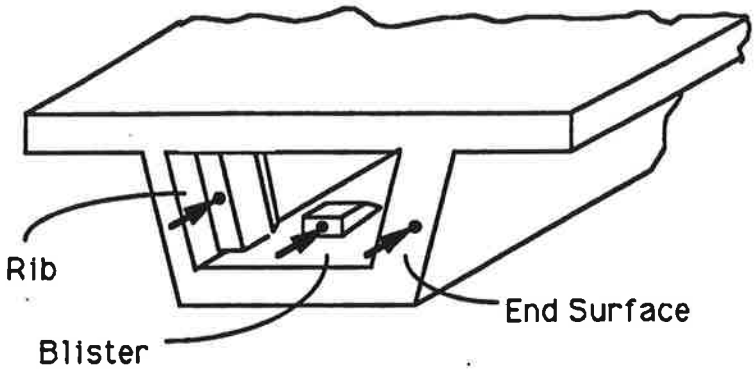

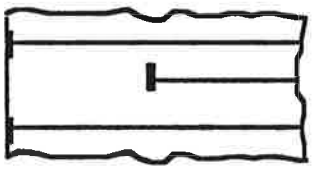

Plan

Interior

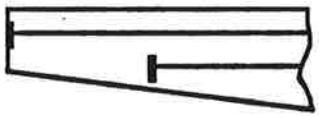

Elevation

C) Geometry

1) Anchorages

a) Number

b) Layout of Multiple Anchorages

1) Spacing between Anchors

2) Spacing between Anchorage Groups

c) Eccentricity

1) Section

2) Element

d) Inclination- Vertical and/or Lateral

e) Proportional Size- Anchor to Effective Confining Concrete(A_1/A_2)

f) Cover

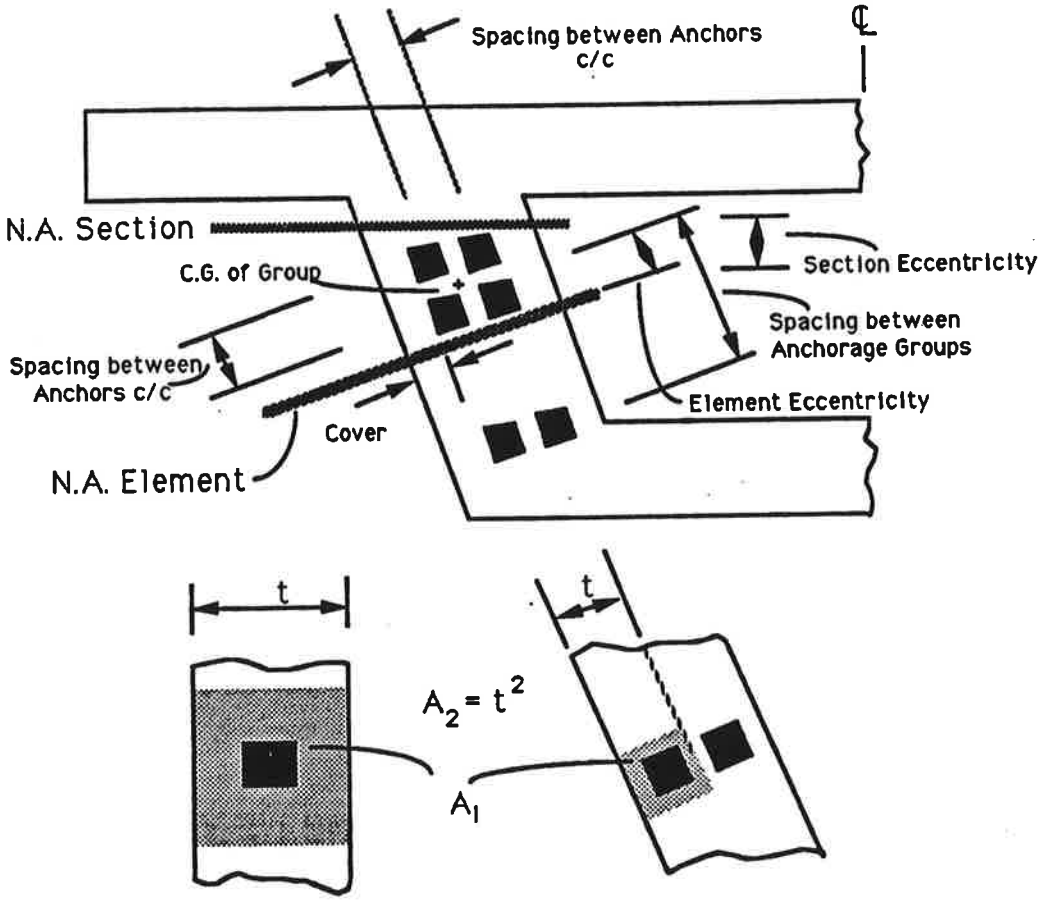

2) Tendon in Anchor Zone

a) Tangent Zone
b) Curvature
c) Number of Strands, Bars or Wires

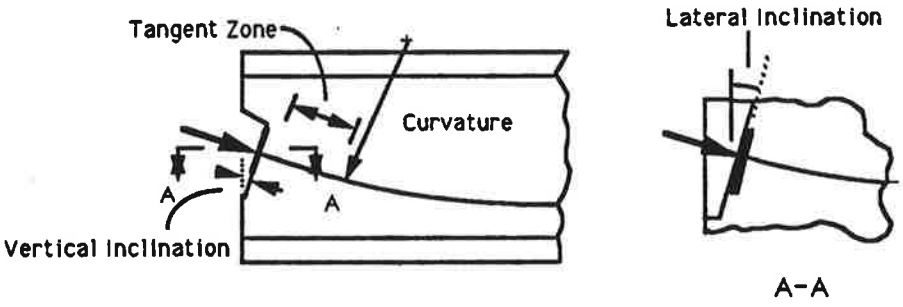

D) Loads

1) Prestressing
   a) Load
   b) Sequence or Staging
2) Other Loads- Magnitude, Angle and Distance from Anchor
   a) Reactions
   b) Applied Forces

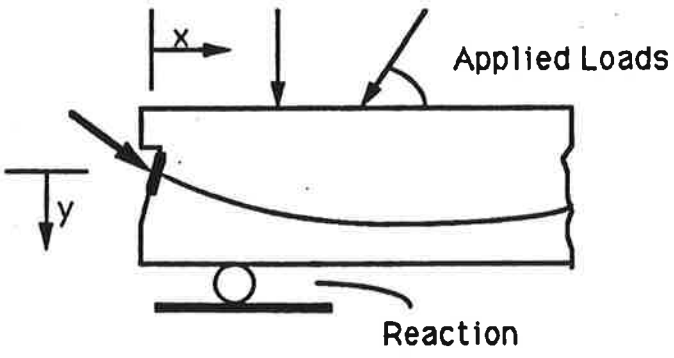

E) Concrete

1) Type
   a) Normal
   b) Lightweight

2) Strength
   a) Initial- at time of prestressing
   b) Final- at 28 days or other specified age

F) Reinforcement-Amount, Layout and Grade

1) Local- Reinforcement Surrounding the Anchorage Device for Splitting and Bearing Stresses(See page 1 for sketch)
   a) Spiral
   b) Orthogonal
   c) Confining Sleeve
   d) Other

2) General- Anchor Zone Reinforcement for Bursting and Spalling Stresses(See page 1 for sketch)
   a) Spiral
   b) Orthogonal
   c) Post-Tensioning- Vertical and/or Transverse
   d) Other

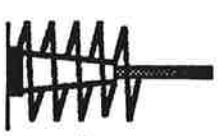

Spiral

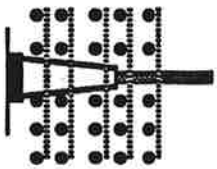

Orthogonal

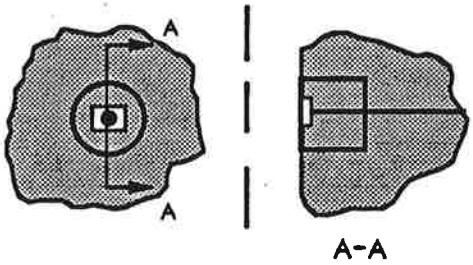

Confining Sleeve

G) Hardware

1) Anchor*
   a) Single Bearing Surface with Trumpet
   b) Multiple Bearing Surface
   c) Flat Bearing Surface
   d) Other

* Fixed End Loop and Strand Anchors, and Couplers excluded from study by NCHRP

Single Bearing Surface with Trumpet

Multiple Bearing Surface

Flat Bearing Surface

2) Grips
   a) Multiple Strand with Single Central Cone
   b) Wedges
   c) Threaded
   d) Button Head
   e) Other

Multiple Strand with Single Central Cone

Wedges

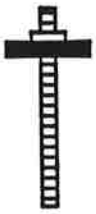

Threaded

Button Head

H) Other Design Criteria

1) Factor of Safety
2) Permissible Crack Width
3) Allowable Tensile Stress

APPENDIX C

DETAILS OF PHYSICAL TEST SPECIMENS

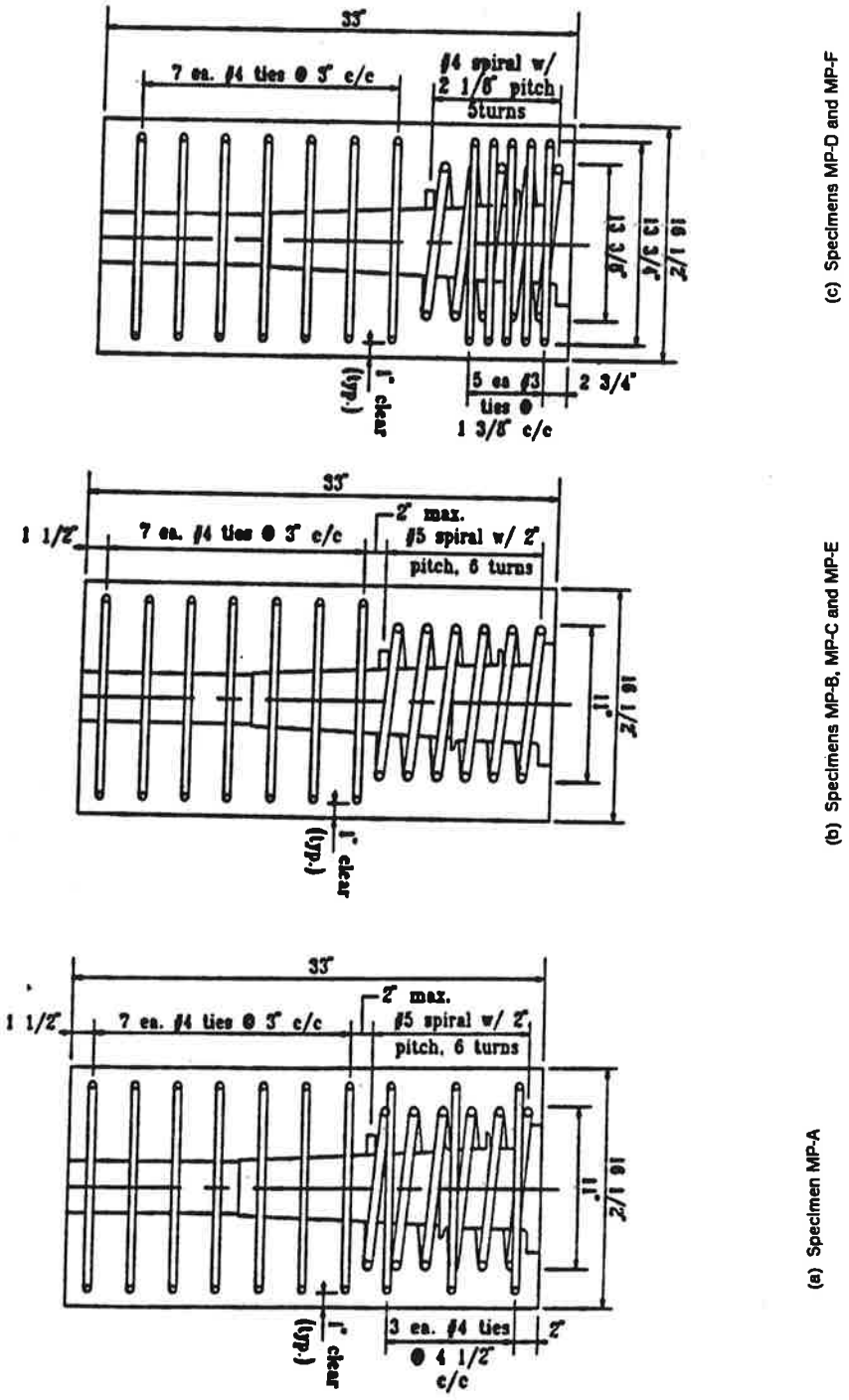

(c) Specimens MP-D and MP-F

(b) Specimens MP-B, MP-C and MP-E

(a) Specimen MP-A

Figure C.1 Series MP Details

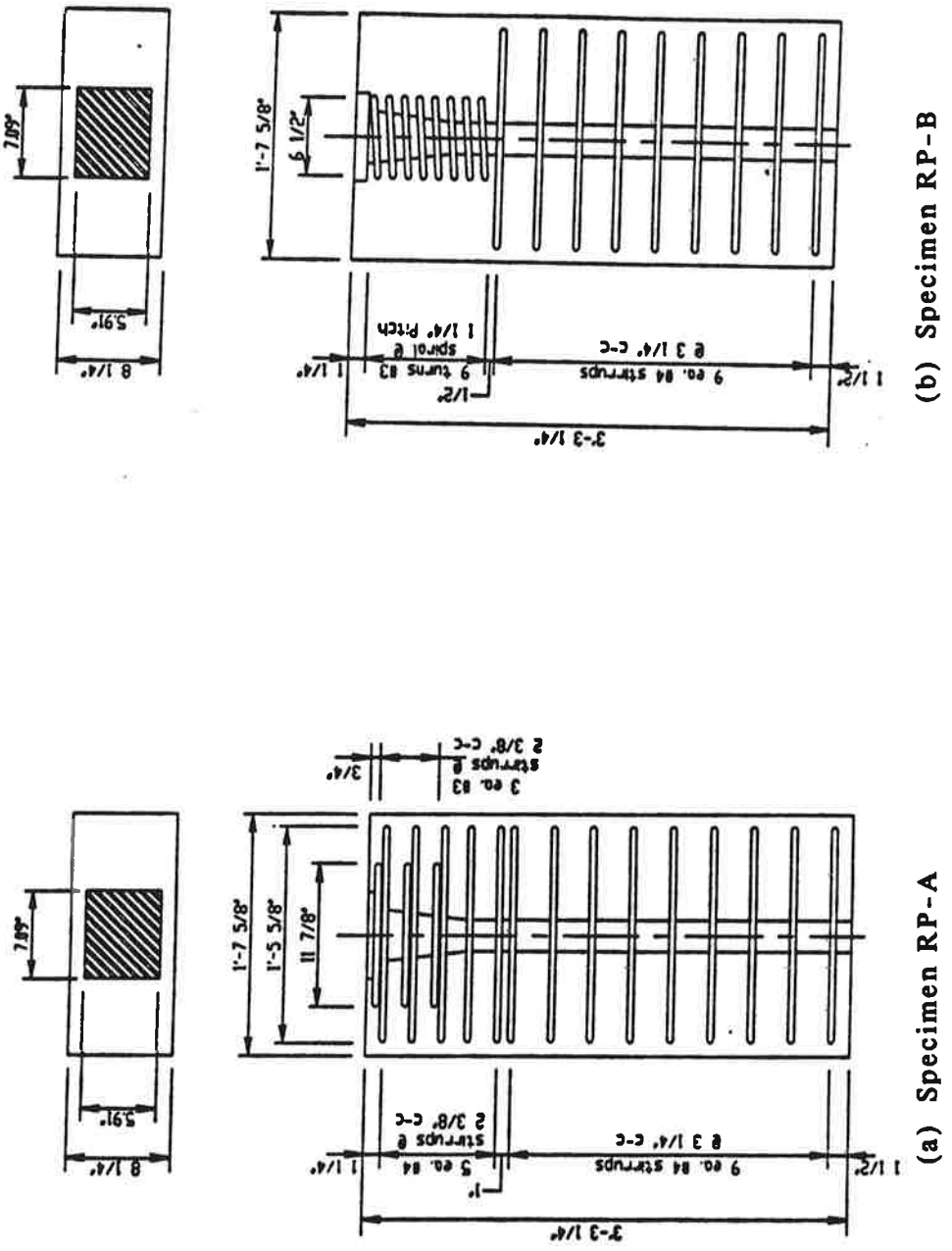

Figure C2 Specimens RP-A and RP-B

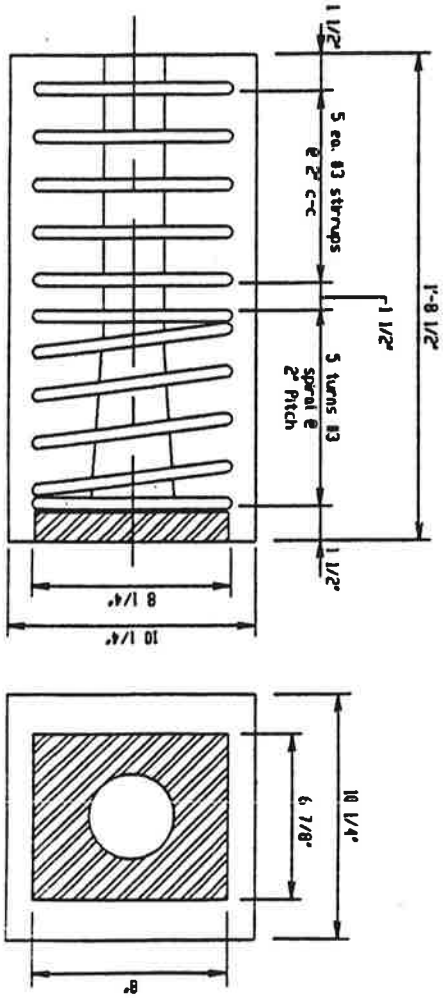

Figure C3 Series LH Details

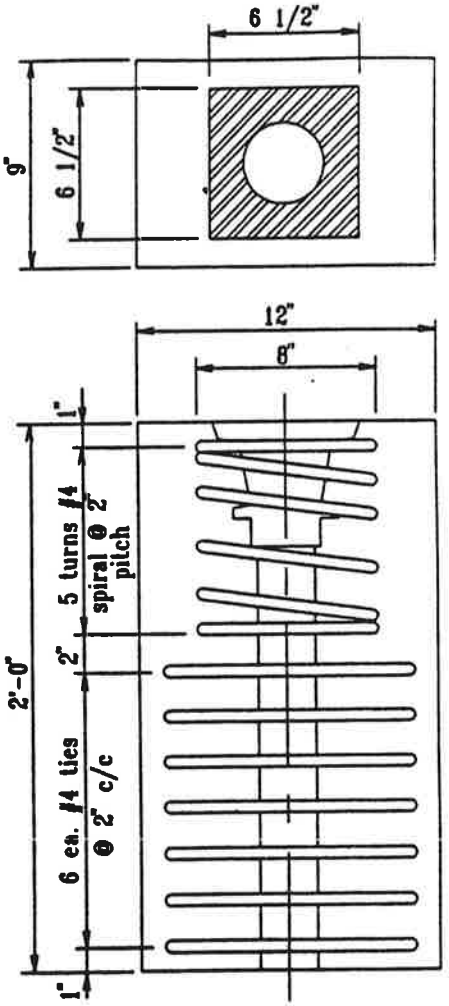

Figure C4 Series MB Details.

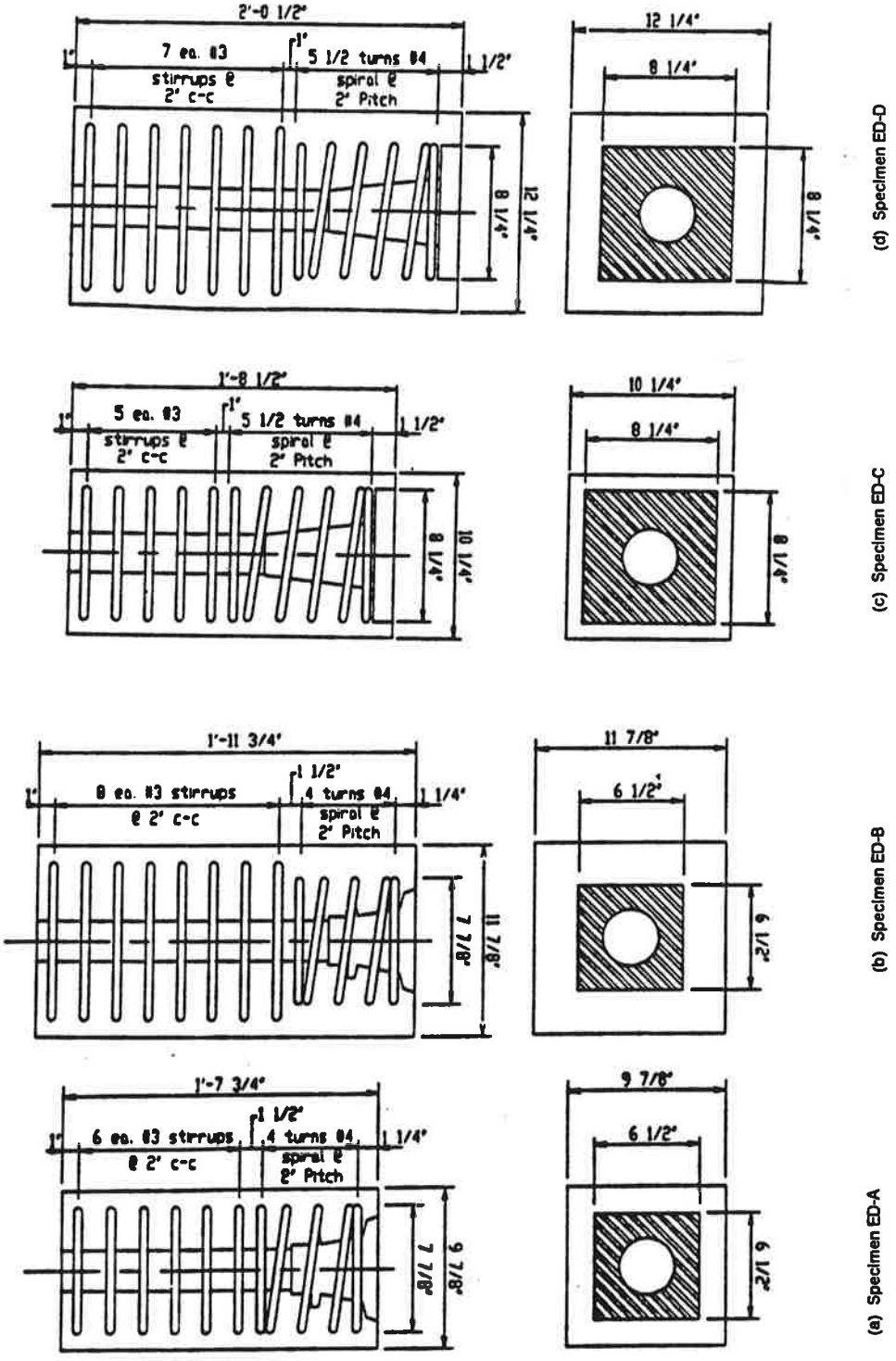

Figure C5 Series ED Details

Figure C6 Series SP Details

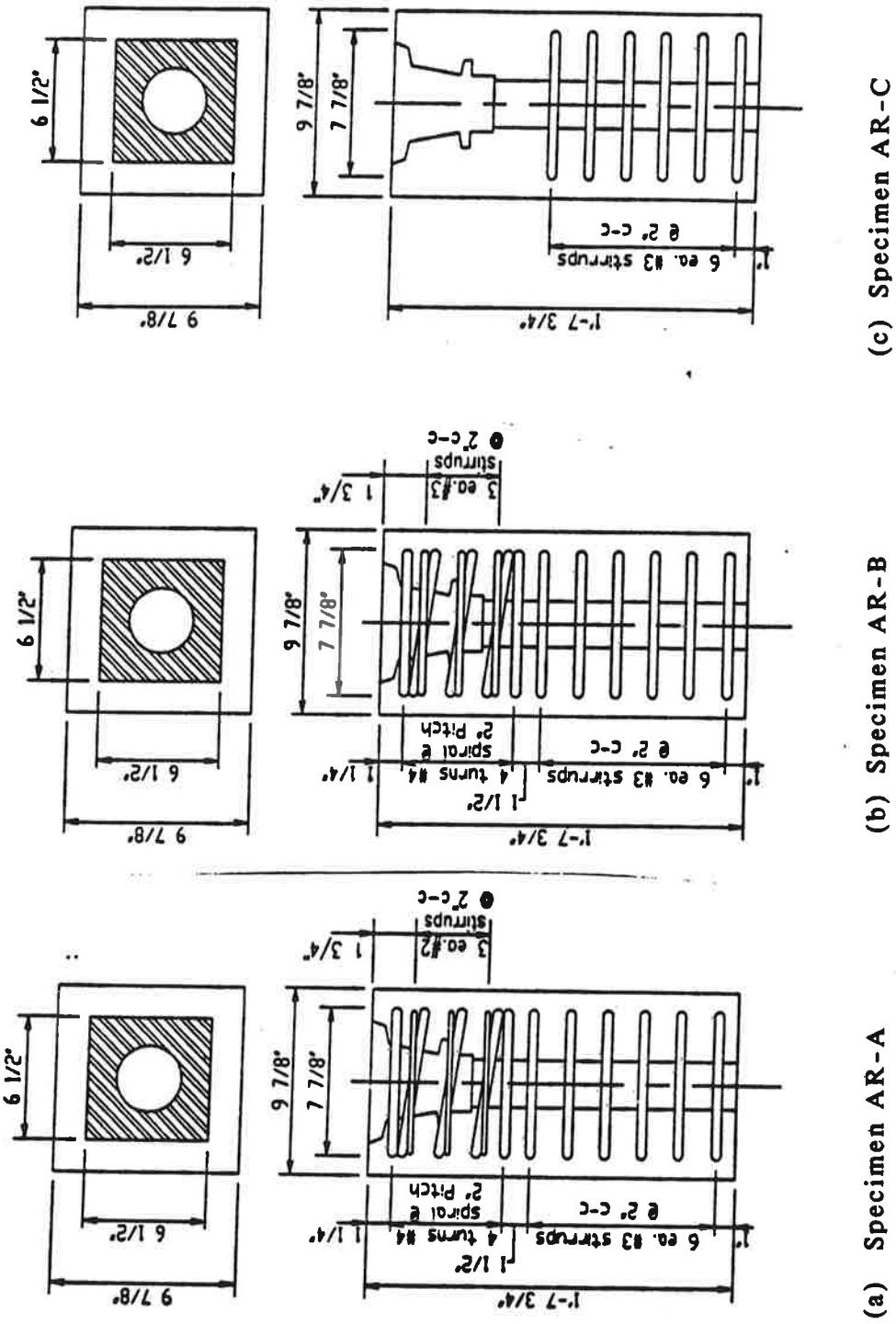

Figure C7 Series AR Details

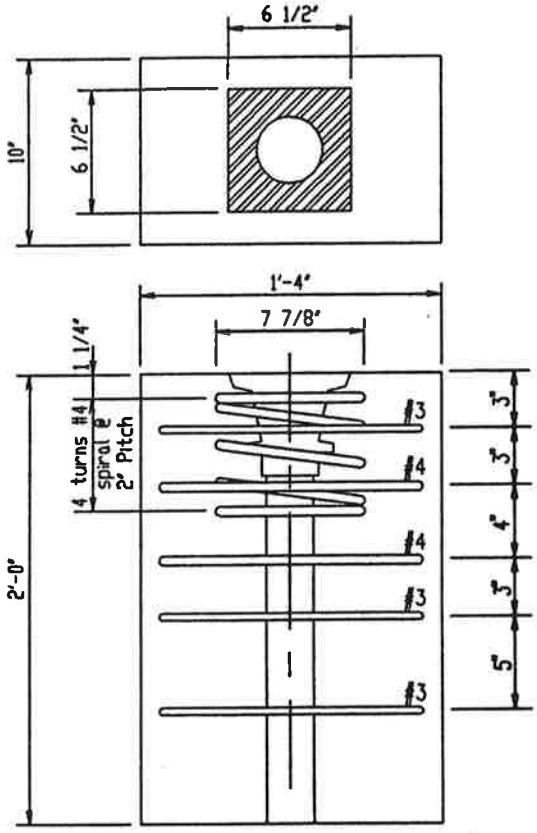

Figure C8 Specimen LG-A Details

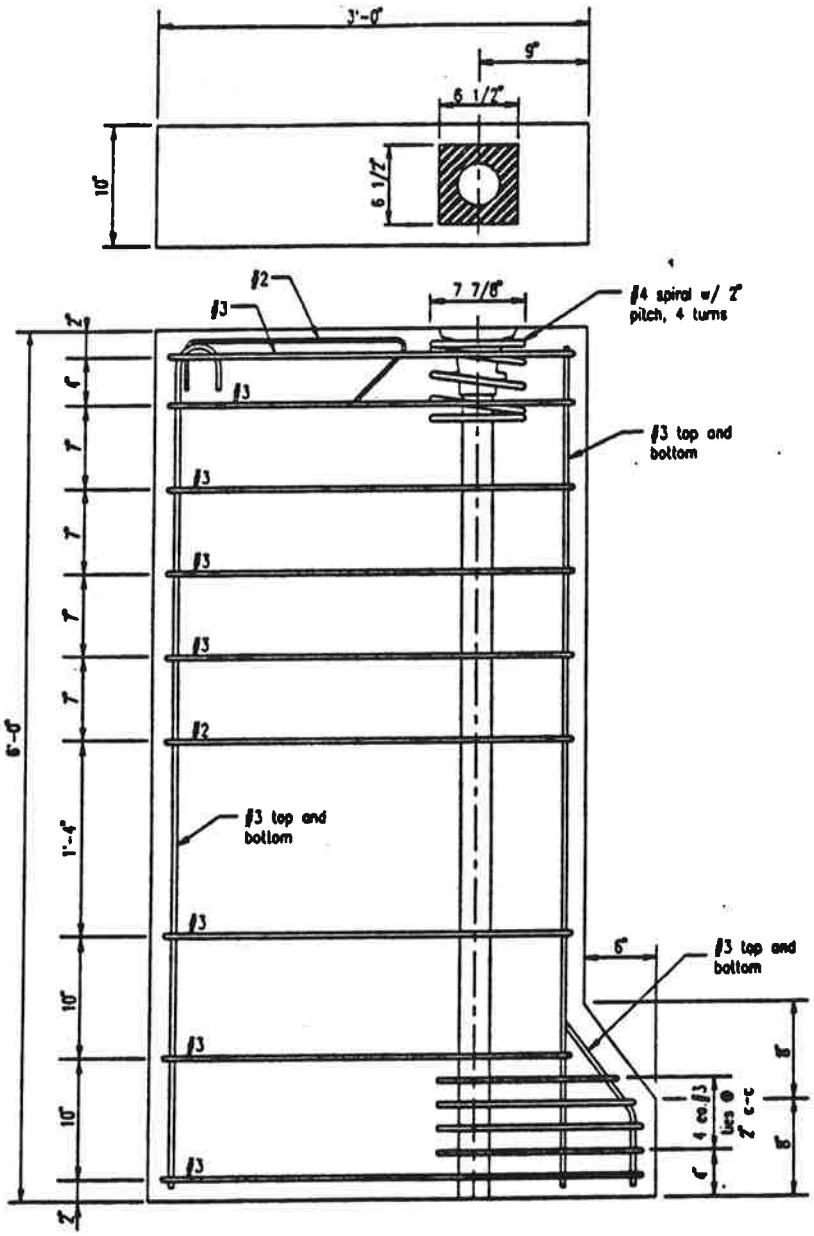

Figure C9 Specimen LG-B Details

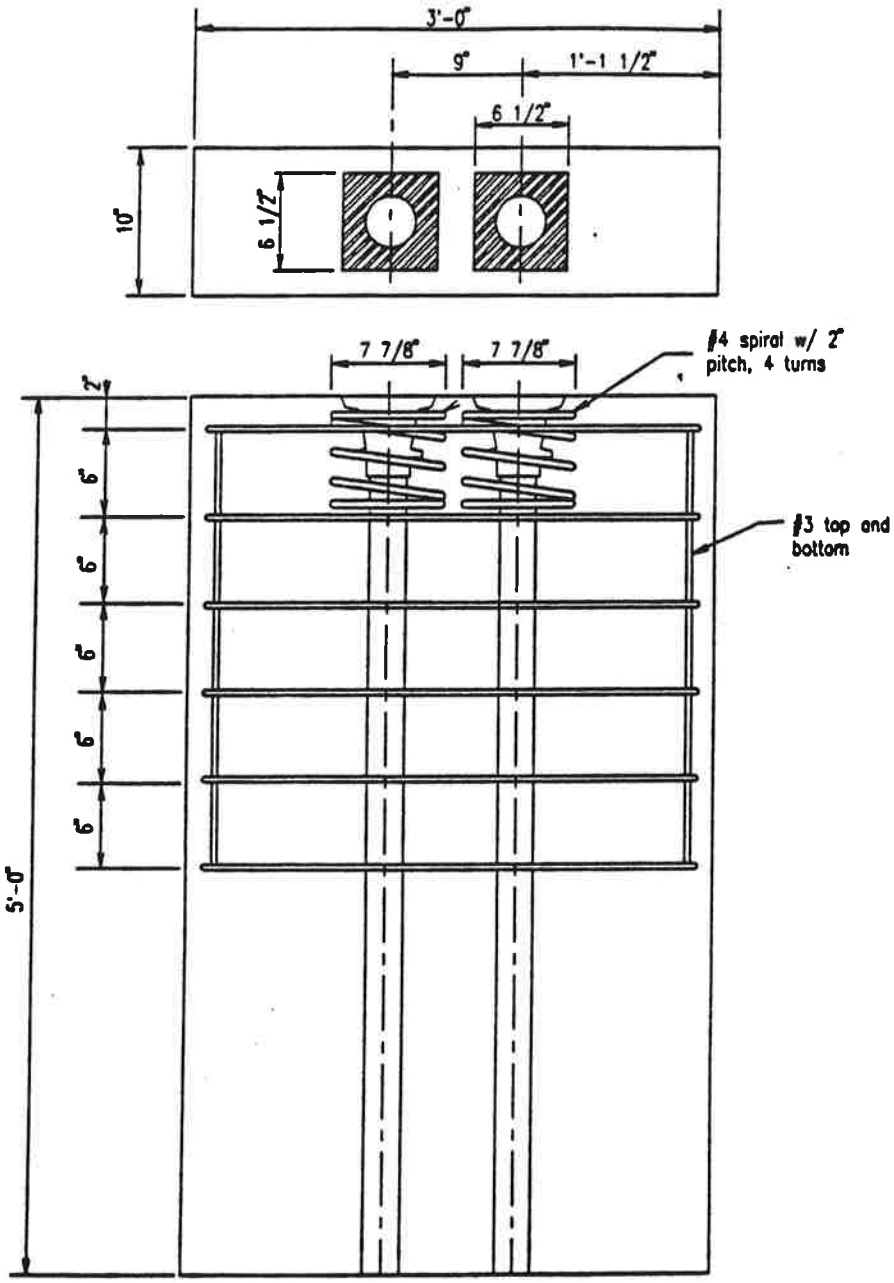

Figure C10 Specimen LG-C Details

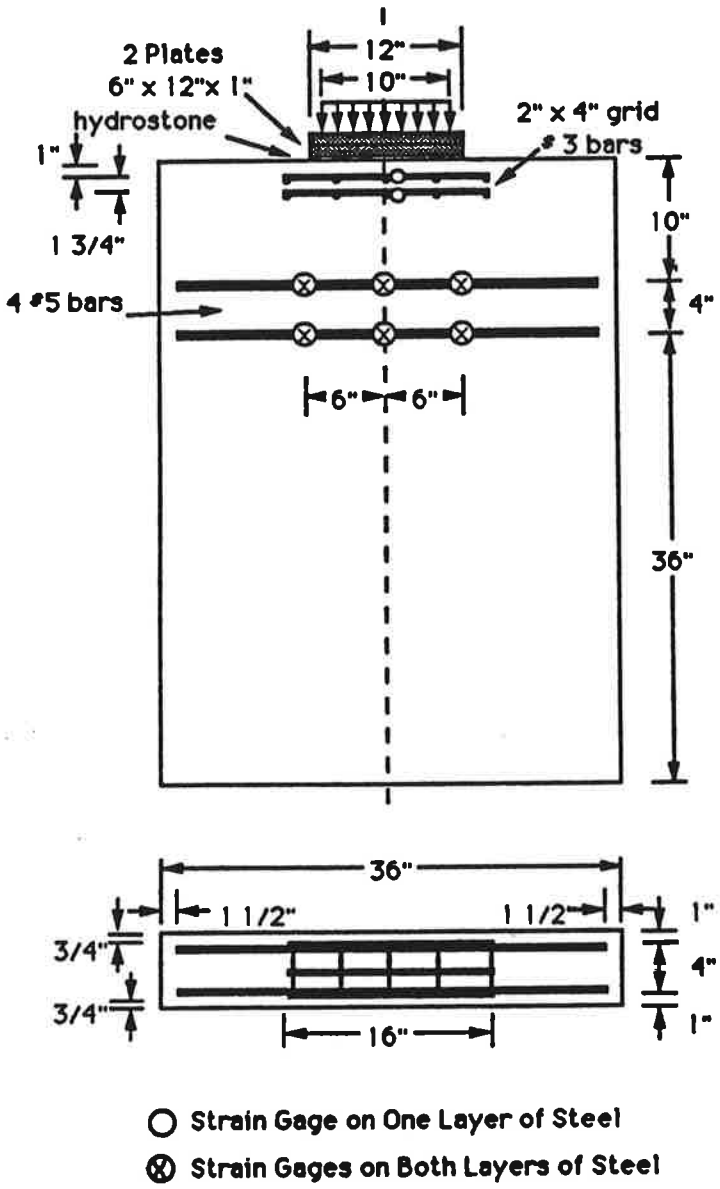

Figure C11 Specimen A1 Detail

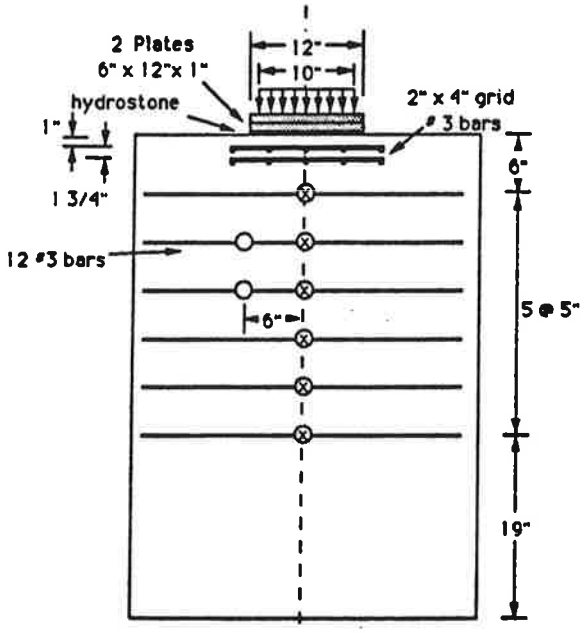

(a) Specimen A2

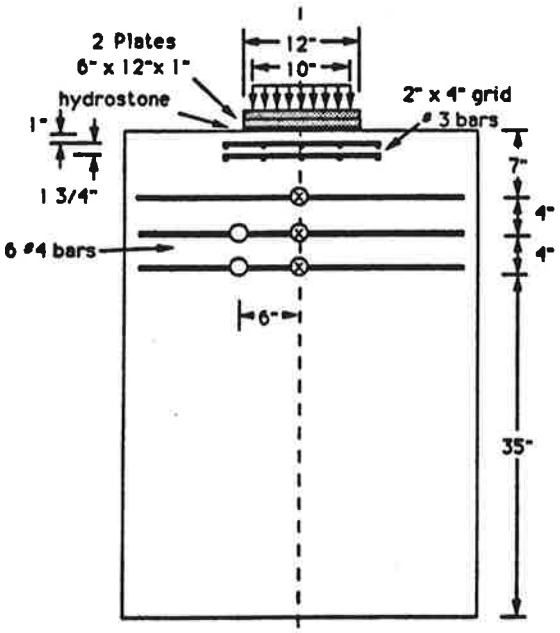

(b) Specimen A3

Figure C12 Reinforcement details for Specimens A2 and A3

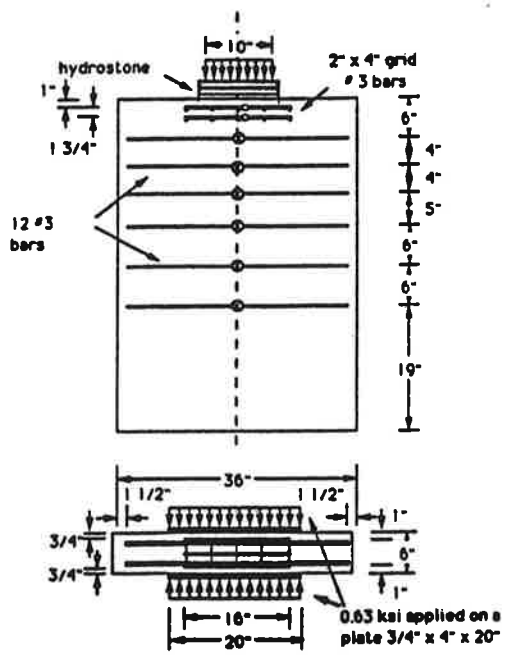

(a) Reinforcement and transverse loads

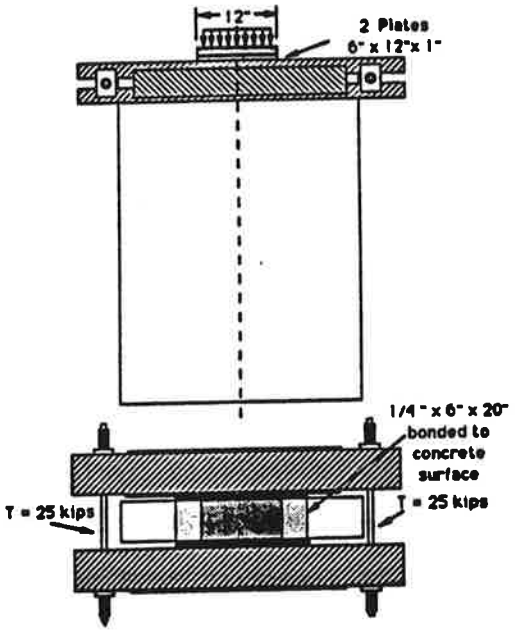

(b) Transverse post-tensioning details

Figure C13 Details for Specimens A4

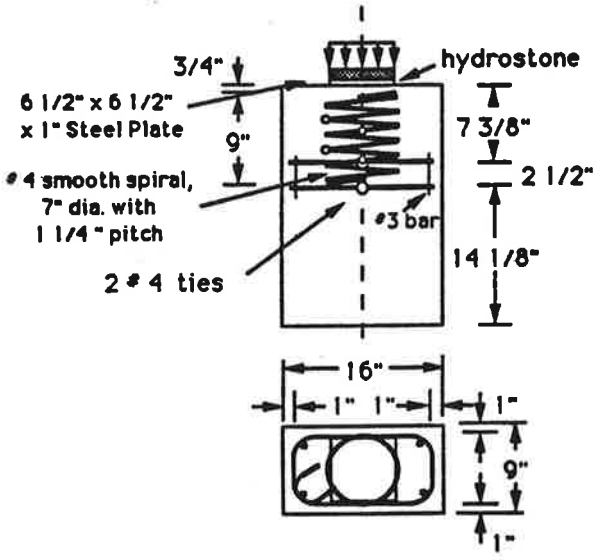

Figure C14 Specimen B1 Detail

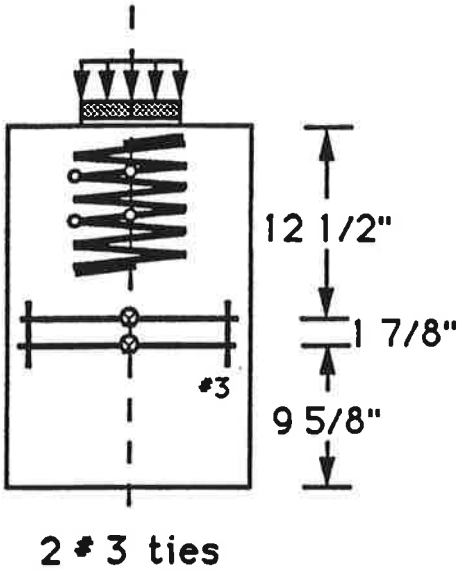

(a) Specimen B2

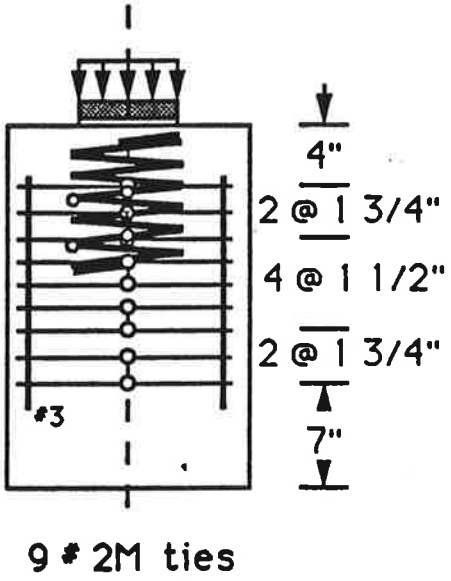

(b) Specimen B3

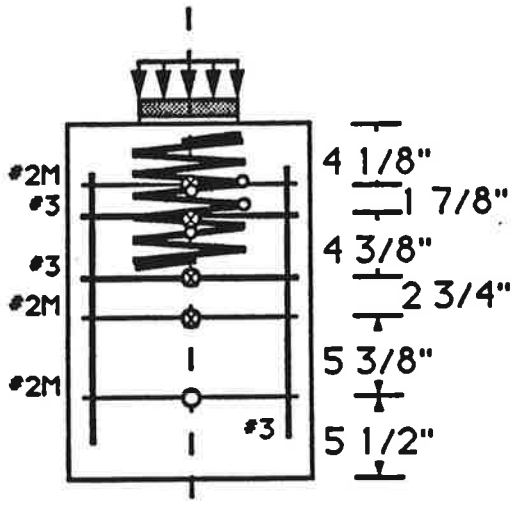

(c) Specimen B4

Figure C15 Details for Specimens B2, B3 and B4

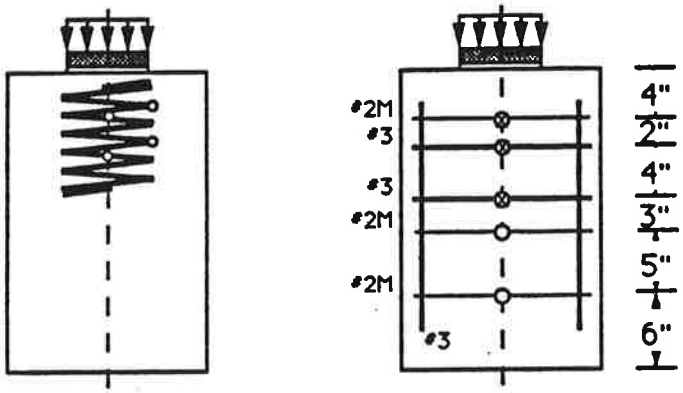

Figure C16 specimen B5 and B6 Details

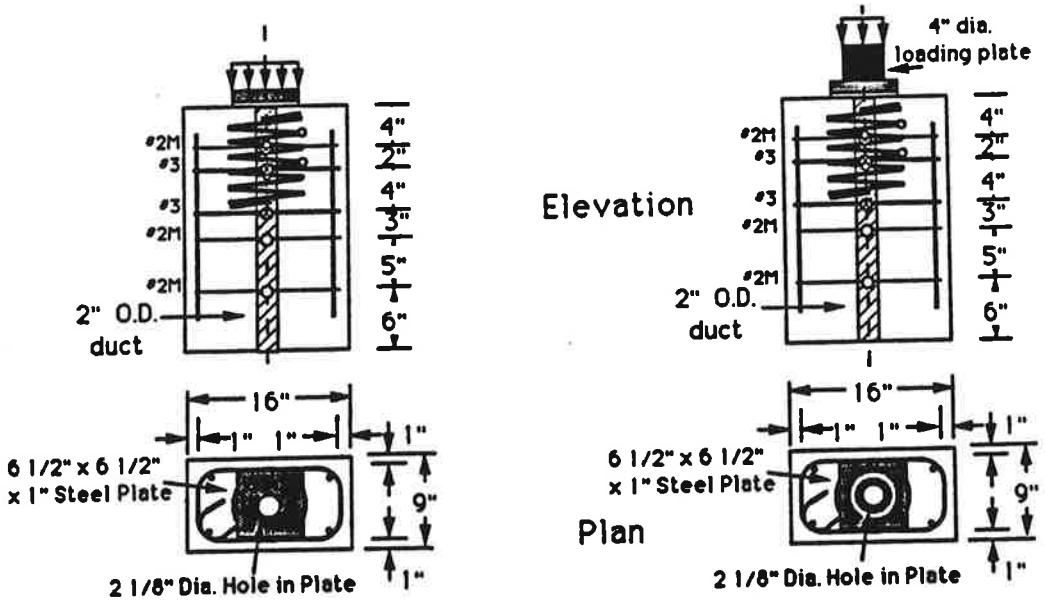

(a) Specimen B7 (b) Specimen B8

Figure C17 Specimens Details for Specimens B7 and B8

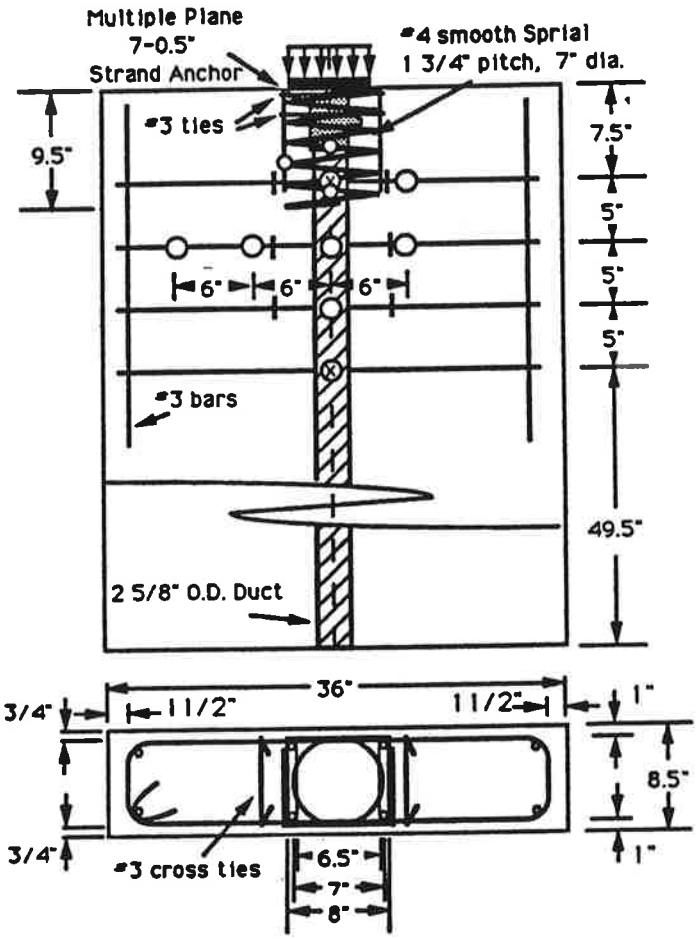

Figure C18 Specimen C1 Detail

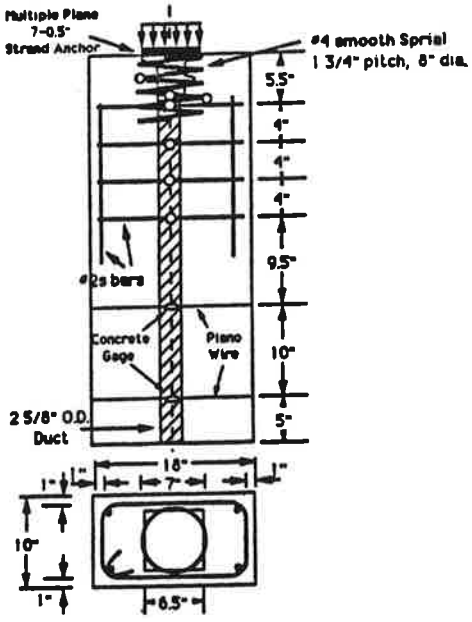

(a) Specimen TPT1

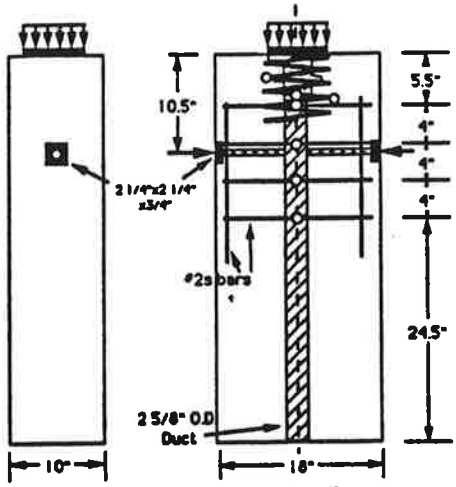

(b) Specimen TPT2

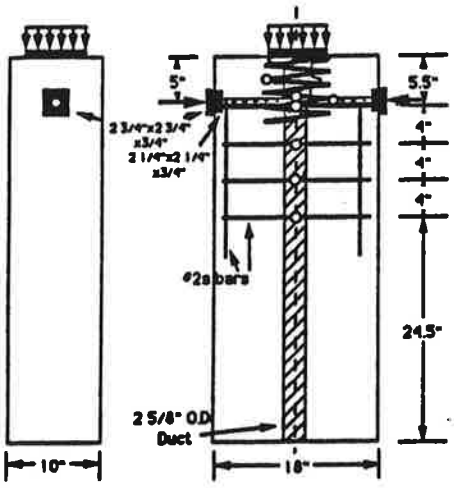

(c) Specimen TPT3

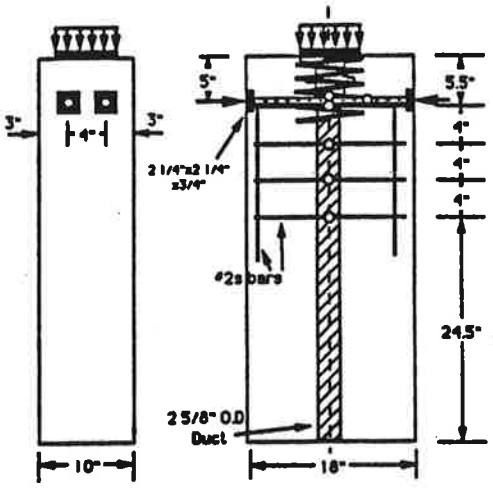

(d) Specimen TPT4

Figure C19 Series TPT Details

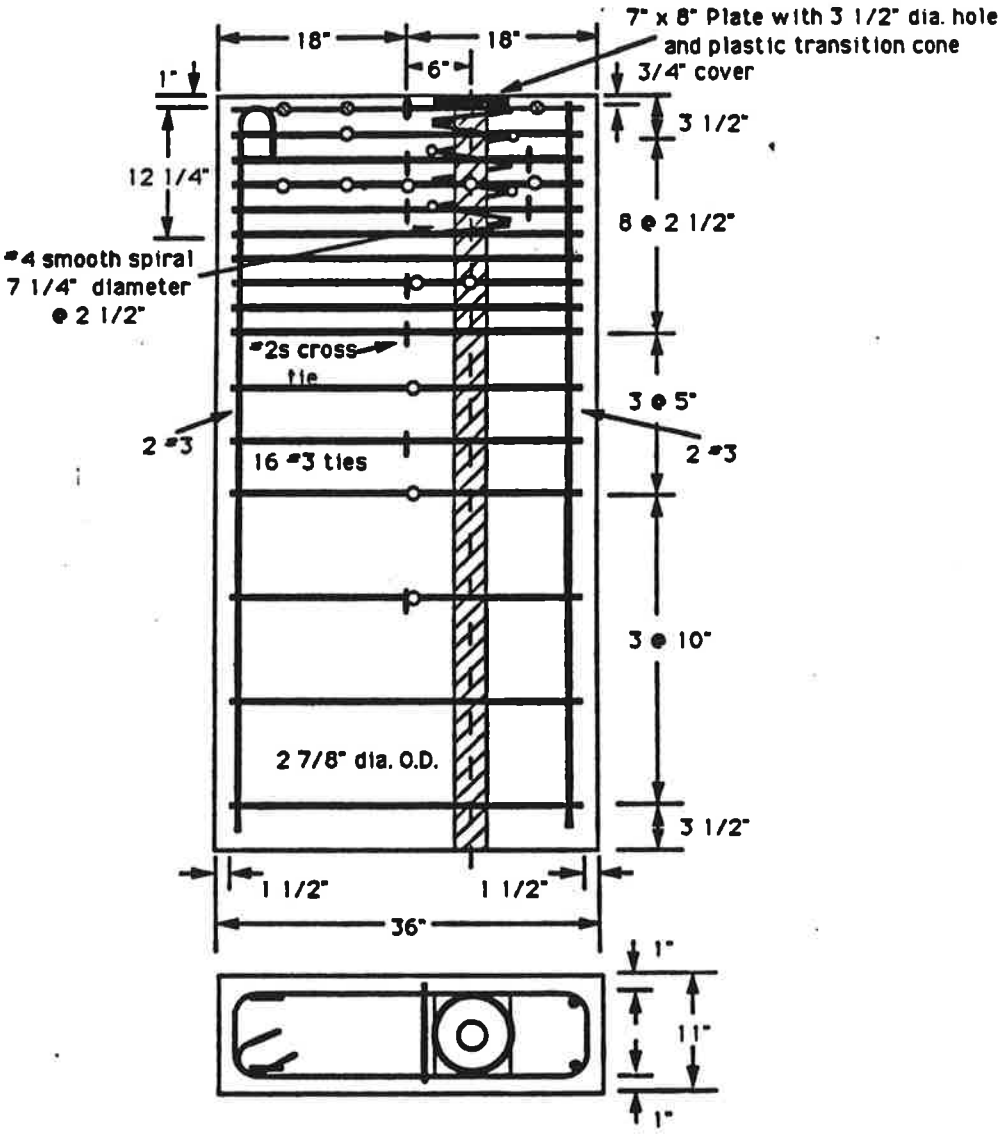

Figure C20 Specimen E1 Details

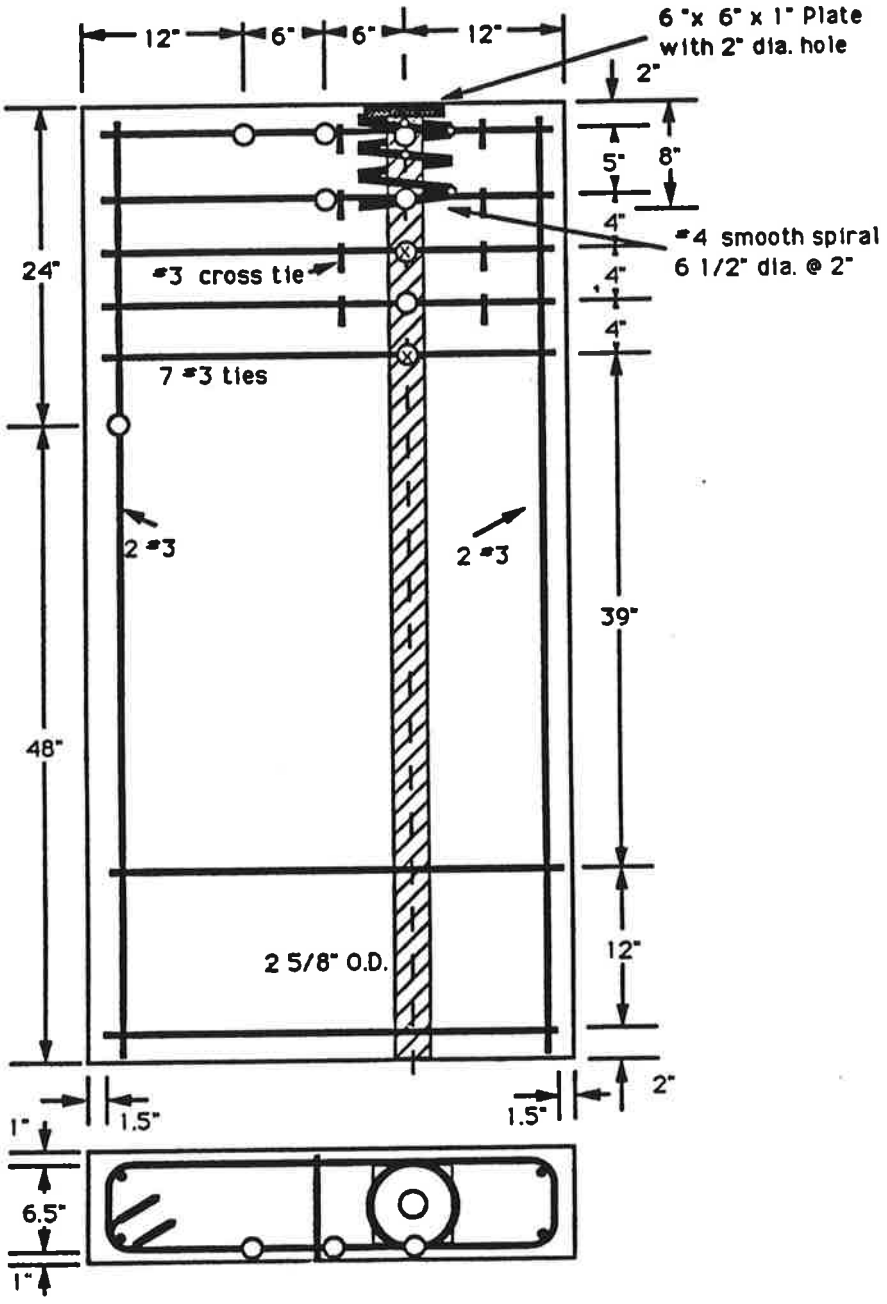

Figure C21 Specimen E5 Details

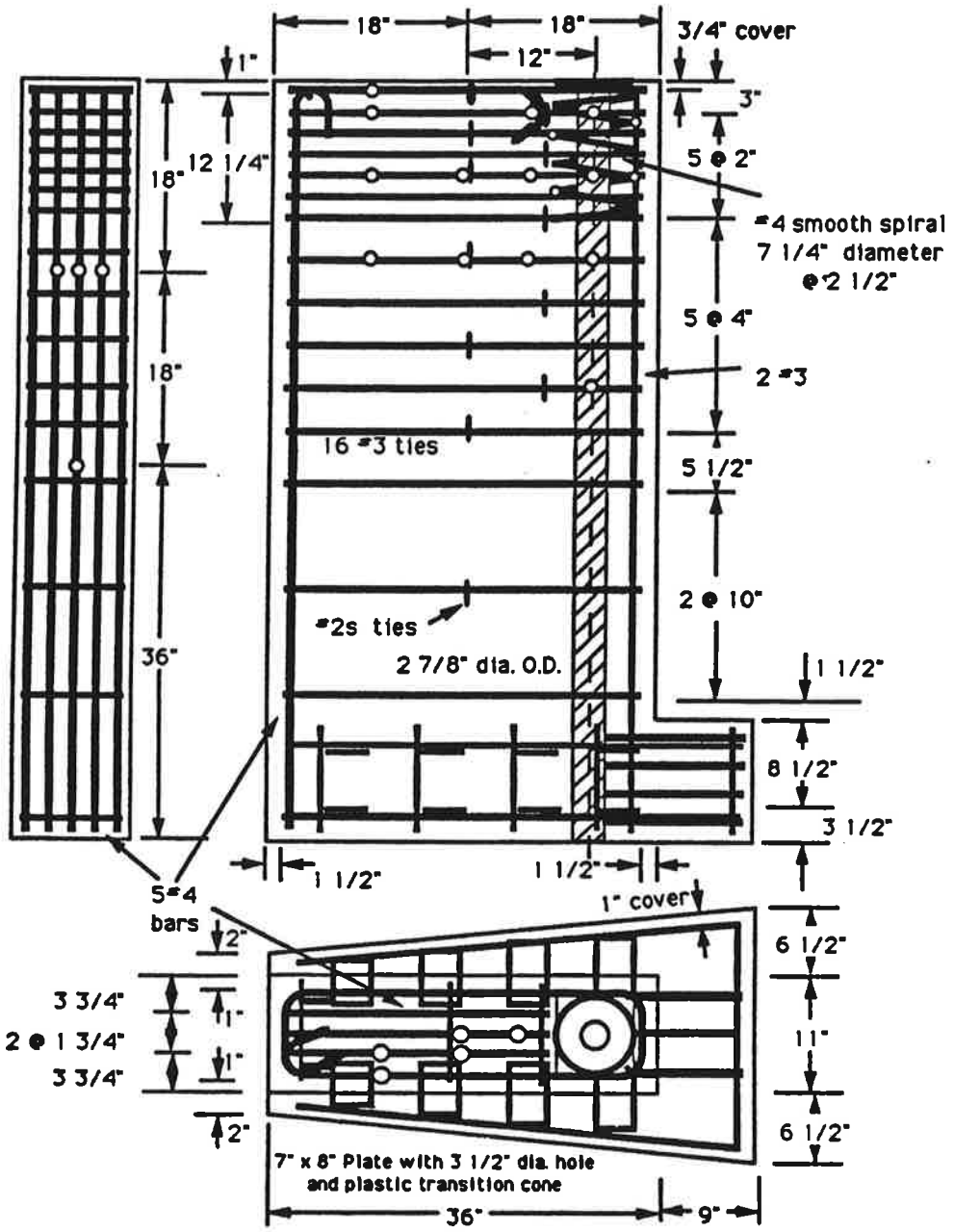

Figure C22 Specimen E2 Details

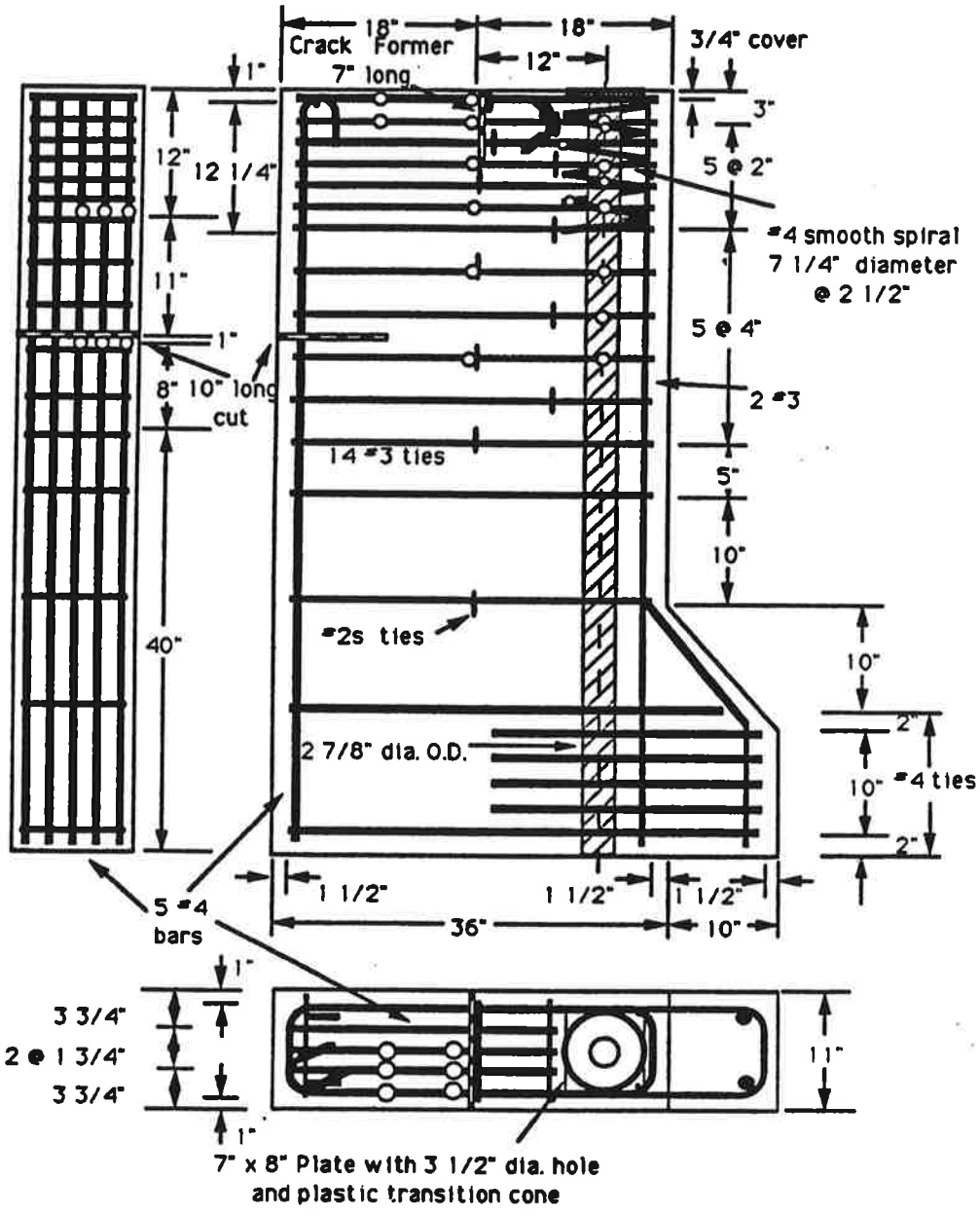

Figure C23 Specimen E3 Details

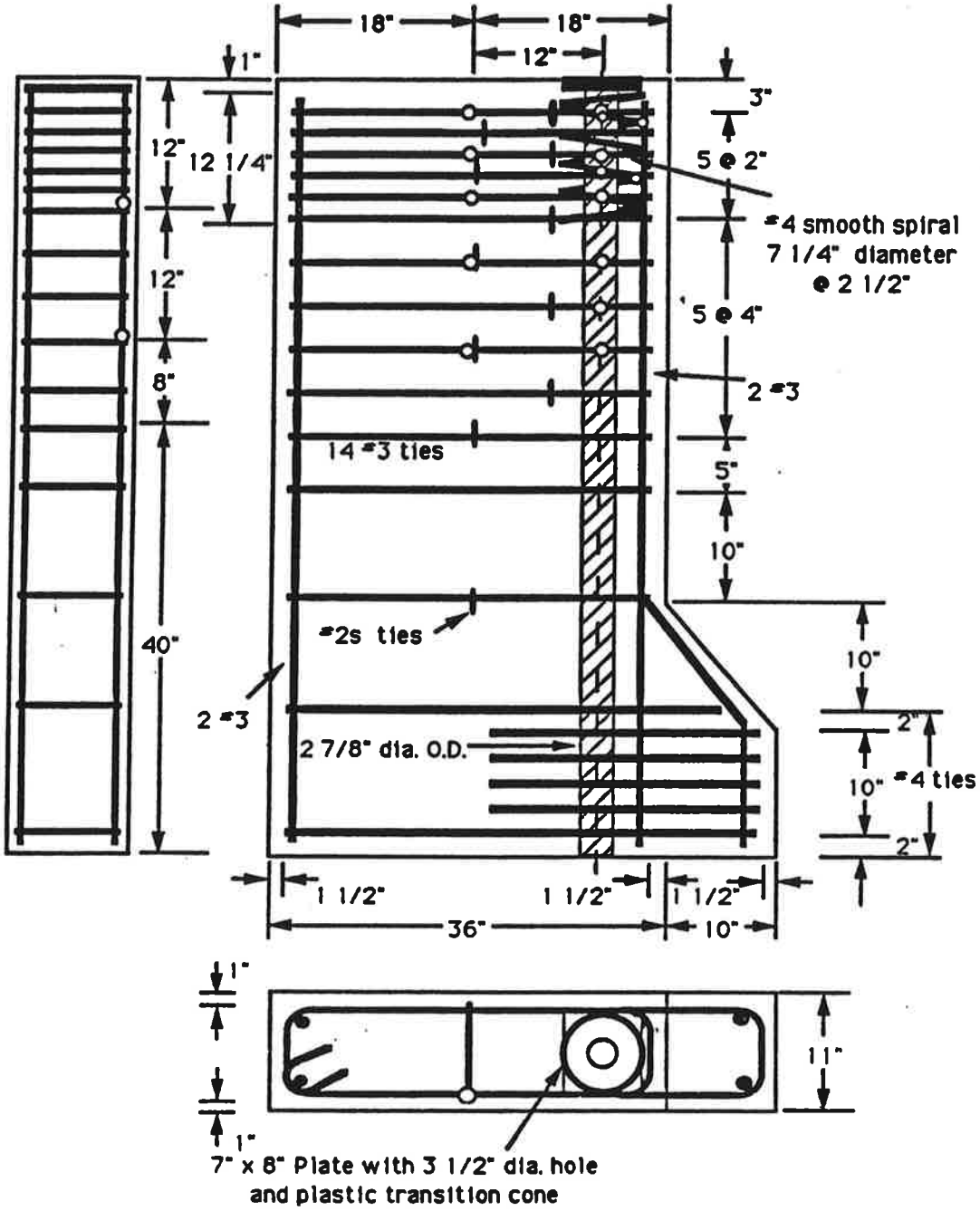

Figure C24 Specimen E4 Details

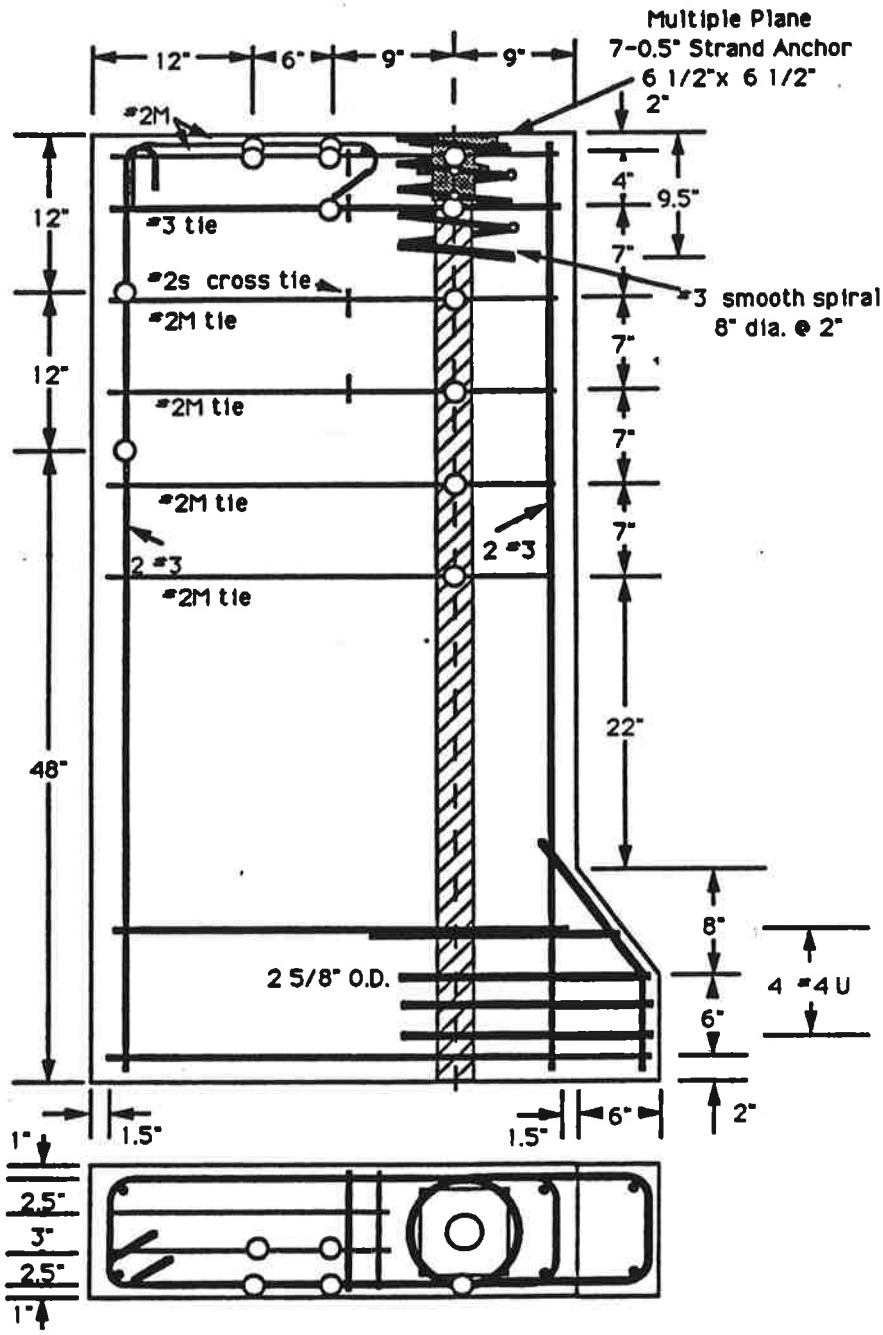

Figure C25 Specimen E6 Details

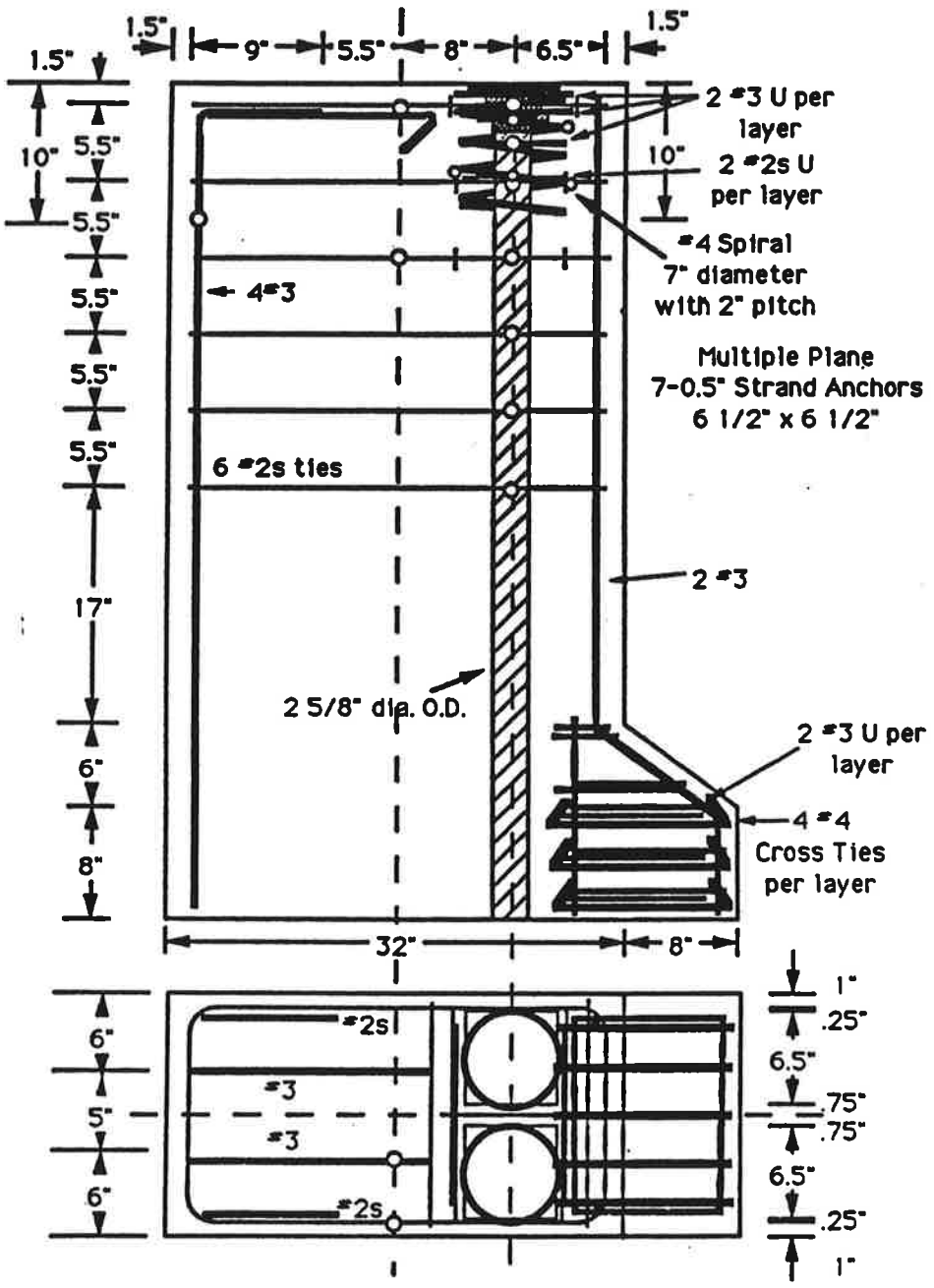

Figure C26 Specimen M5 Detail

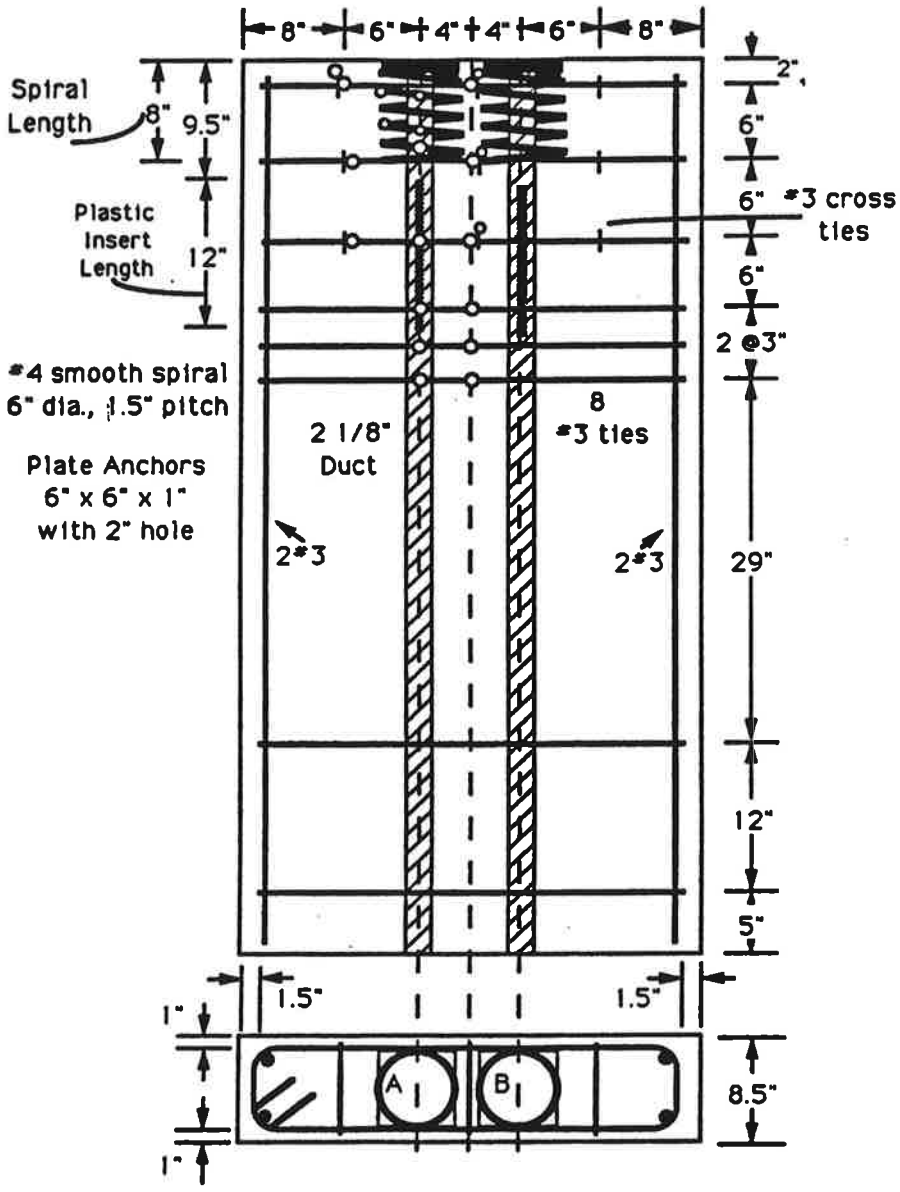

Figure C27 Specimen M1 Detail

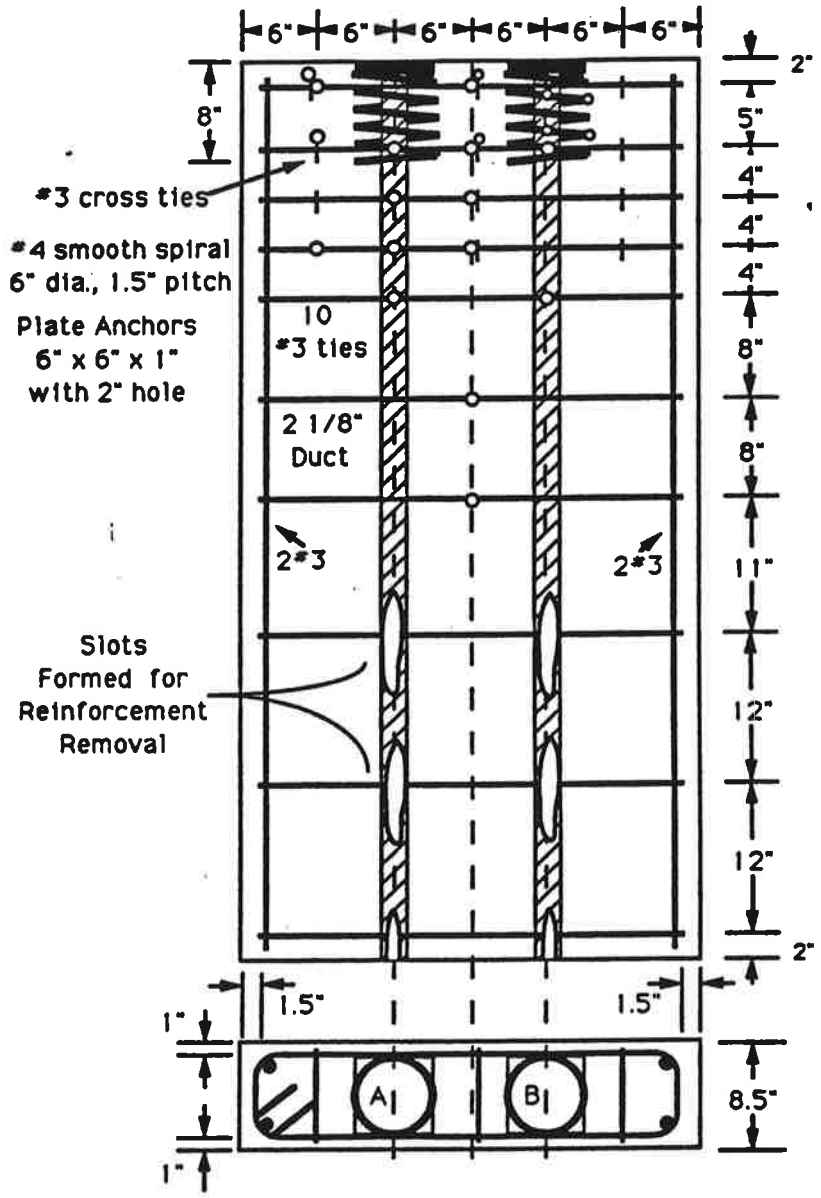

Figure C28 Specimen M2 Detail

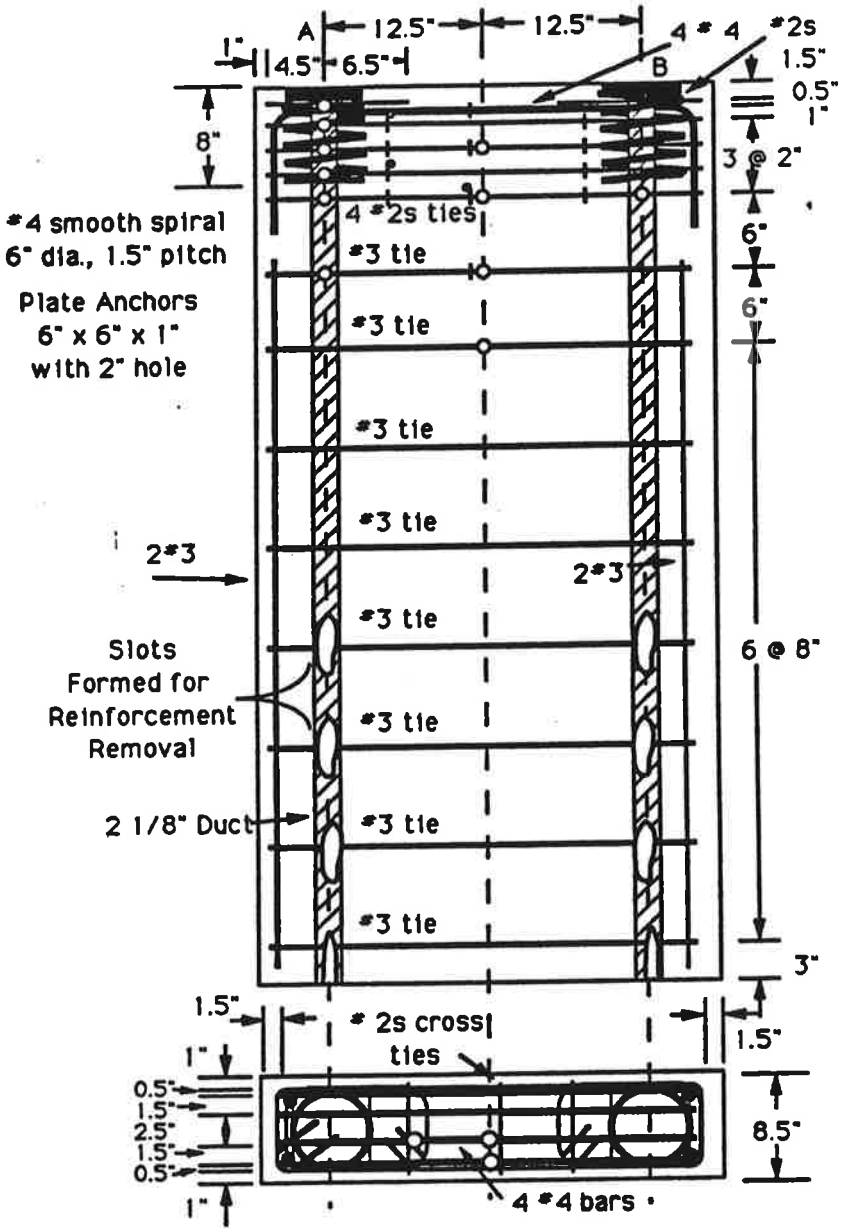

Figure C29 Specimen M3 Detail

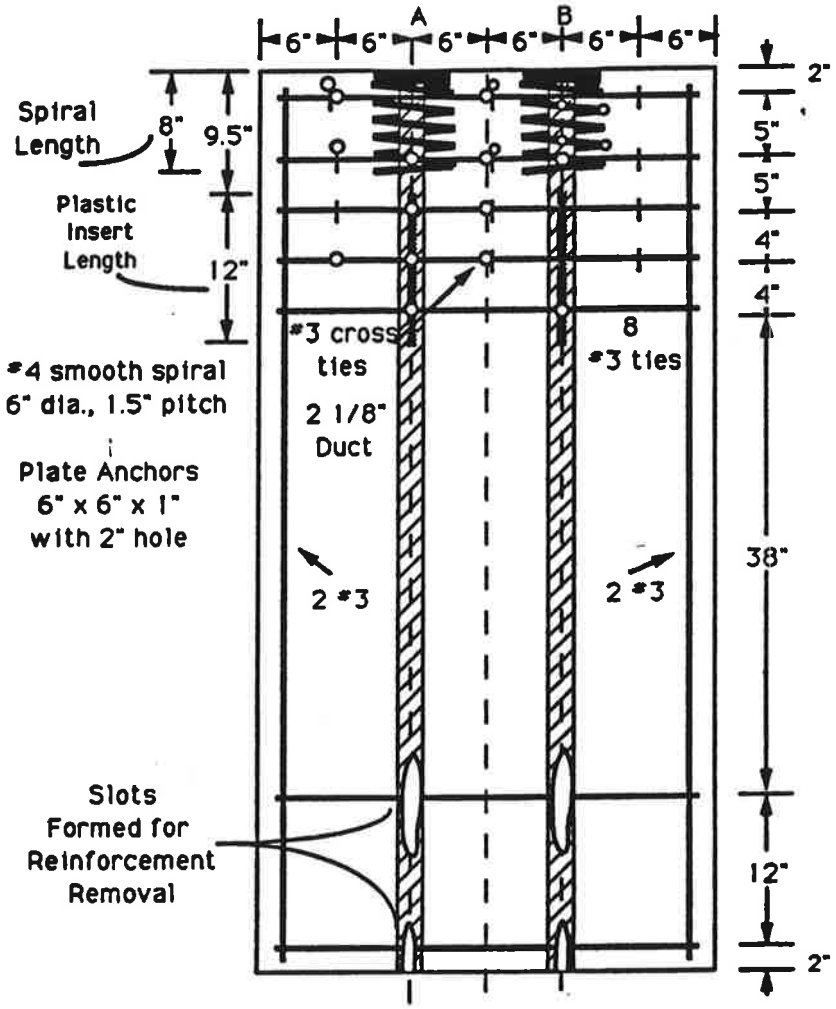

Figure C30 Specimen M4 Detail

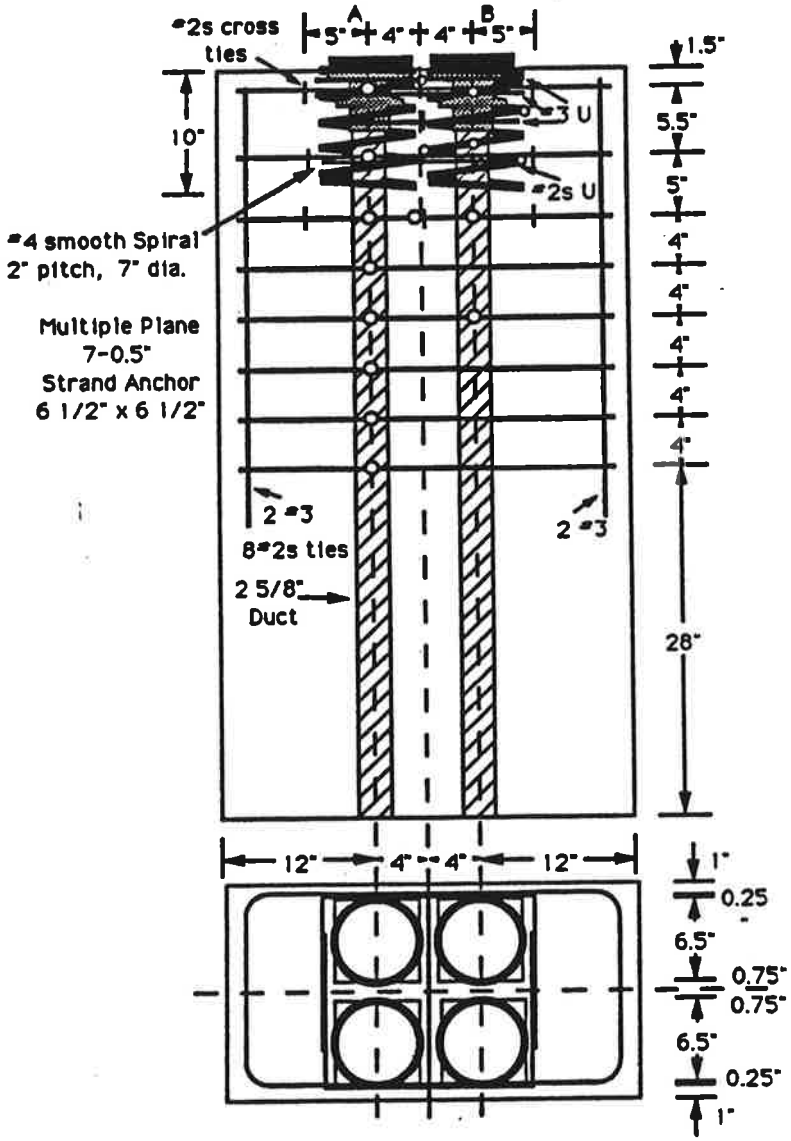

Figure C31 Specimen M6 Detail

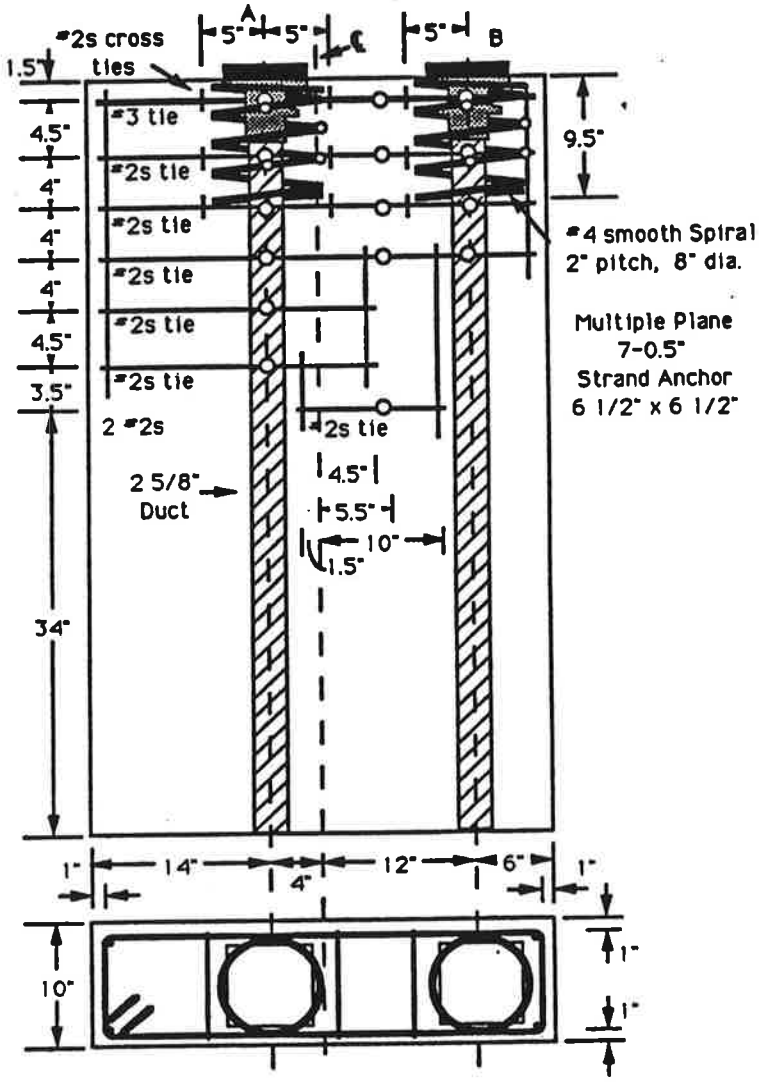

Figure C32 Specimen ME1 Detail

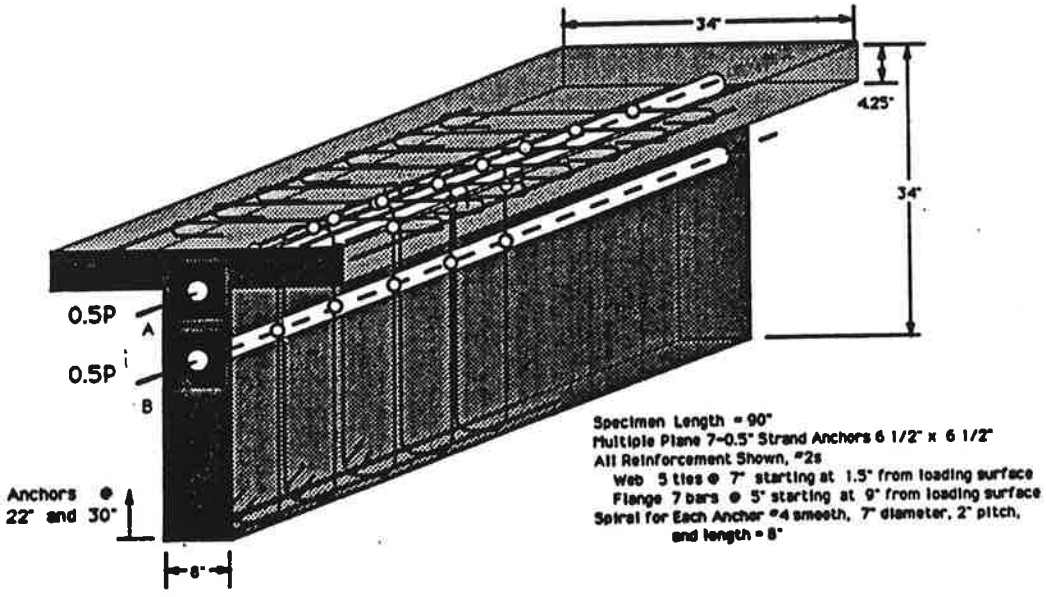

Figure C33 Specimen F1 Detail

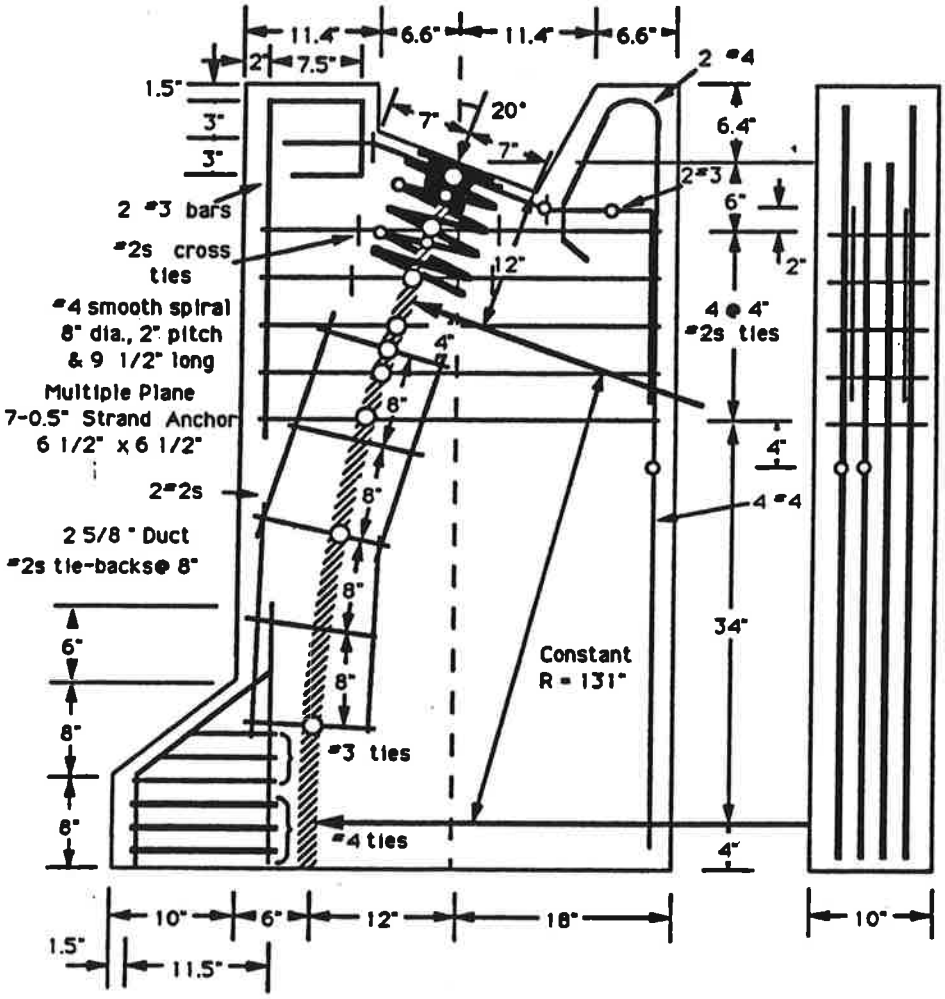

Figure C34 Specimen I1 Detail

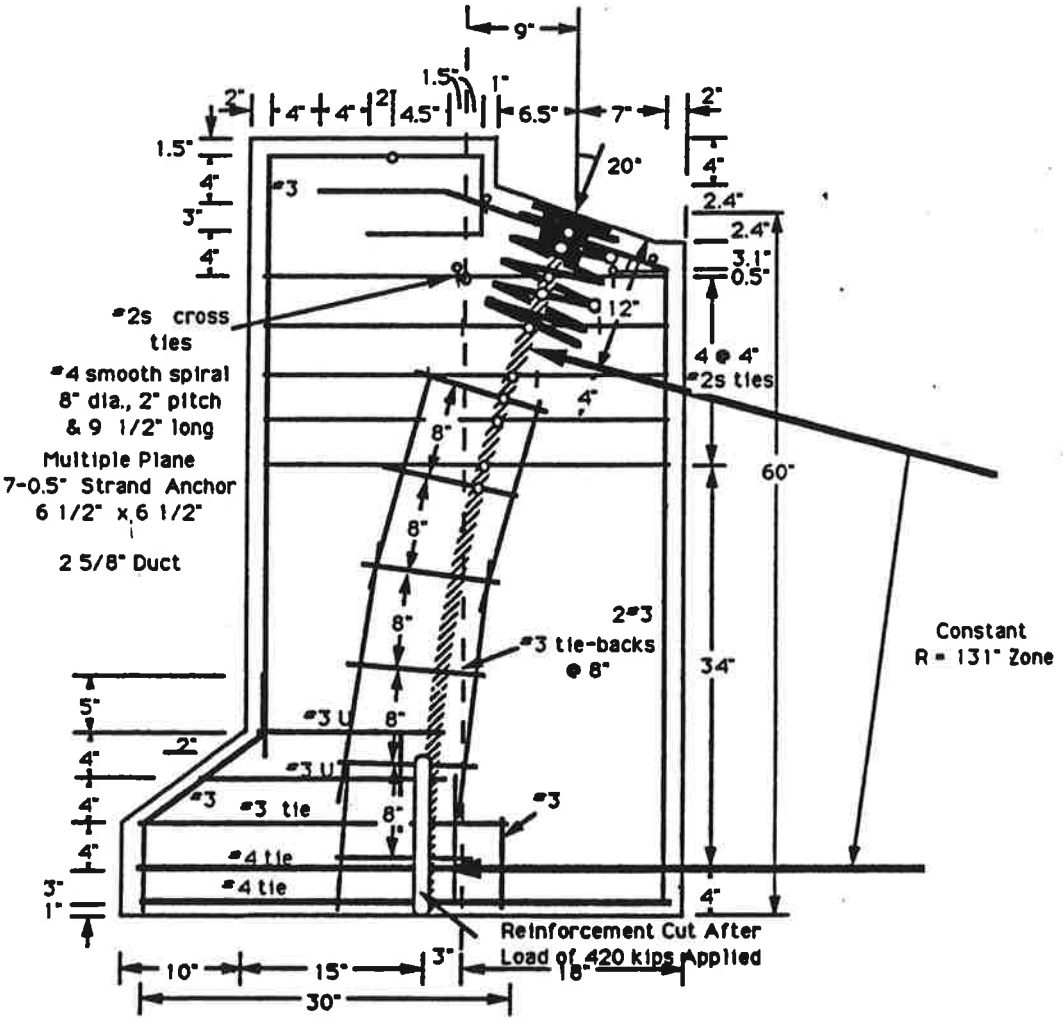

Figure C35 Specimen I2 Detail

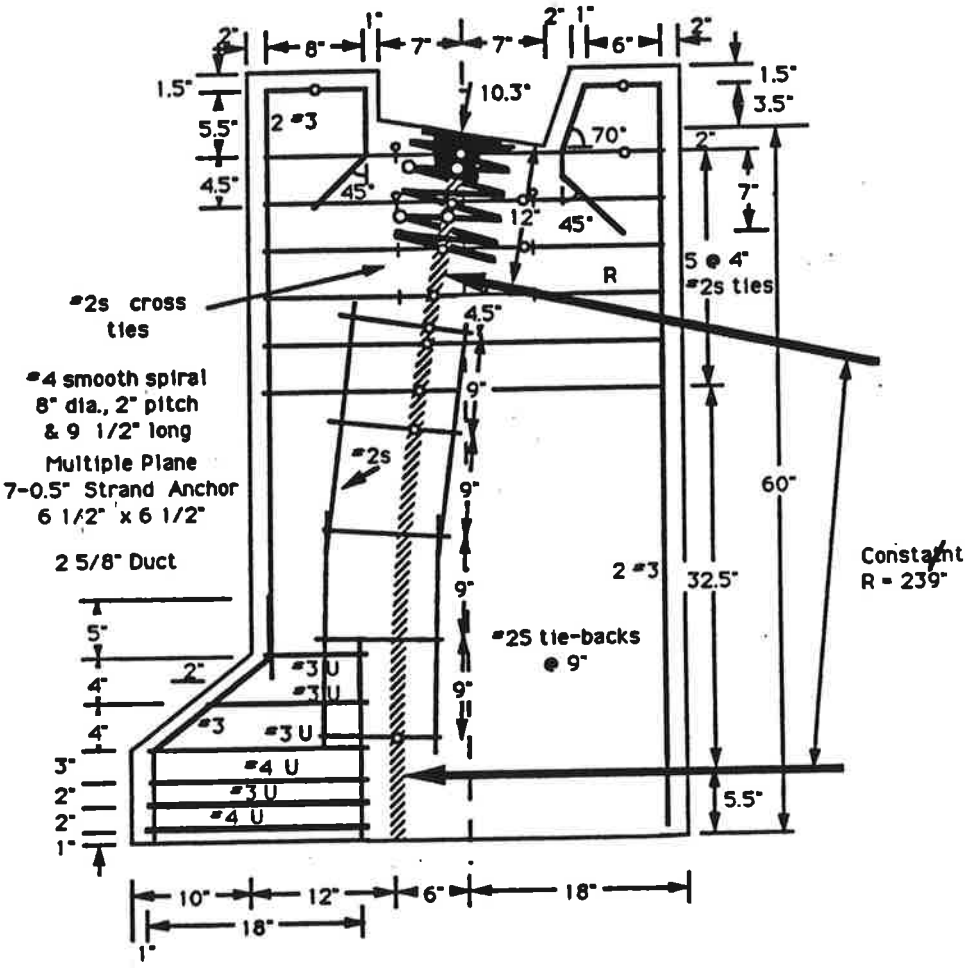

Figure C36 Specimen I3 Detail

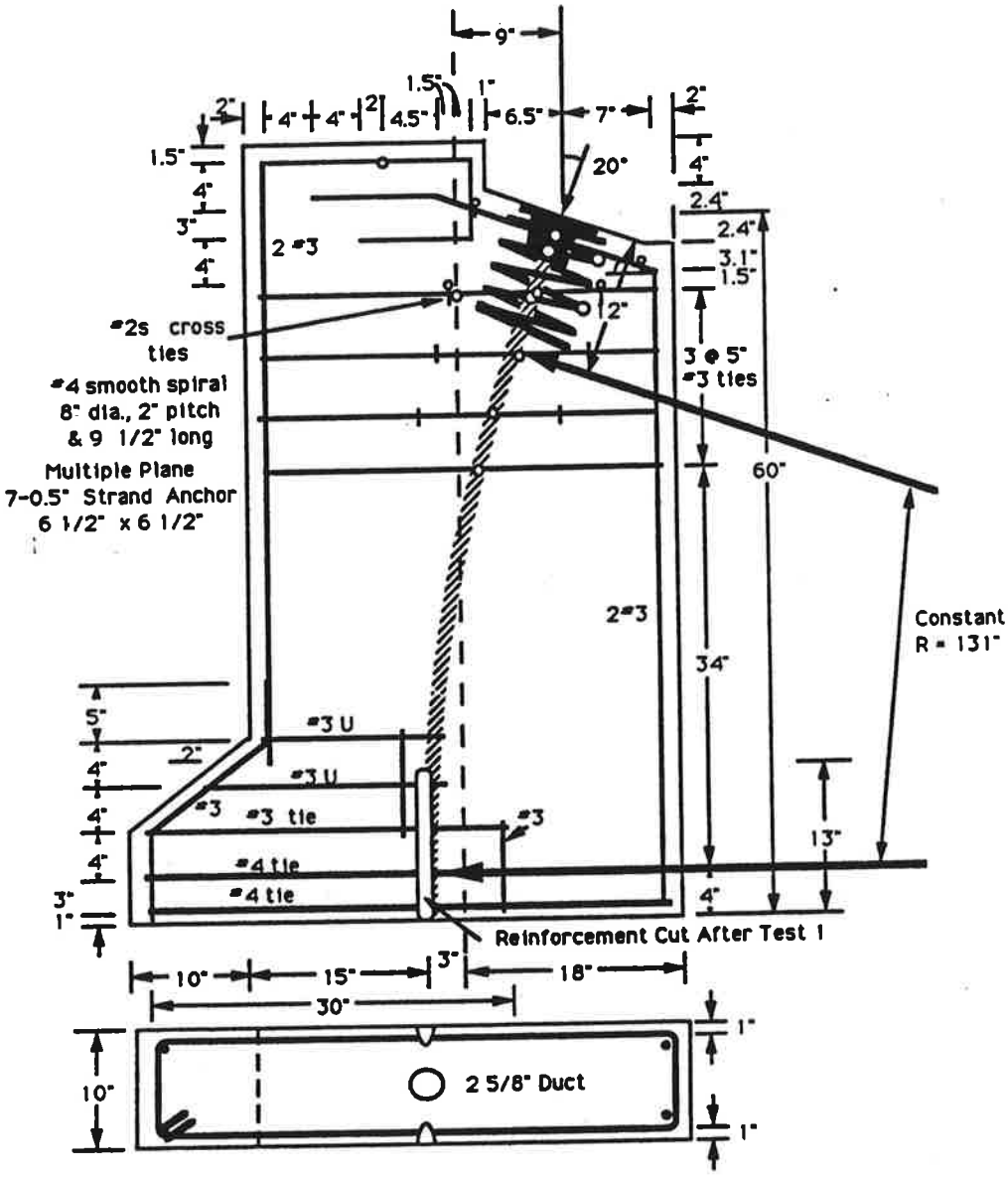

Figure C37 Specimen I4 Detail

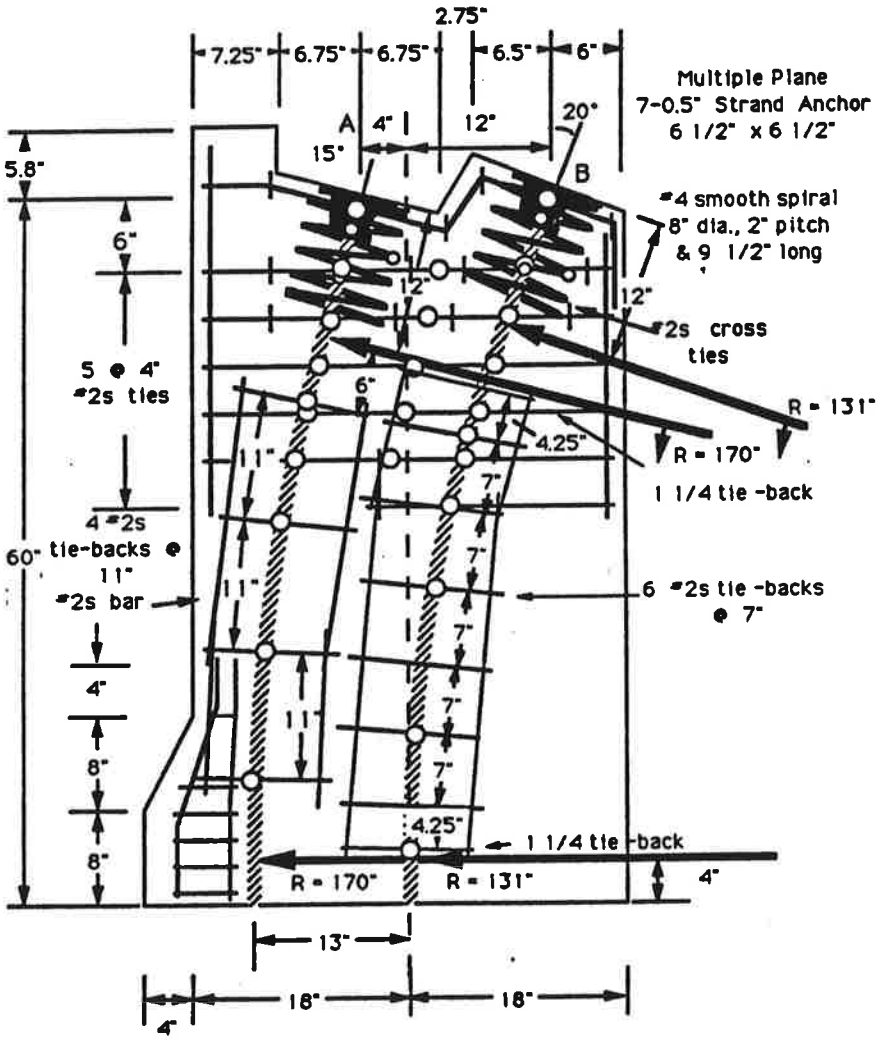

Figure C38 Specimen ME2 Detail

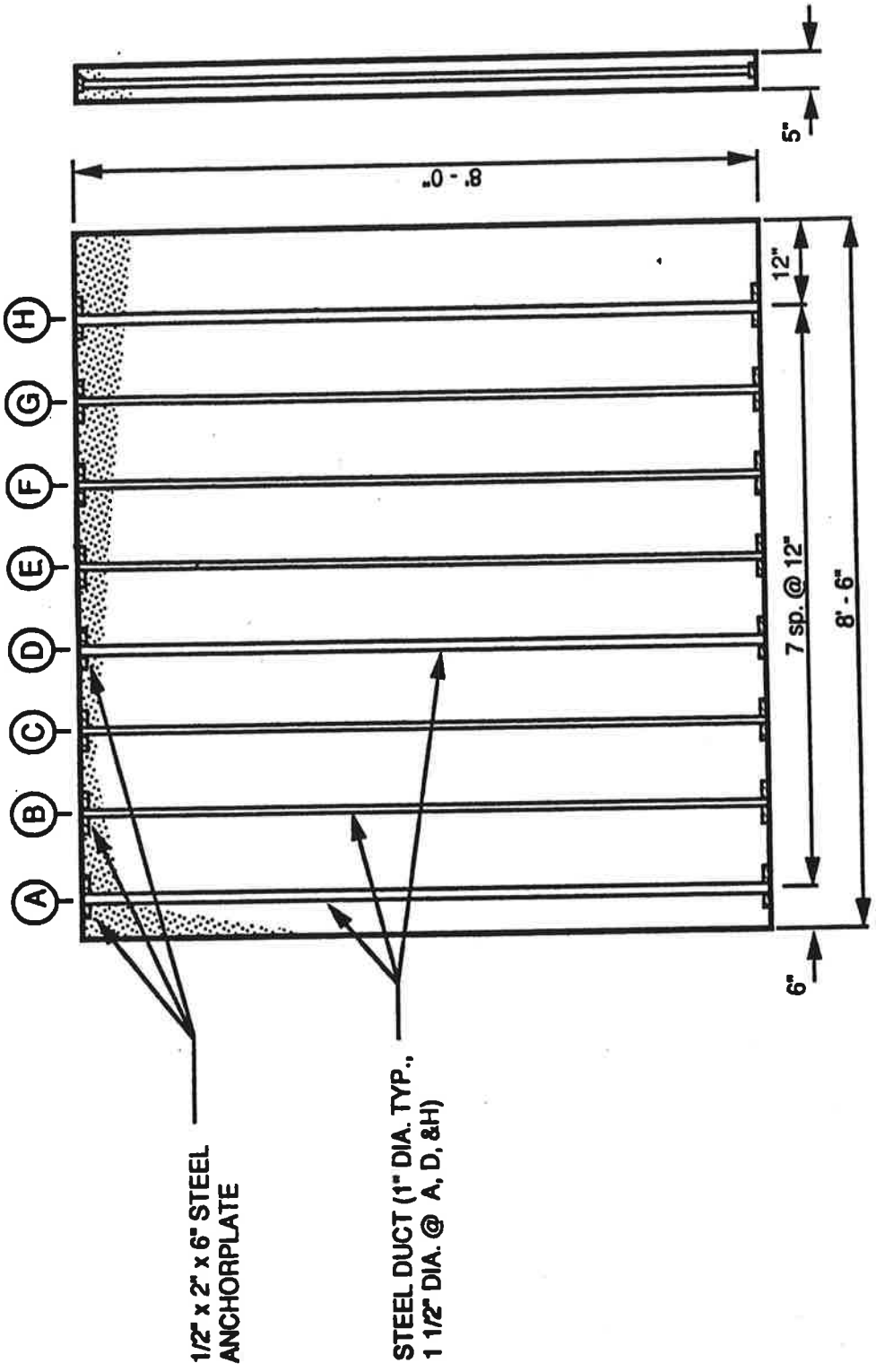

Figure C39 Plan of Slab #1

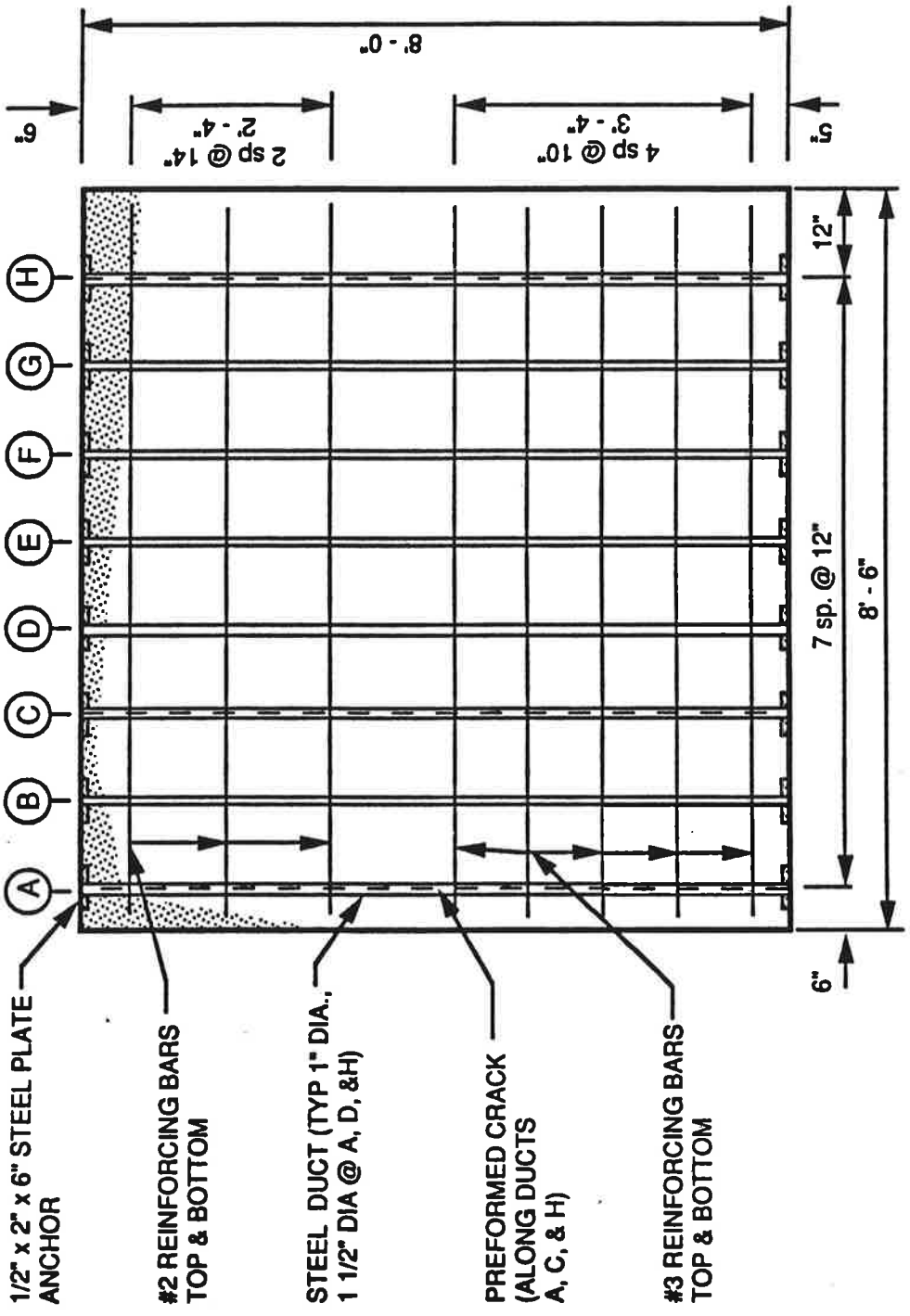

Figure C40 Plan of Slab #2

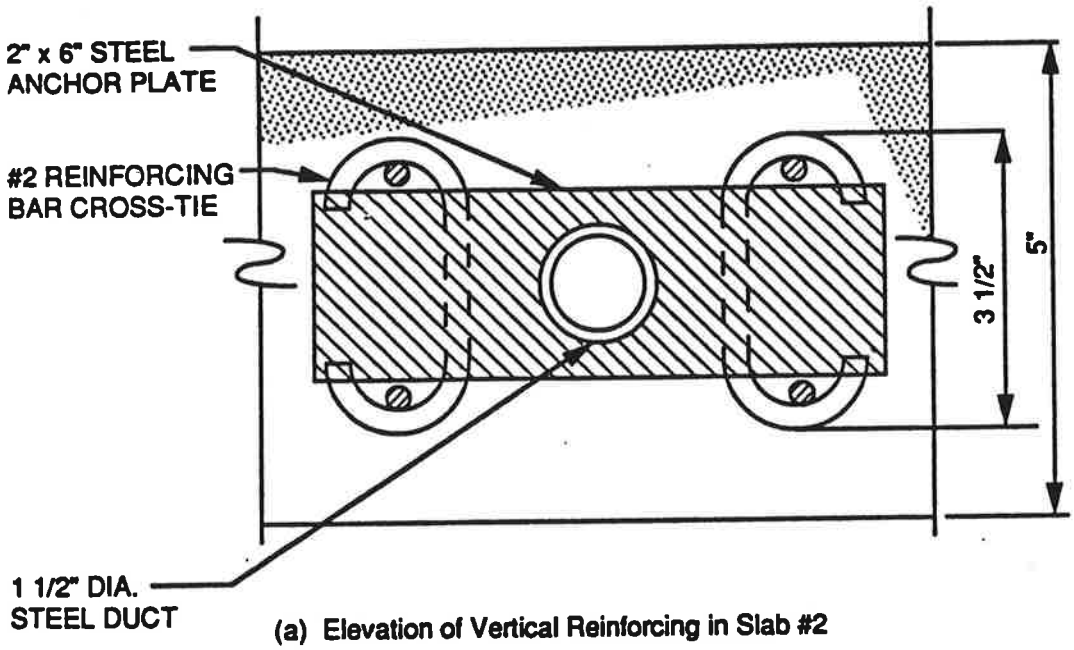

(a) Elevation of Vertical Reinforcing in Slab #2

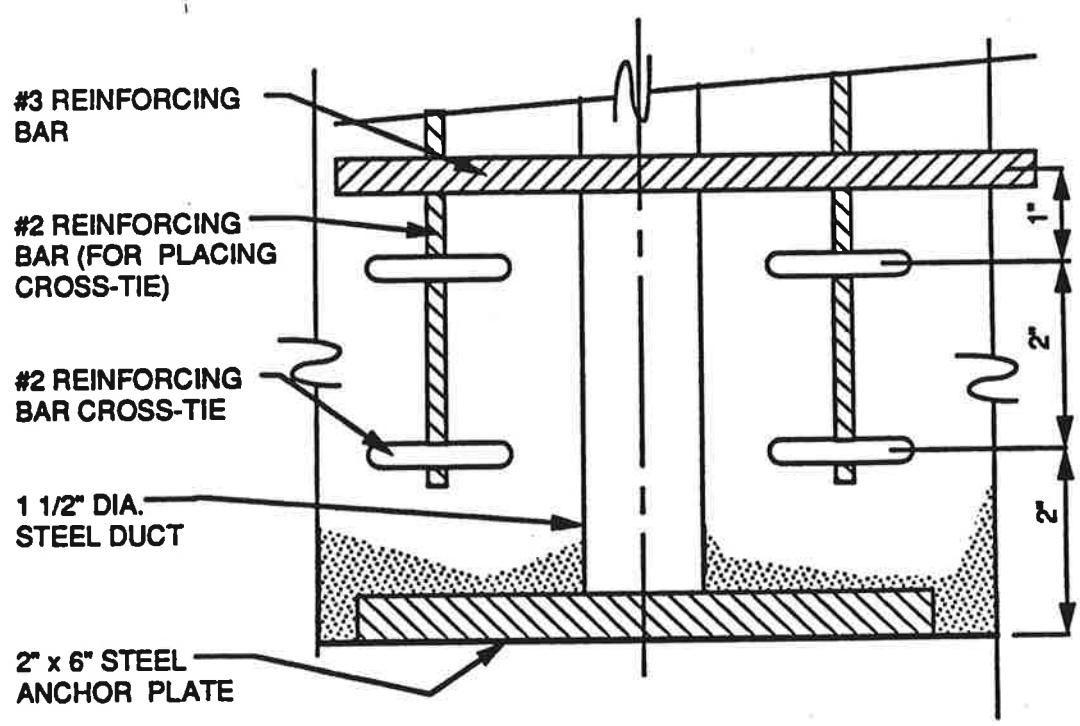

(b) Plan of Vertical Reinforcing Detail

Figure C41 Reinforcing Detail in Slab #2

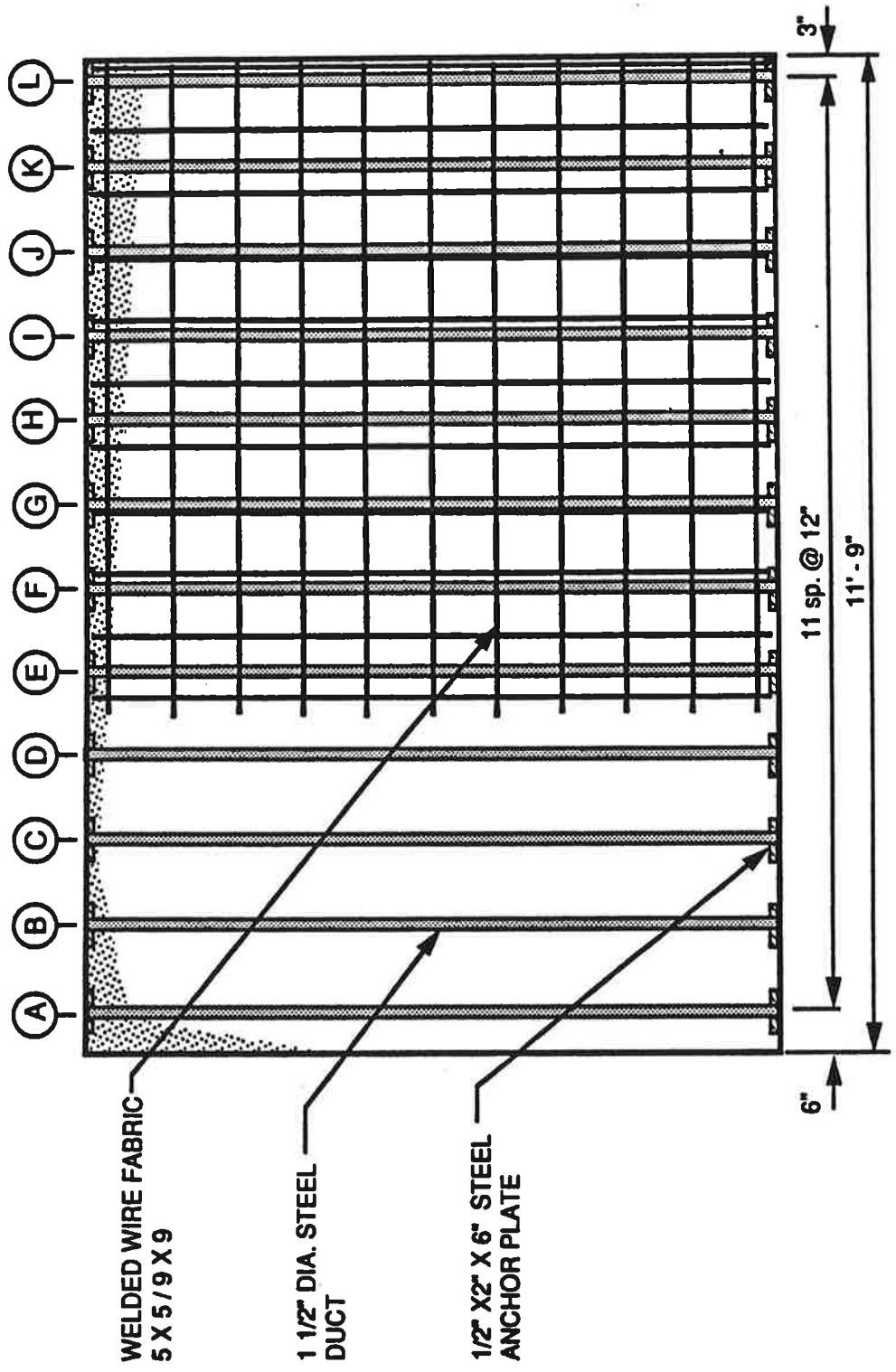

Figure C42 Plan of Slab #3

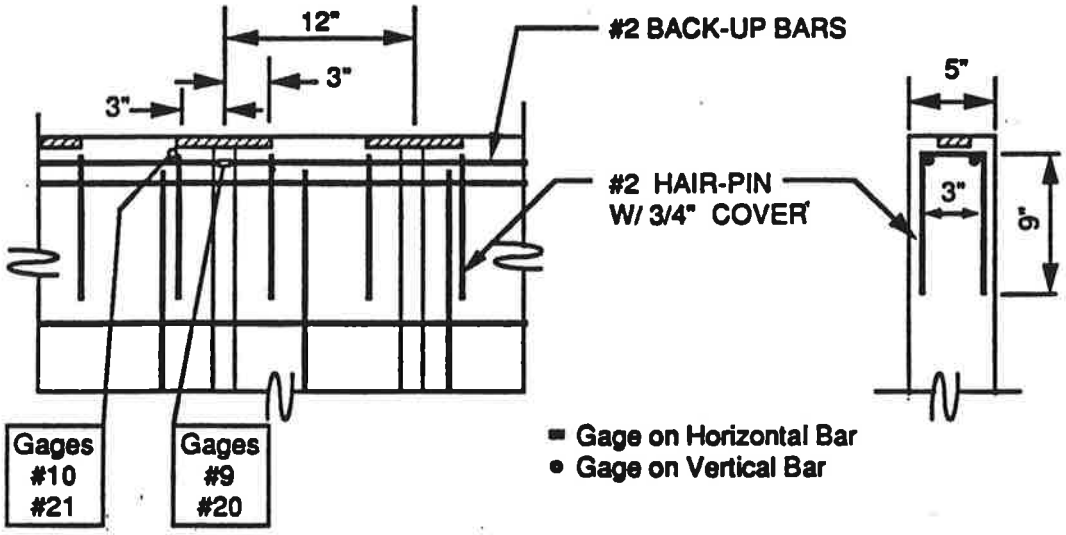

(a) Back-up bars and hair pins at Anchors E and F

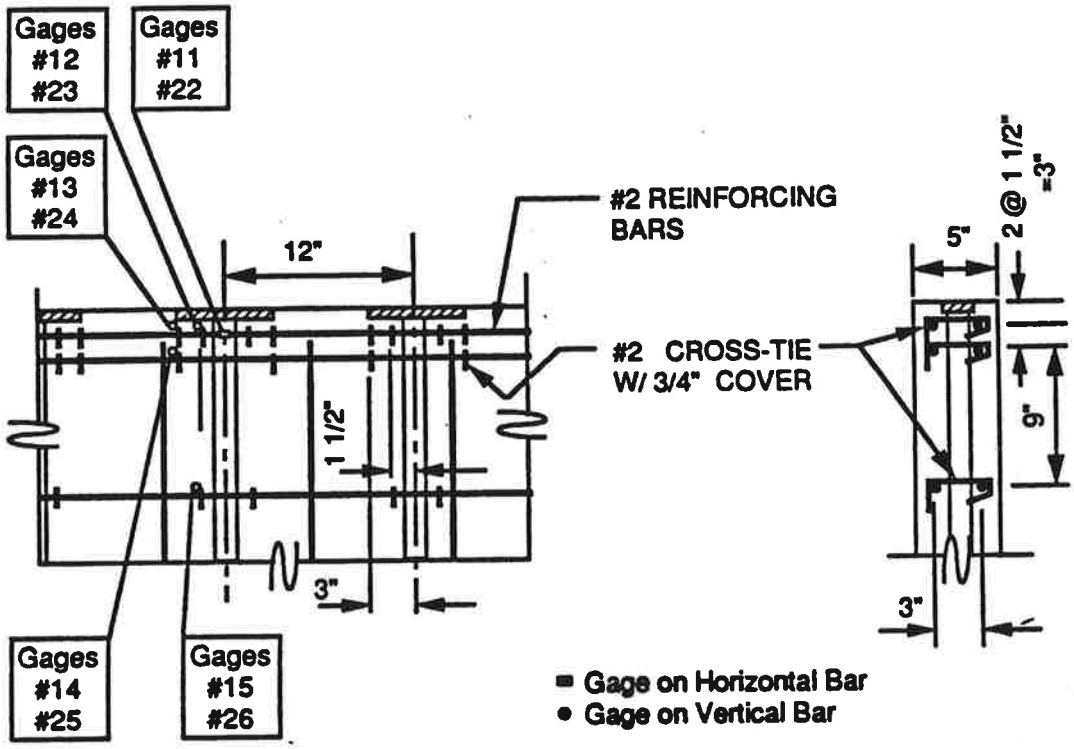

(b) Cross ties at Anchors G and H

Figure C43 Slab #3 Details

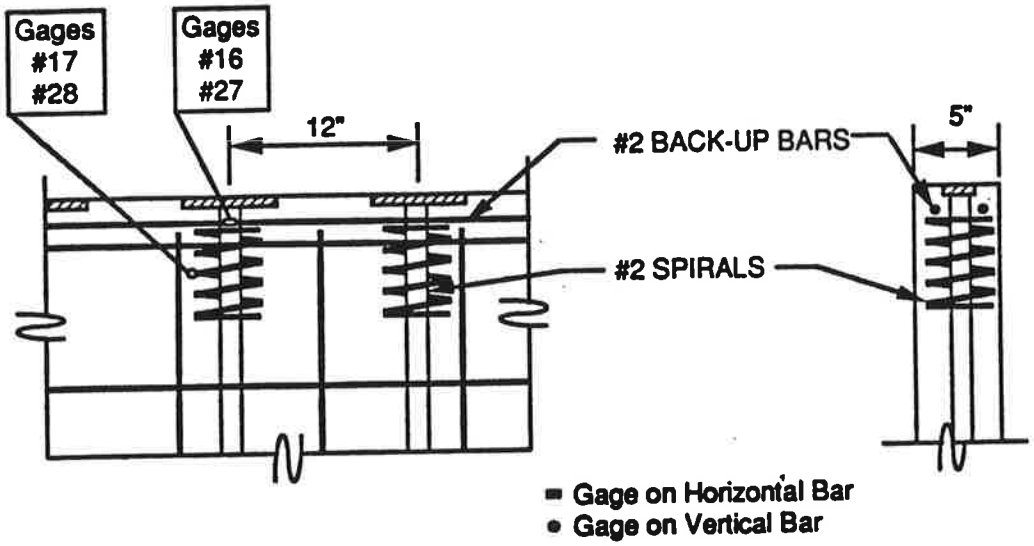

(c) Slab #3 spiral detail at Anchors I and J

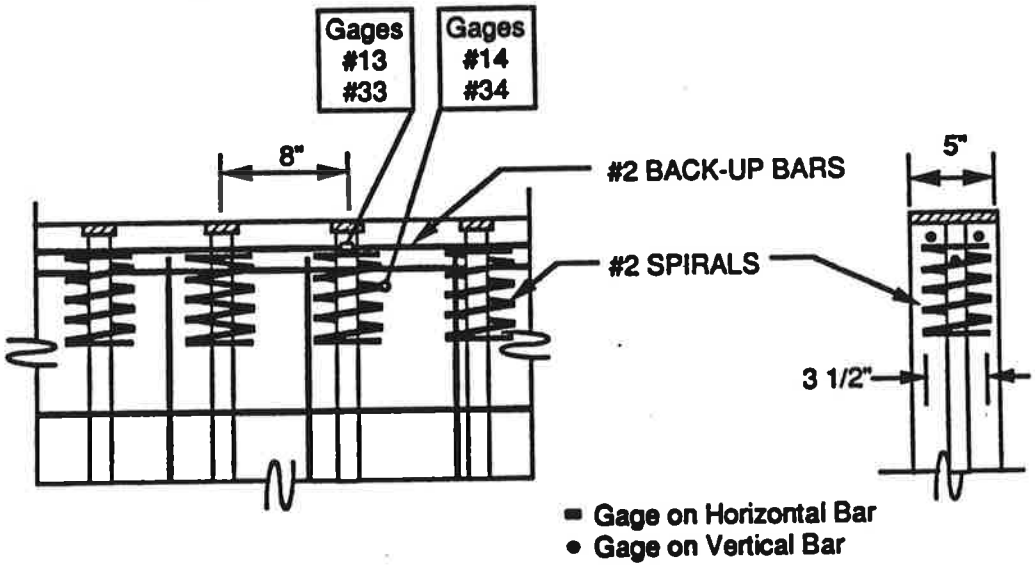

(d) Spiral detail at anchors I and J

Figure C43 Slab #3 Details

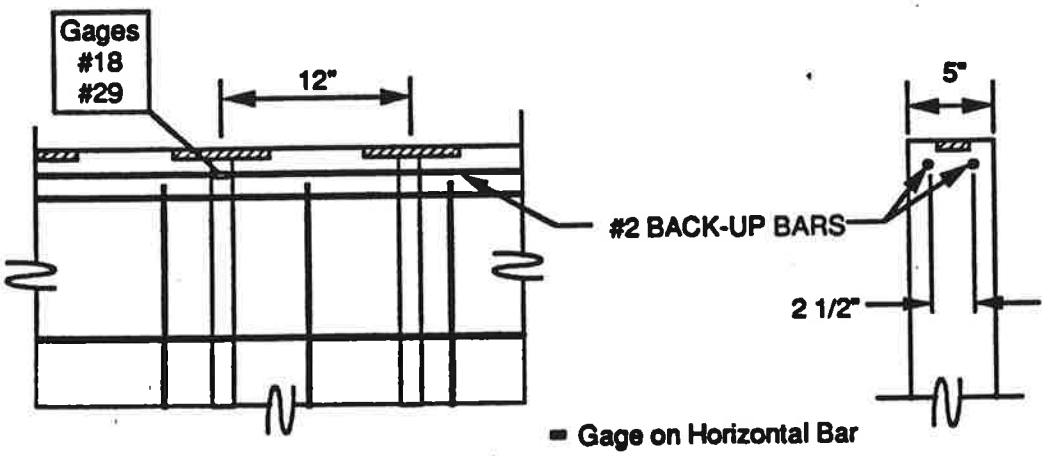

(e) Slab #3 detail at Anchors K and L - Backup bars with gages

Figure C43 Slab #3 Details

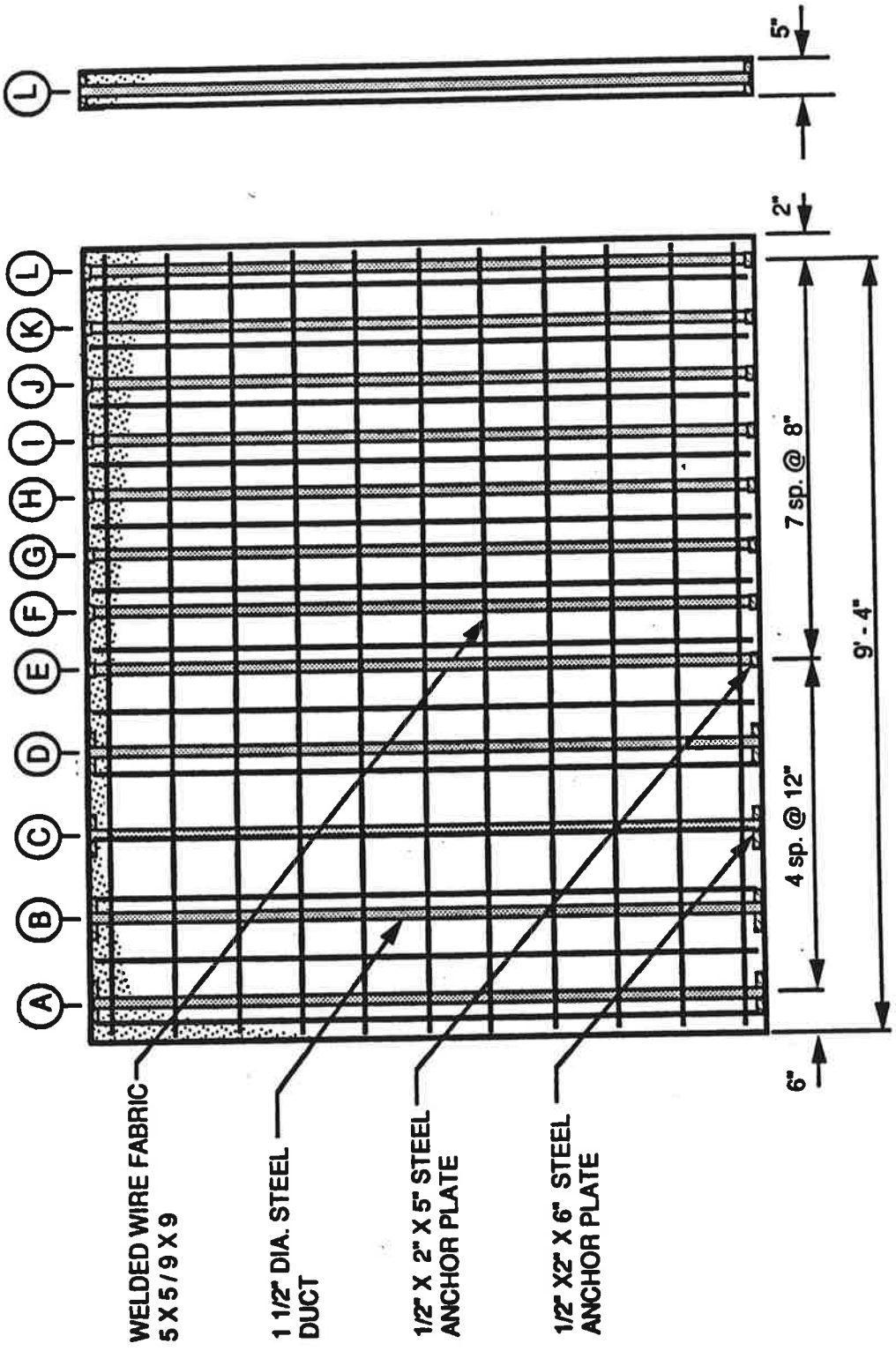

Figure C44 Plan of Slab #4

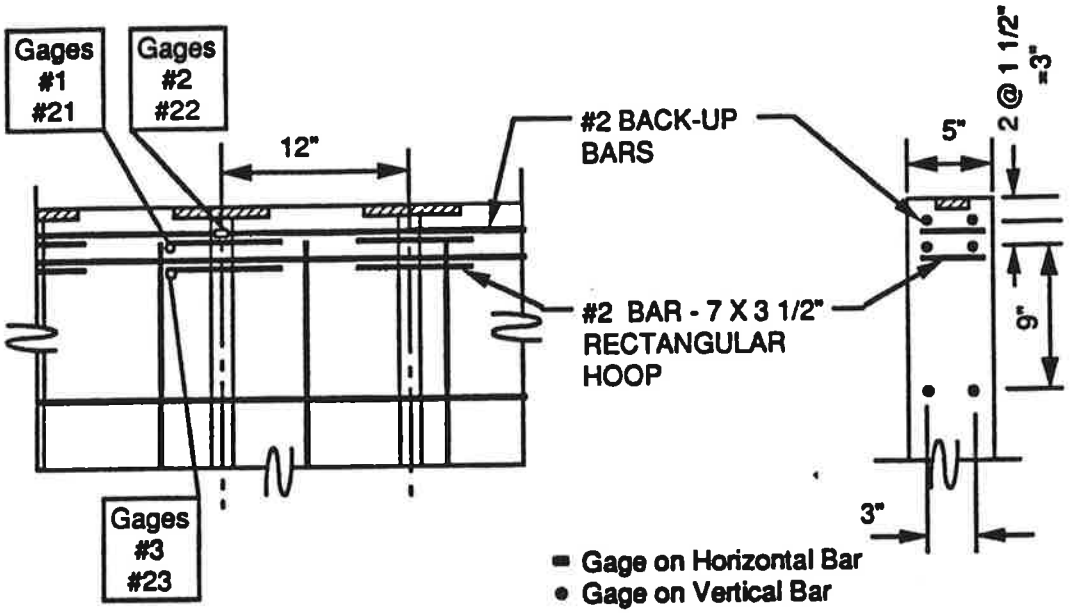

(a) Hoops at Anchors A and B

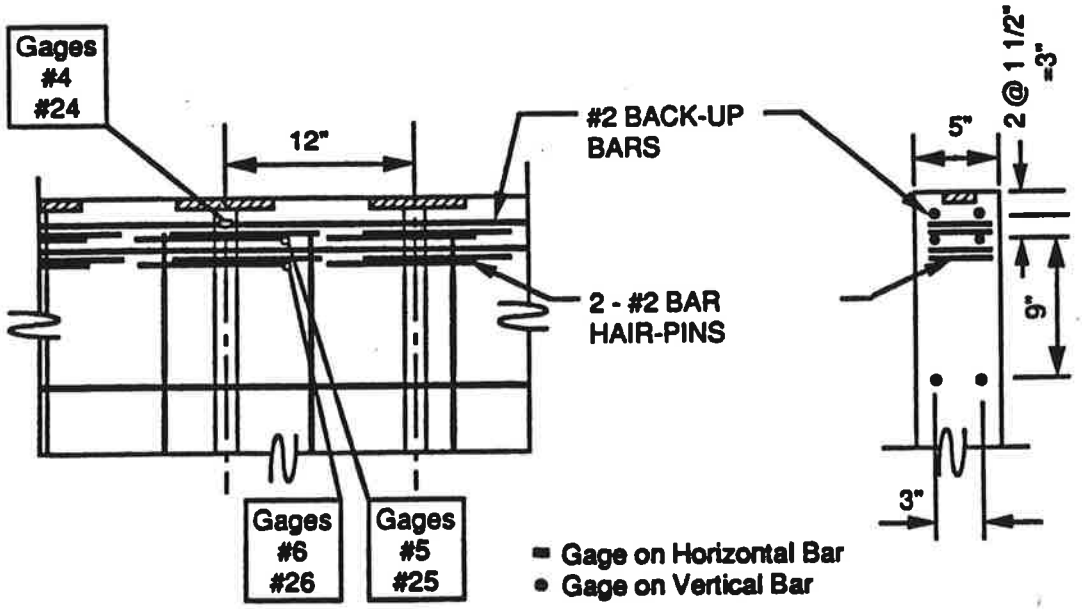

(b) Double hairpins at Anchors C and D

Figure C45 Slab #4 Details

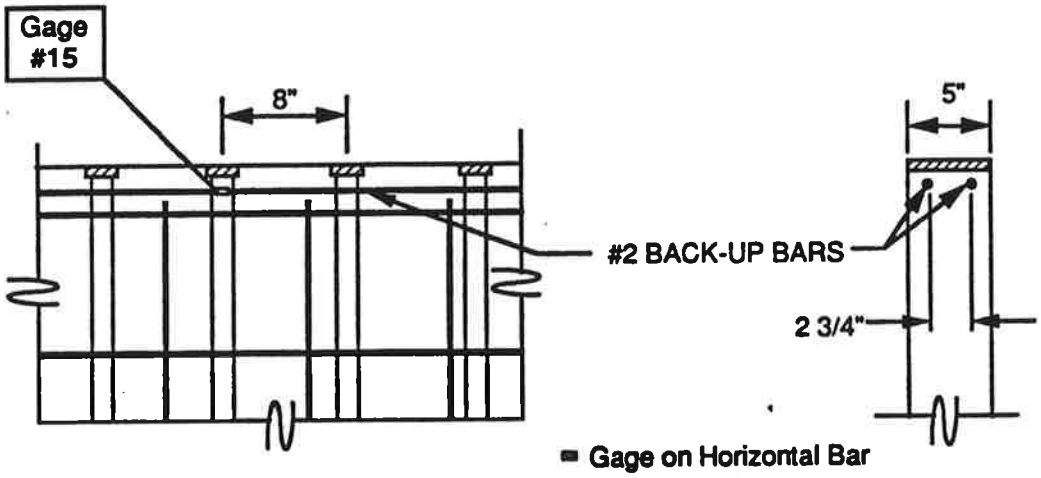

(c) Back-up bars at anchors K and L

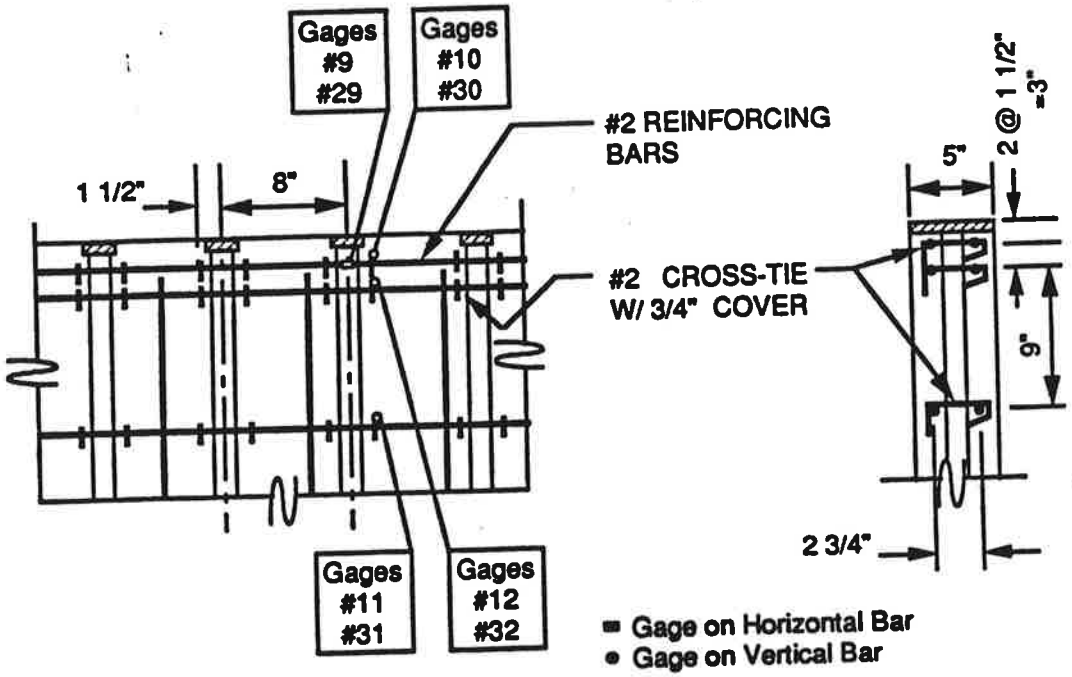

(d) Cross ties at anchors G and H

Figure C45 Slab #4 Details

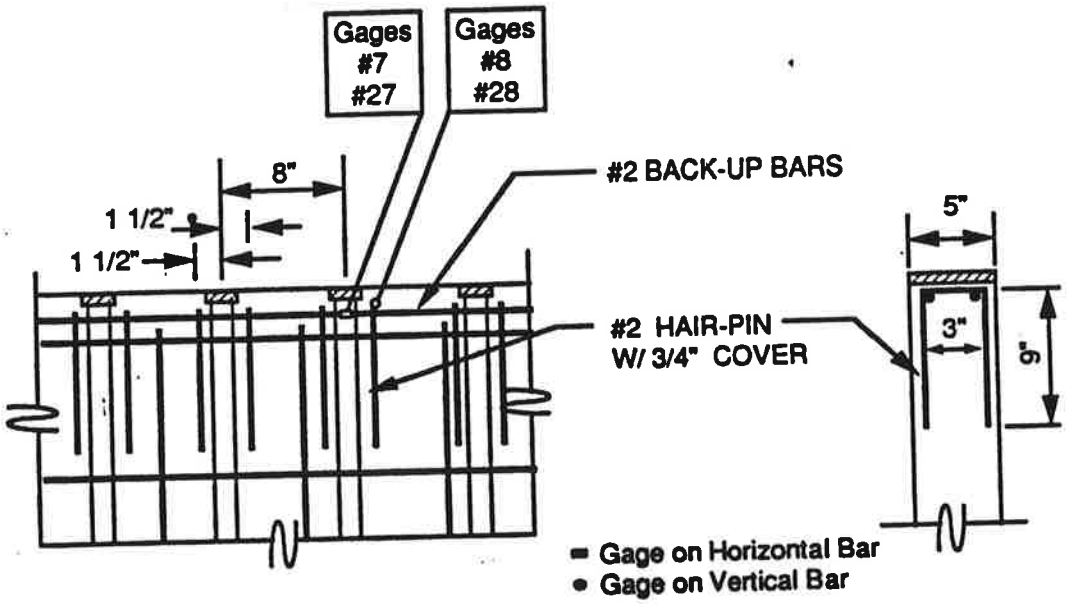

(e) Hairpins at Anchors E and F

Figure C45 Slab #4 Details

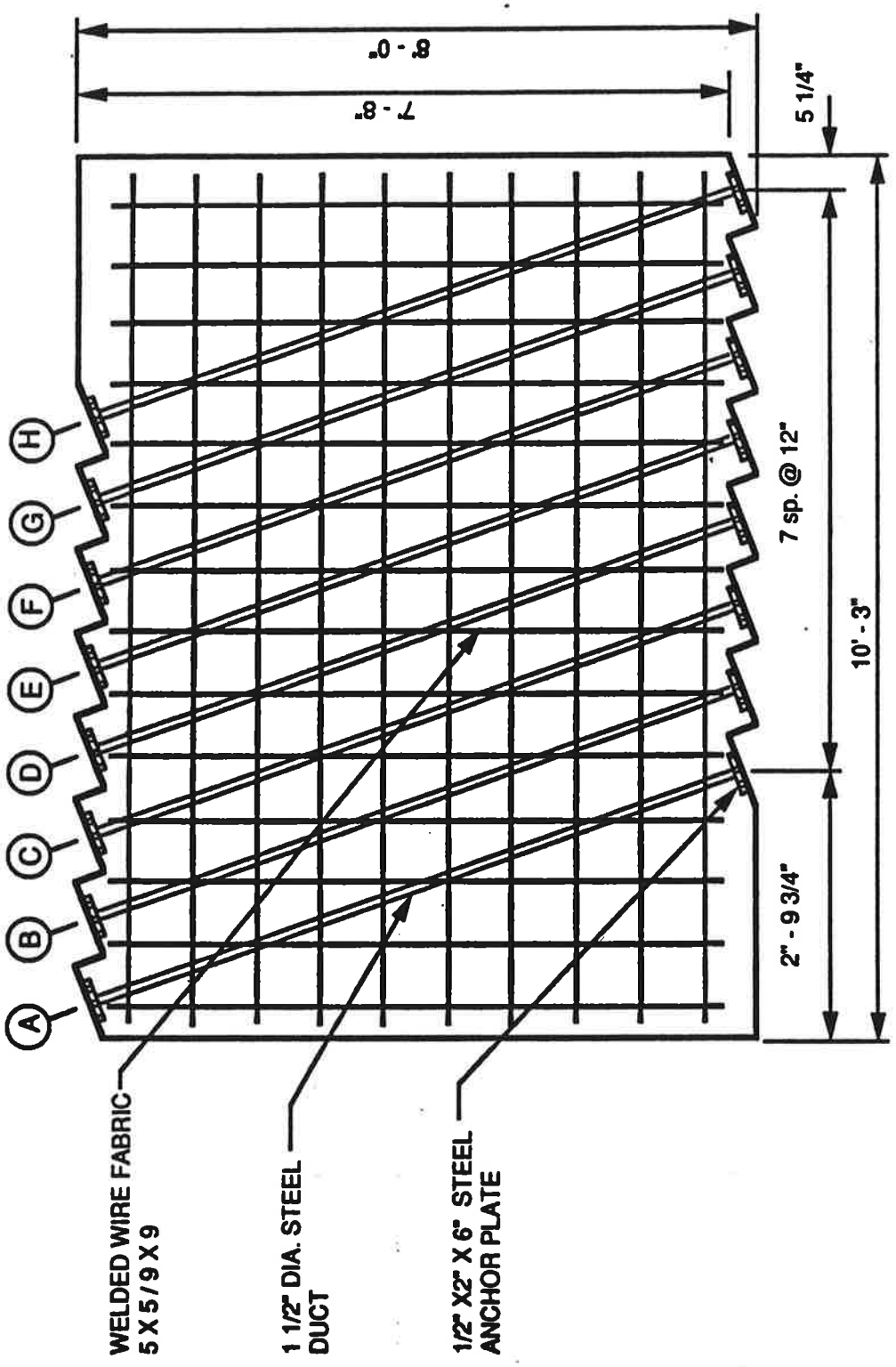

Figure C46 Plan of Slab #5 - 20 Degree Inclined Ducts

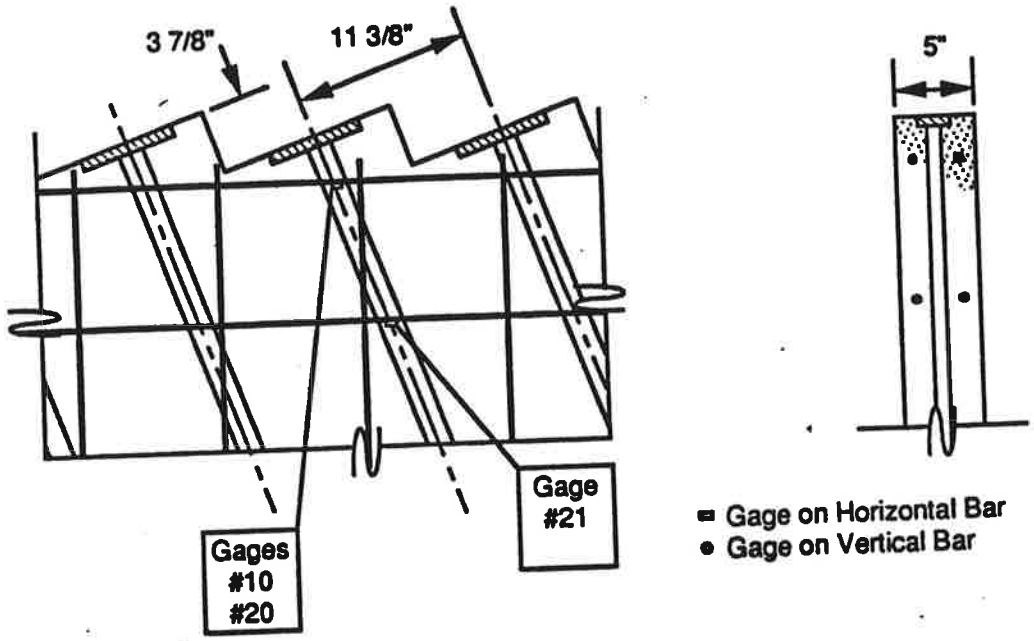

(a) Slab #5 horizontal reinforcing detail at Anchors G and H

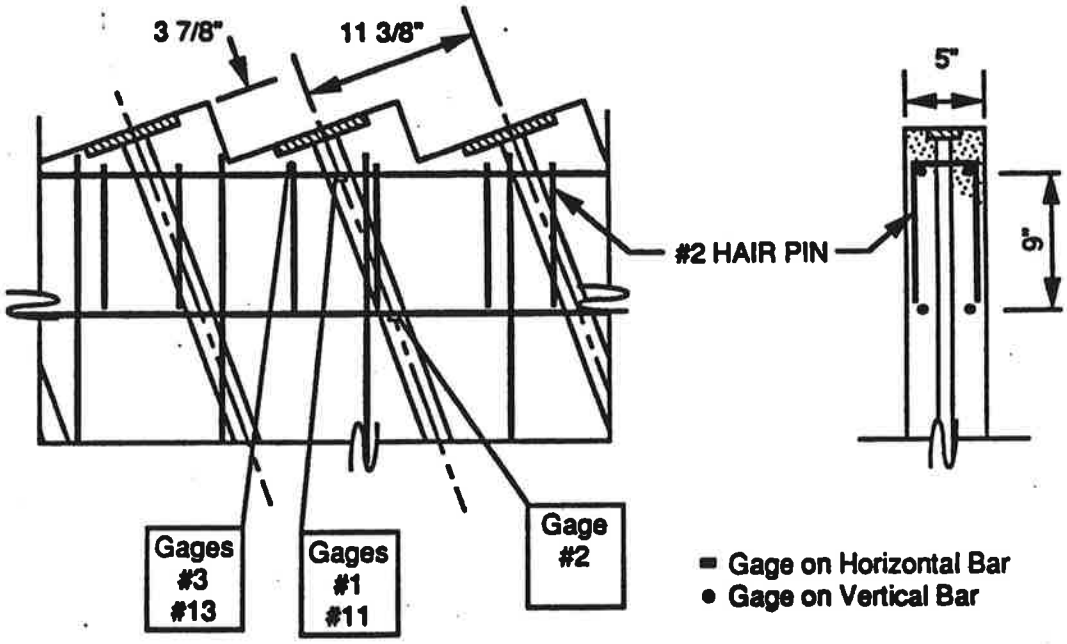

(b) Slab #5 hairpins at Anchors A and B

Figure C47 Slab #5 Details

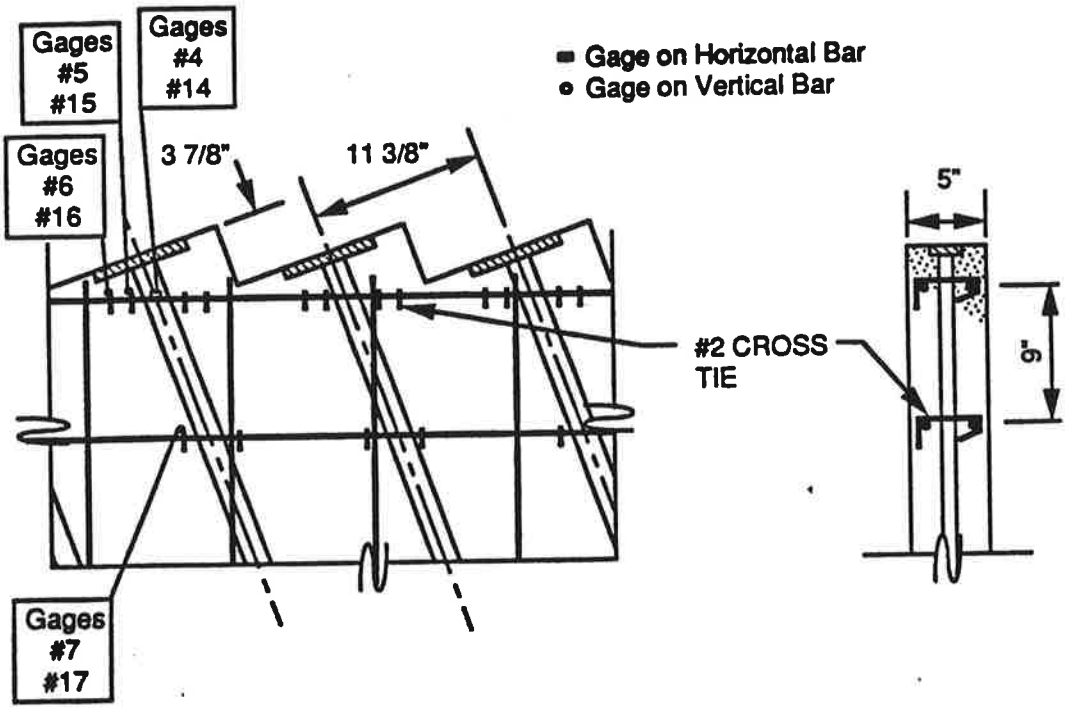

(c) Slab #5 cross ties detail at Anchors C and D

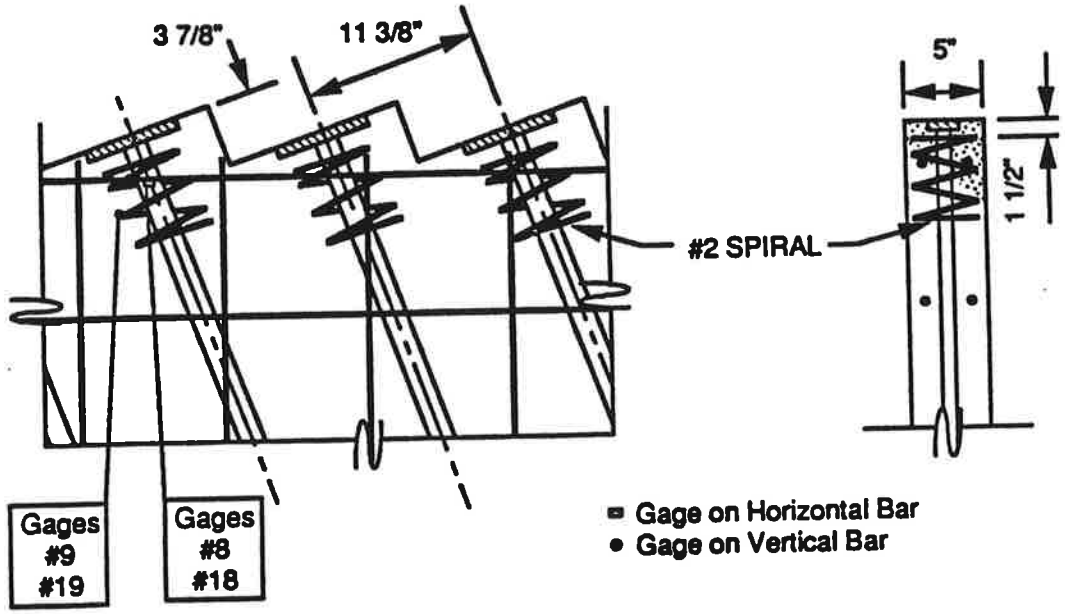

(d) Slab #5 spiral detail at Anchors E and F

Figure C47 Slab #5 Details

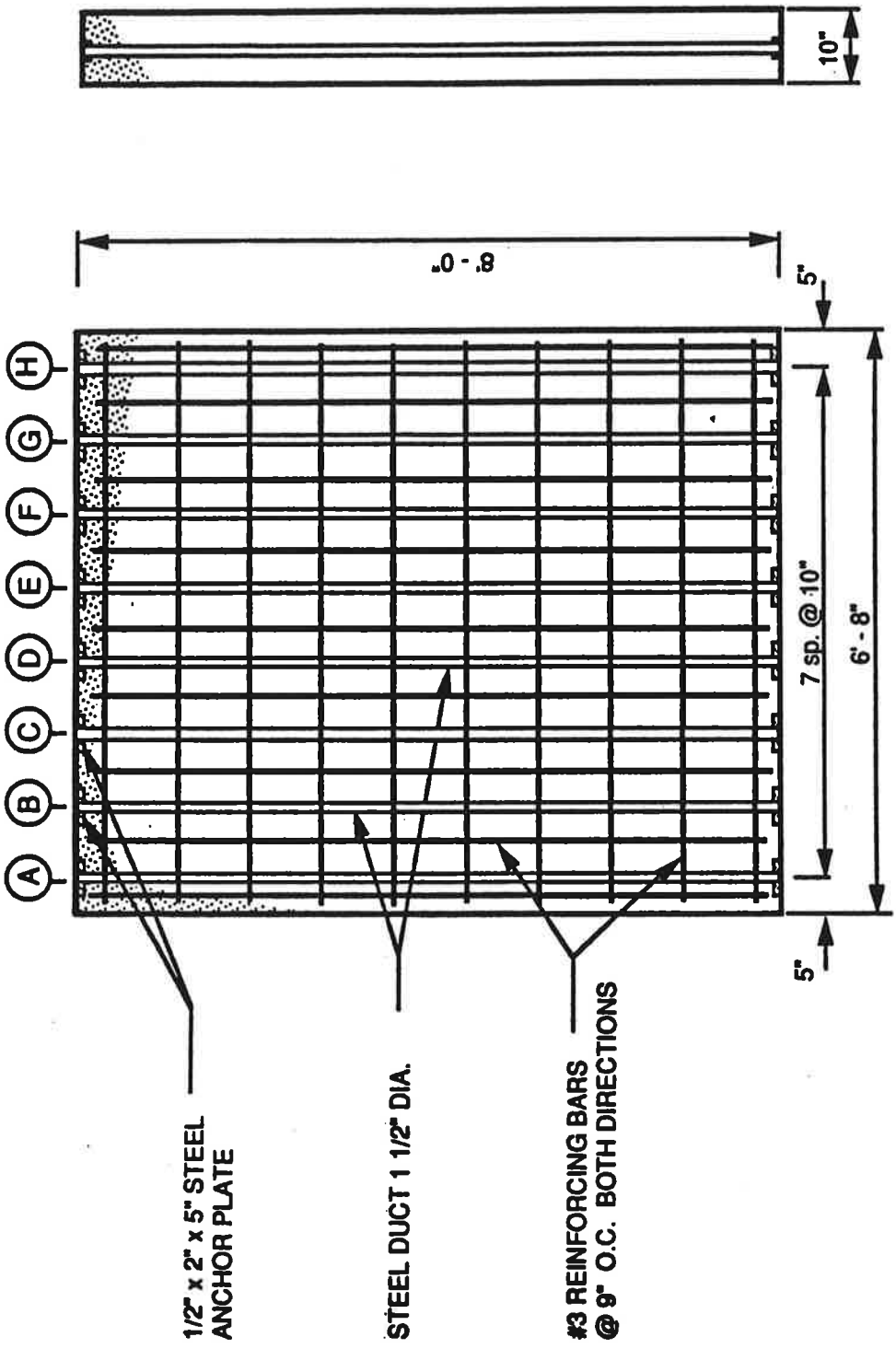

Figure C48 Plan of Slab #6 - Full Scale Monostrand Anchors

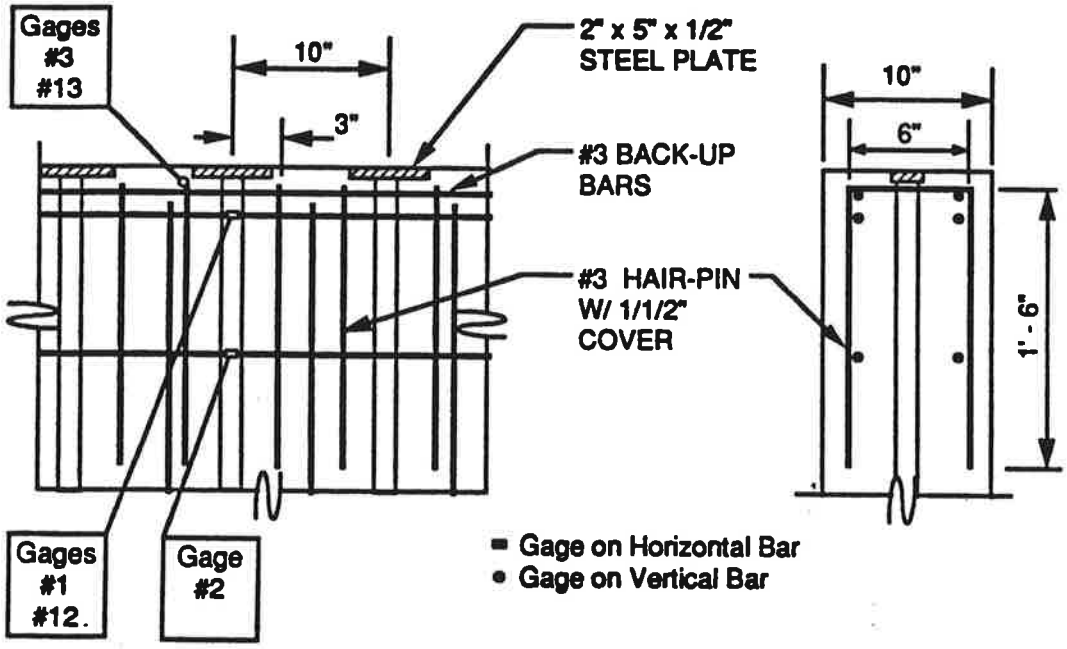

(a) Hairpins at Anchors E and F

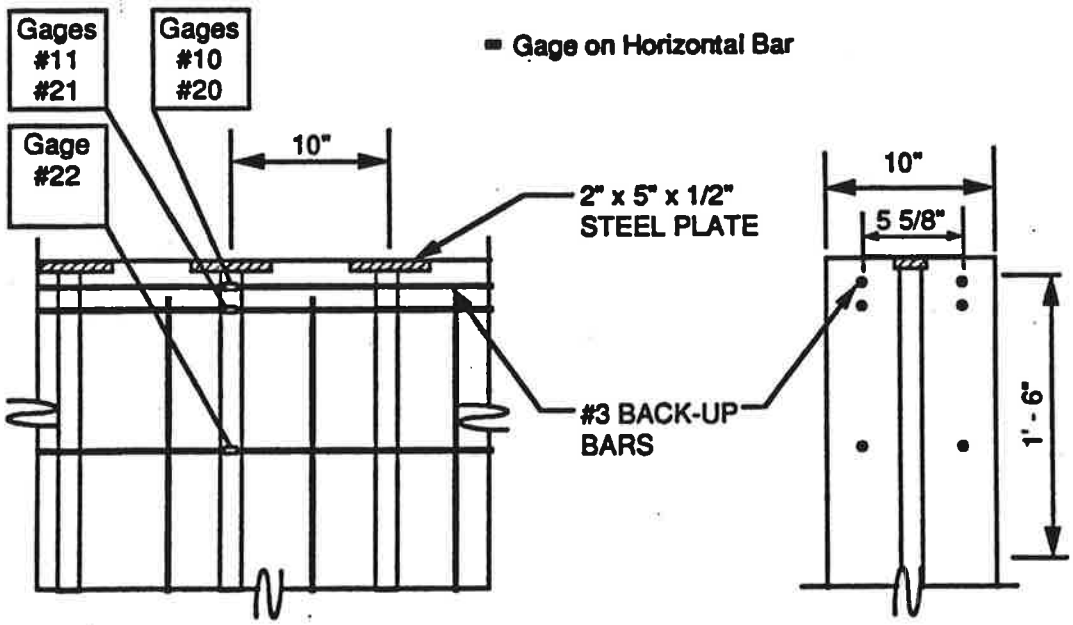

(b) Slab #6 back-up bars detail at Anchors K and L

Figure C49 Slab #6 Details

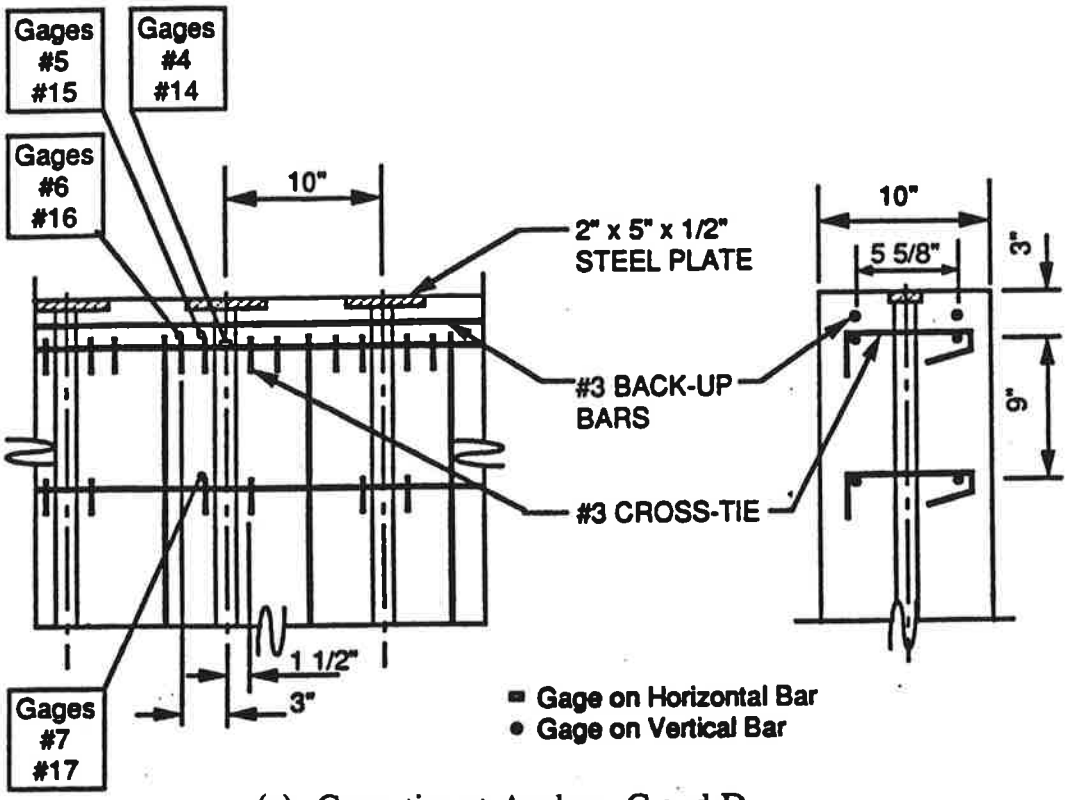

(c) Cross ties at Anchors C and D

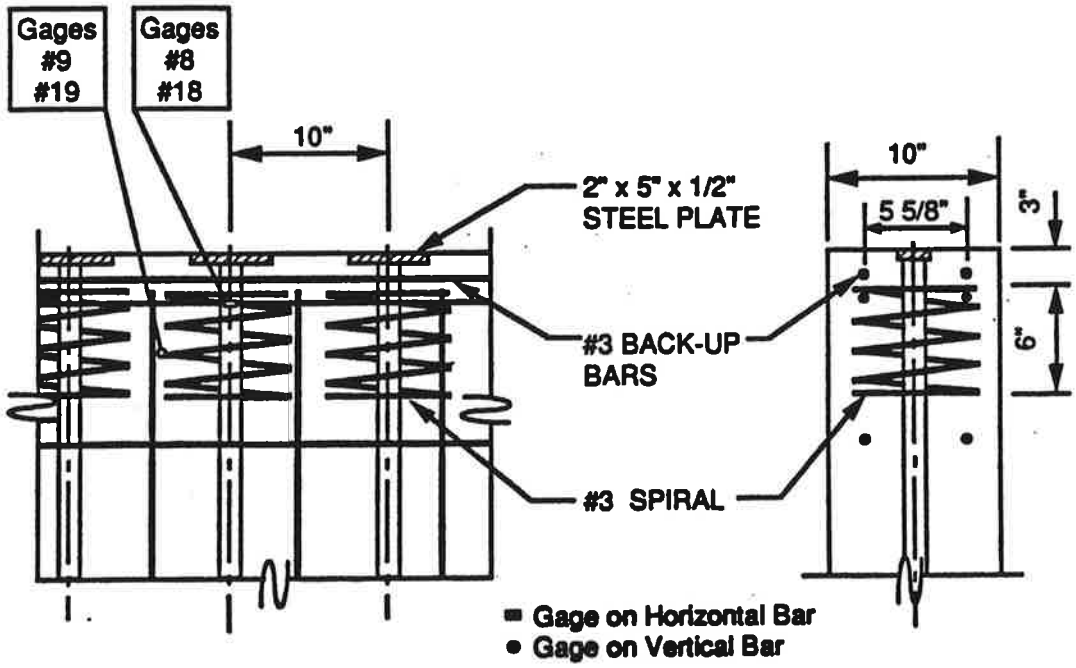

(d) Slab #6 spiral detail at Anchors E and F

Figure C49 Slab #6 Details

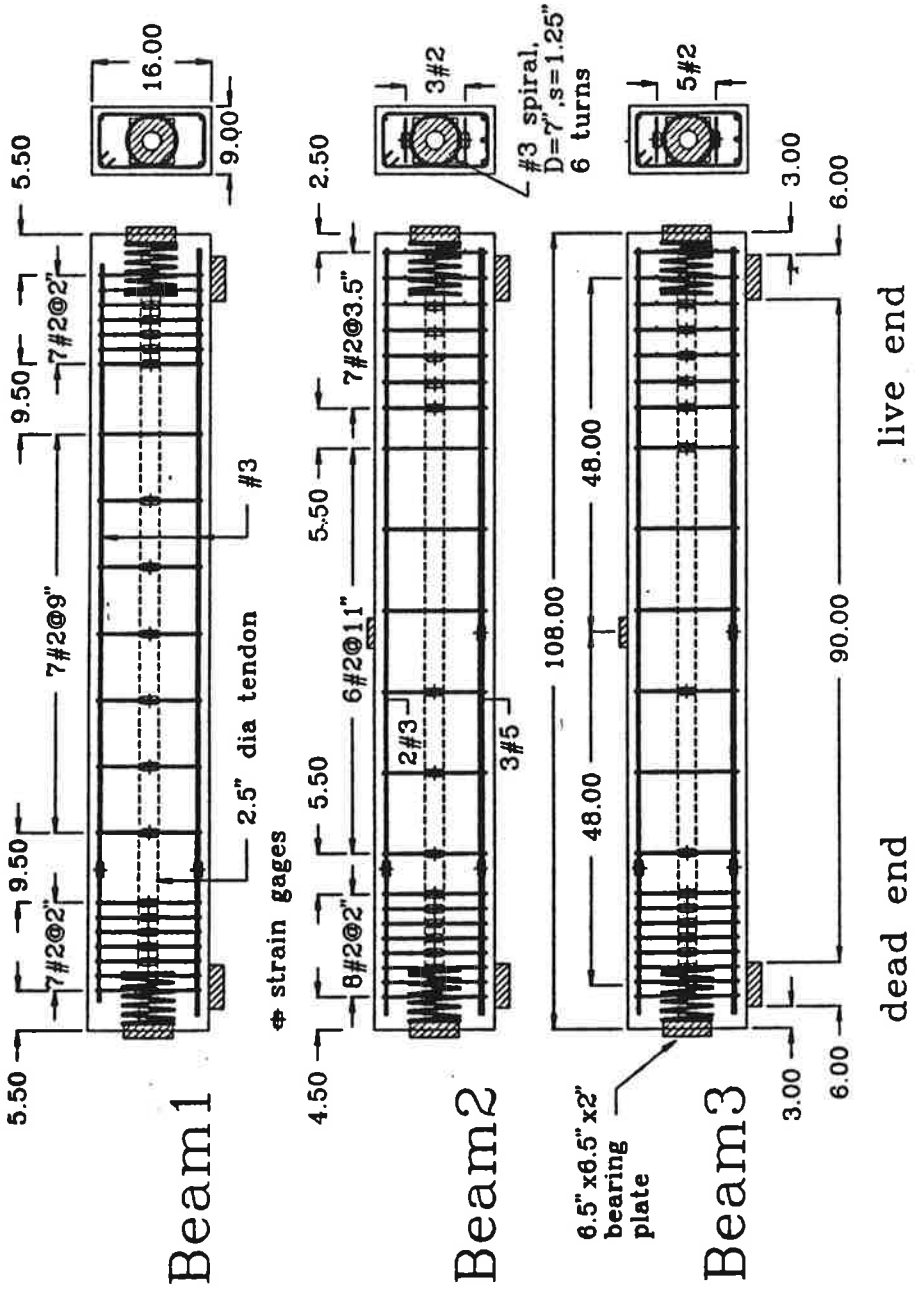

Figure C50 Dimensions and Details for Beam Specimens

Figure C51 Geometry of Slab Blister Specimens

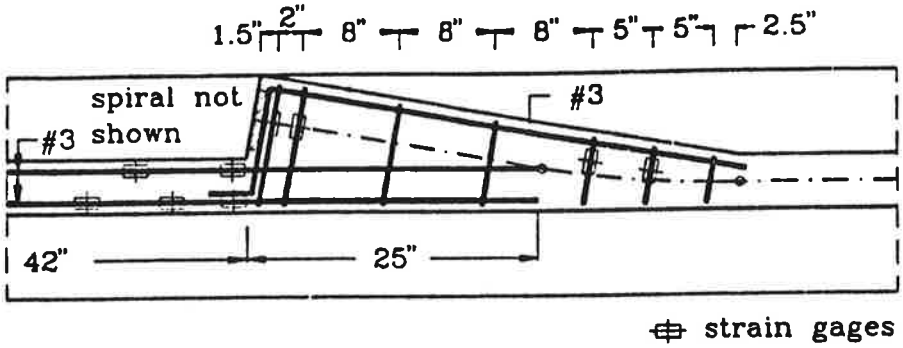

Elevation

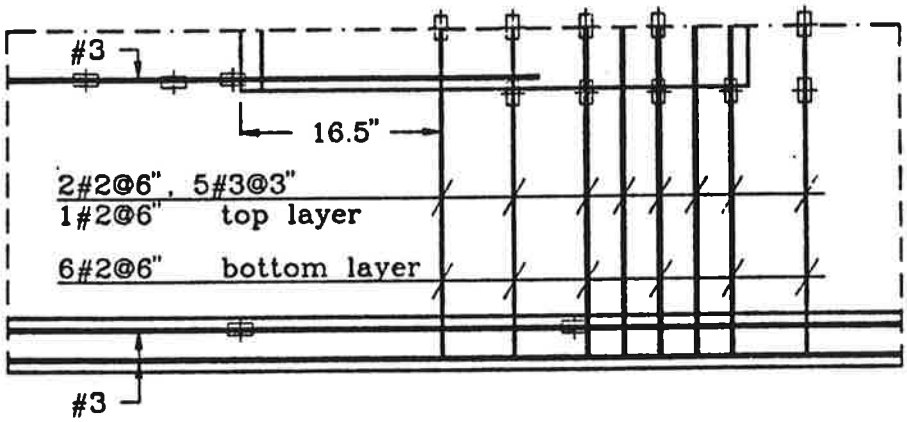

Plan

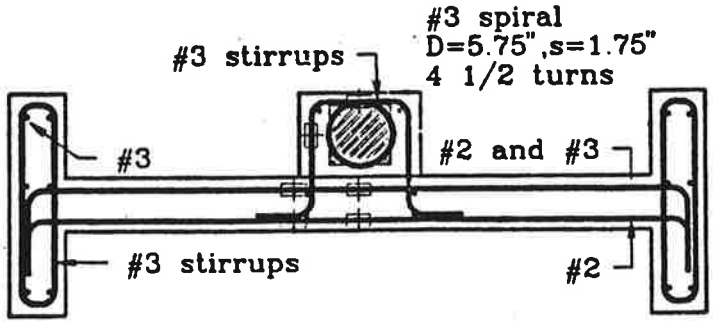

Cross Section

Figure C52 Details for Slab Blister Specimen Blister1

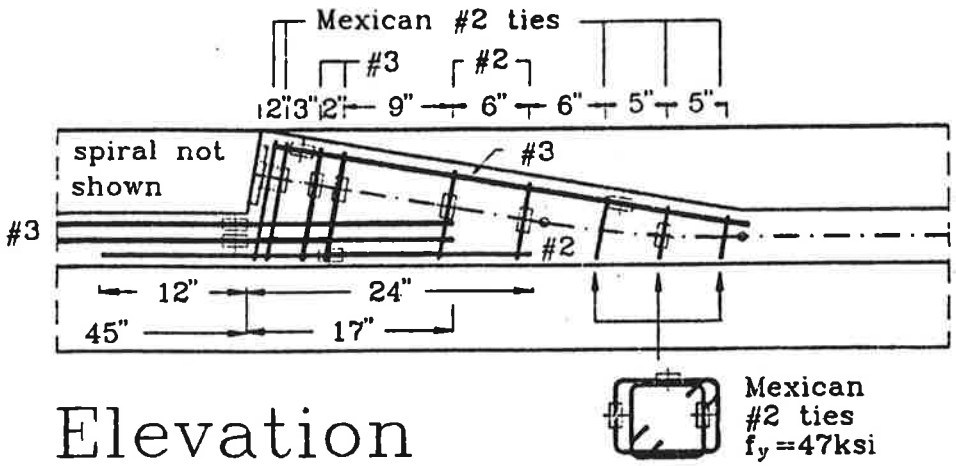

Elevation

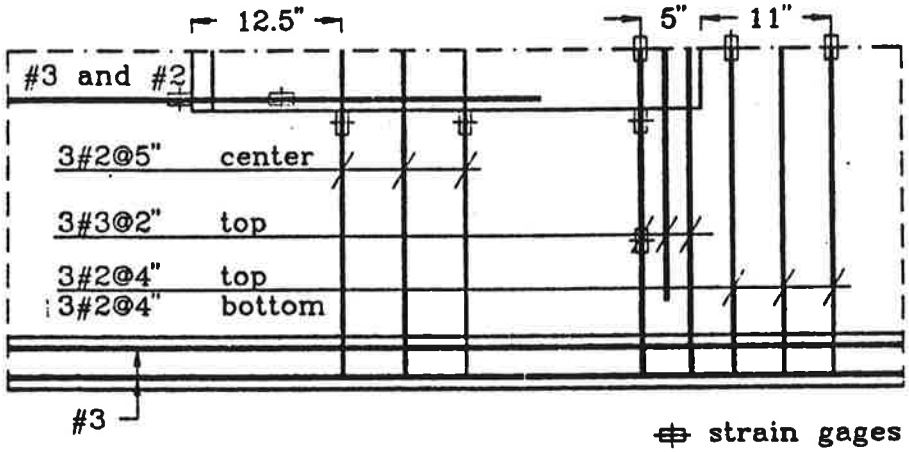

Plan

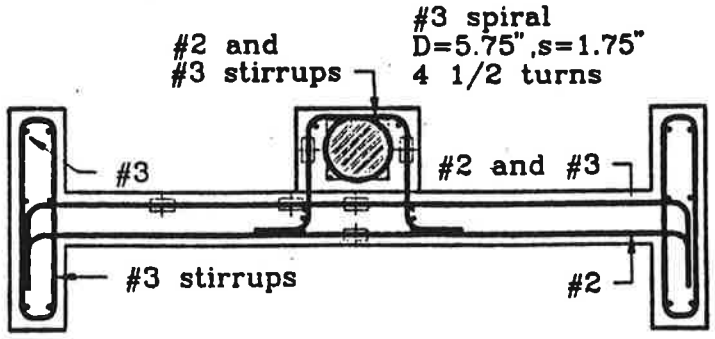

Cross Section

Figure C53 Details for Slab Blister Specimen Blister2

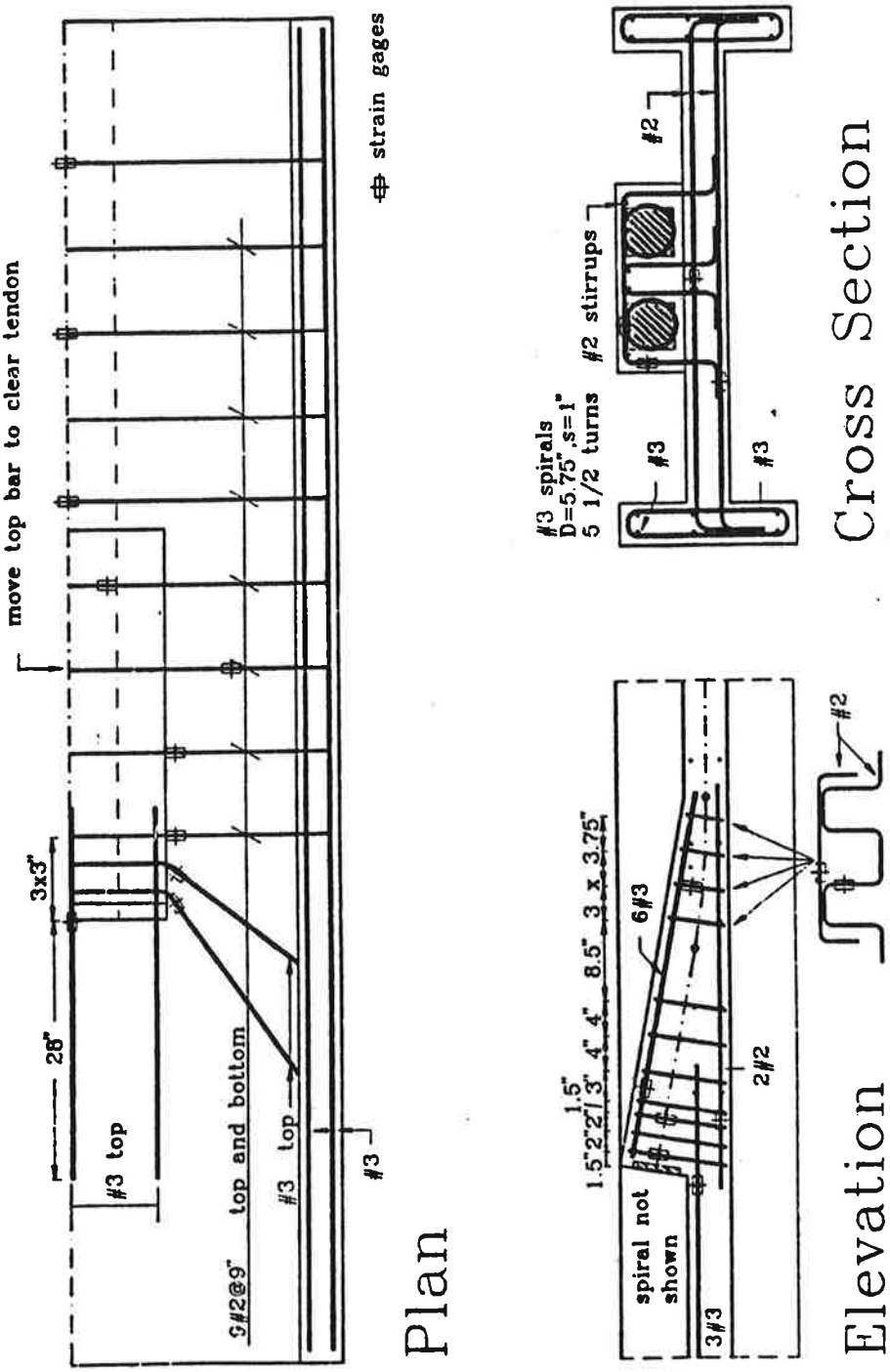

Figure C54 Details for Slab Blister Specimen Blister3

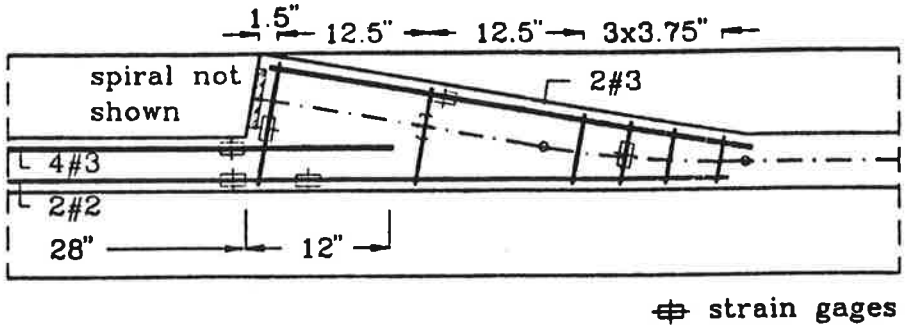

Elevation

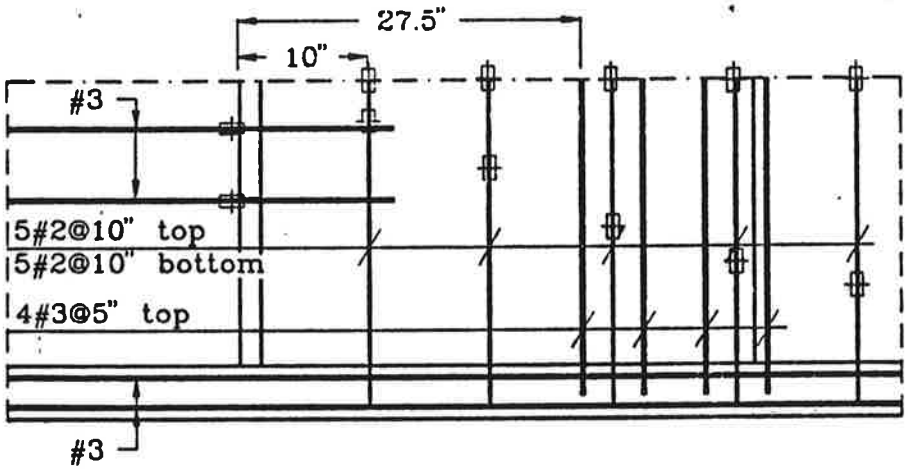

Plan

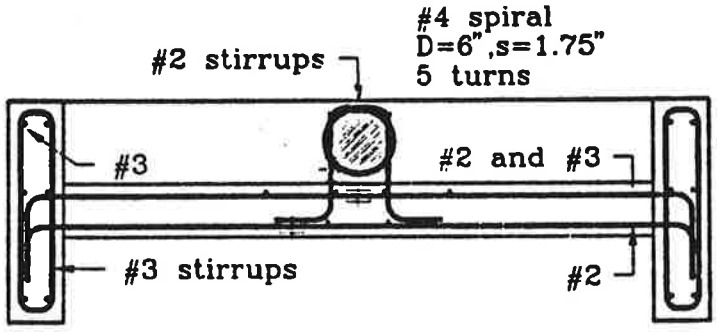

Cross Section

Figure C55 Details for Slab Blister Specimen Blister4

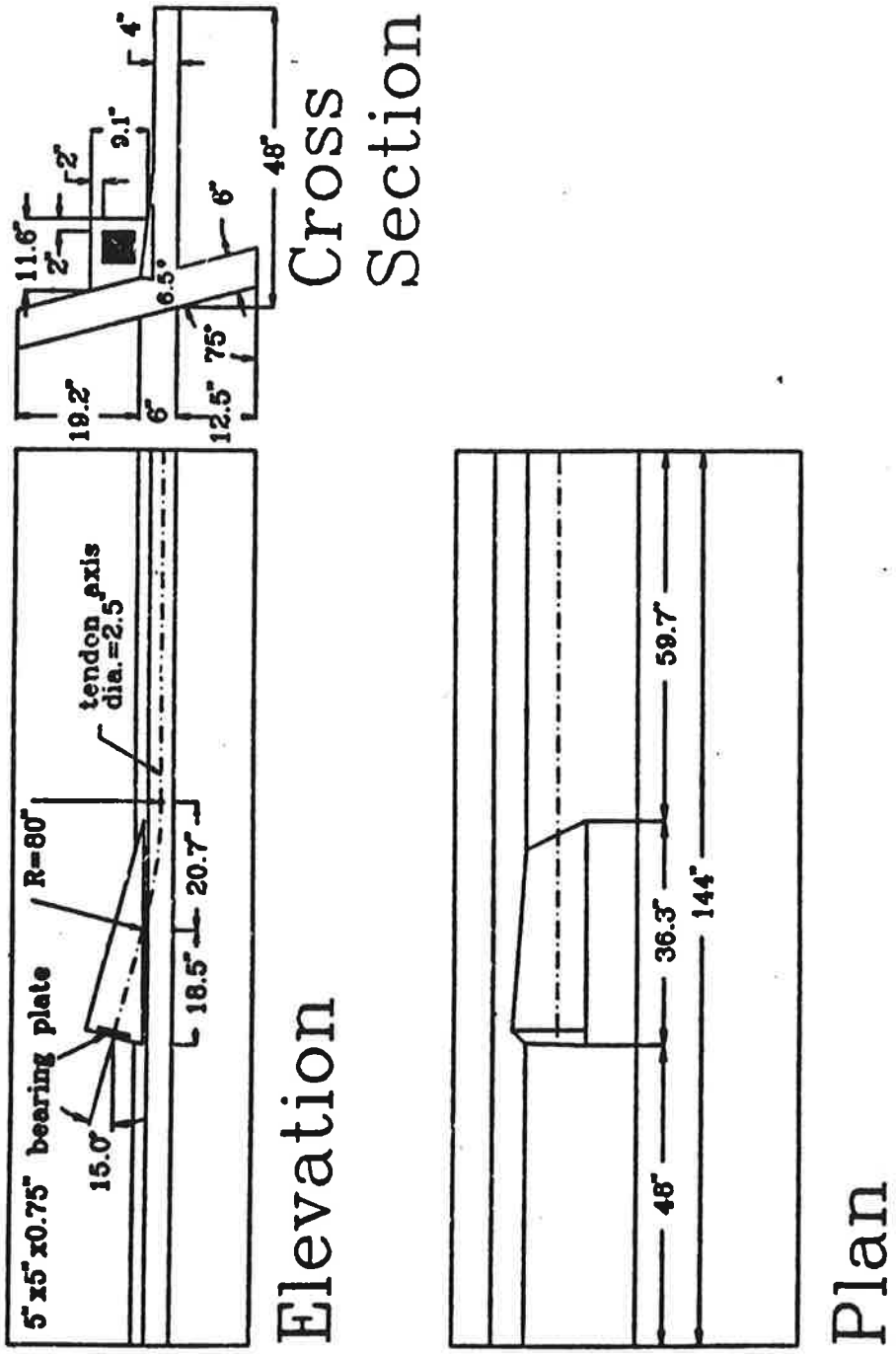

Figure C56 Geometry of Corner Blister Specimens for Internal Tendons

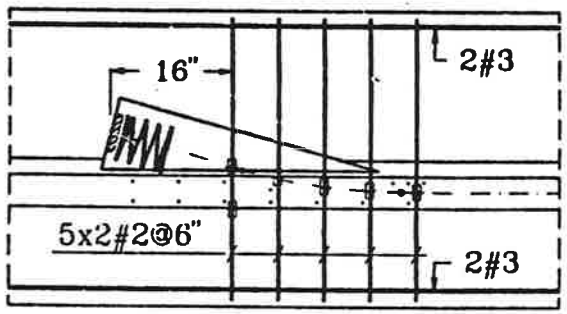

Elevation

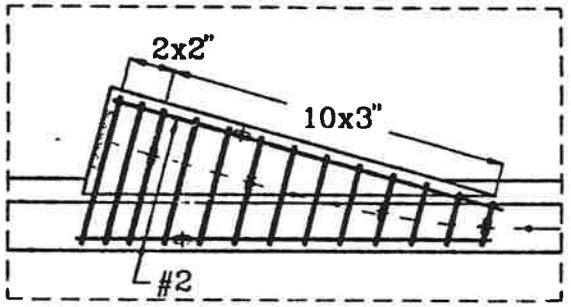

Blister Detail

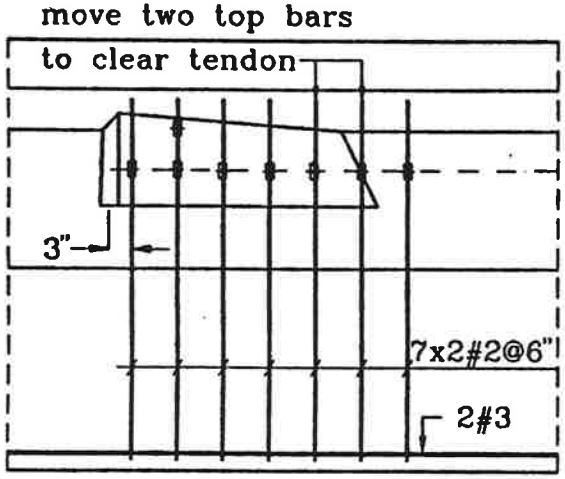

Plan

⊕ strain gages

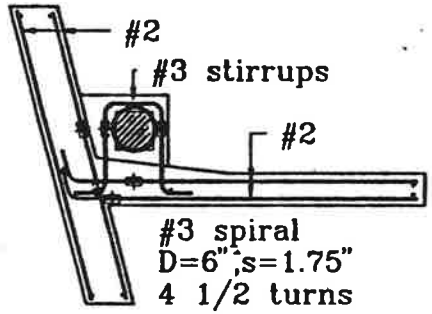

Cross Section

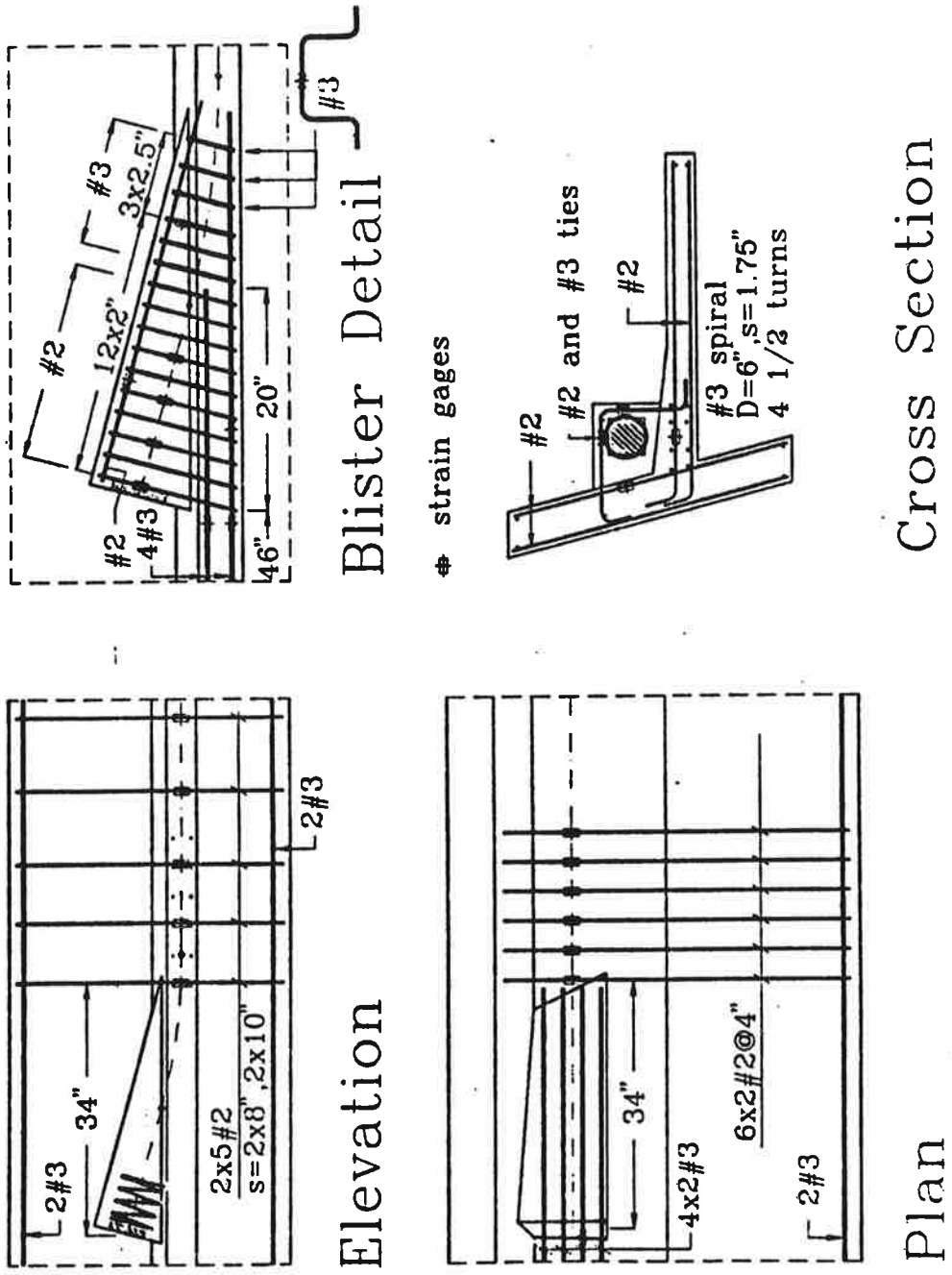

Figure C58 Details for Corner Blister Specimens Corner21 and Corner22

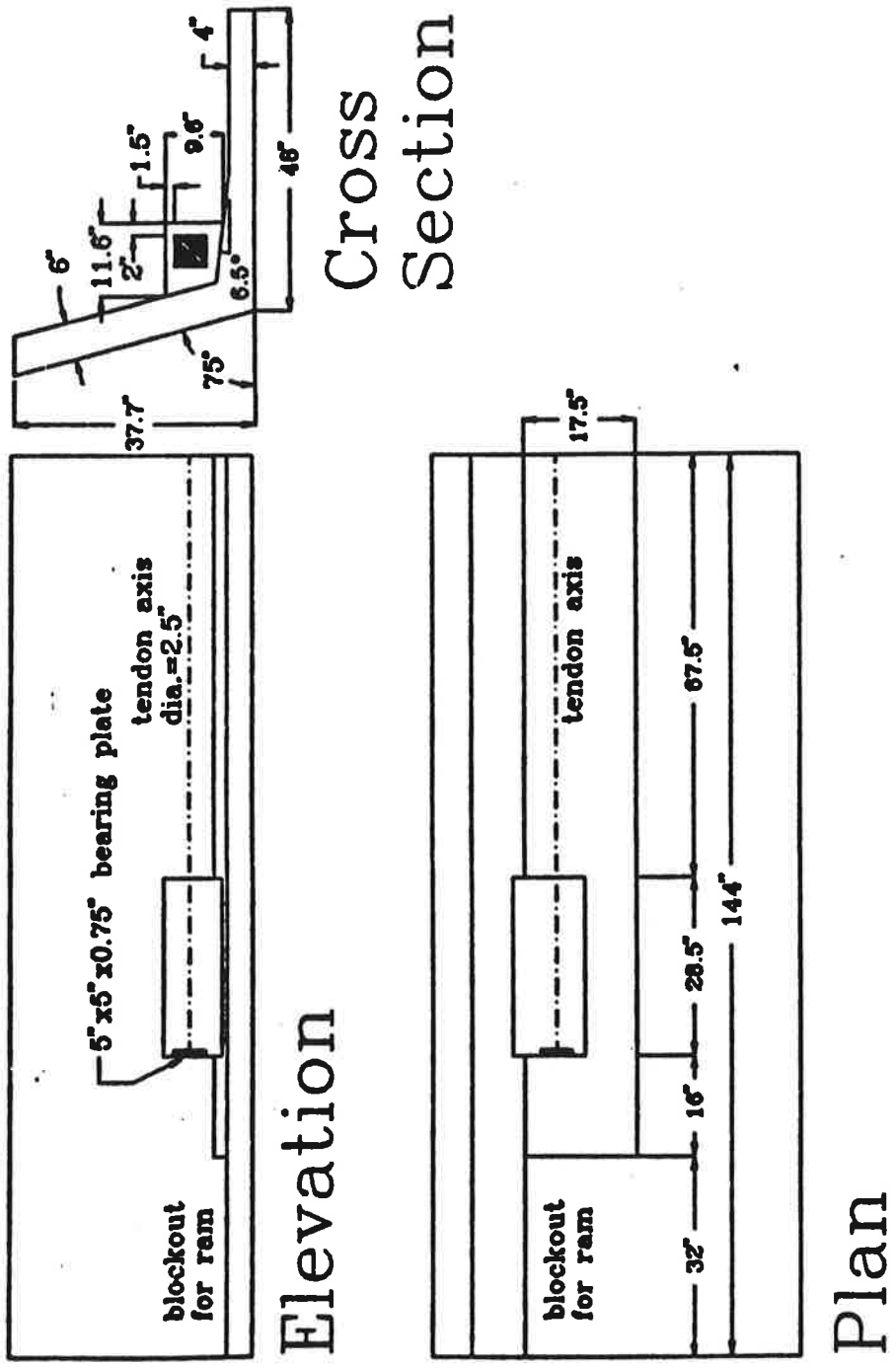

Figure C59 Geometry of Corner Blister Specimen for External Tendon (Corner3)

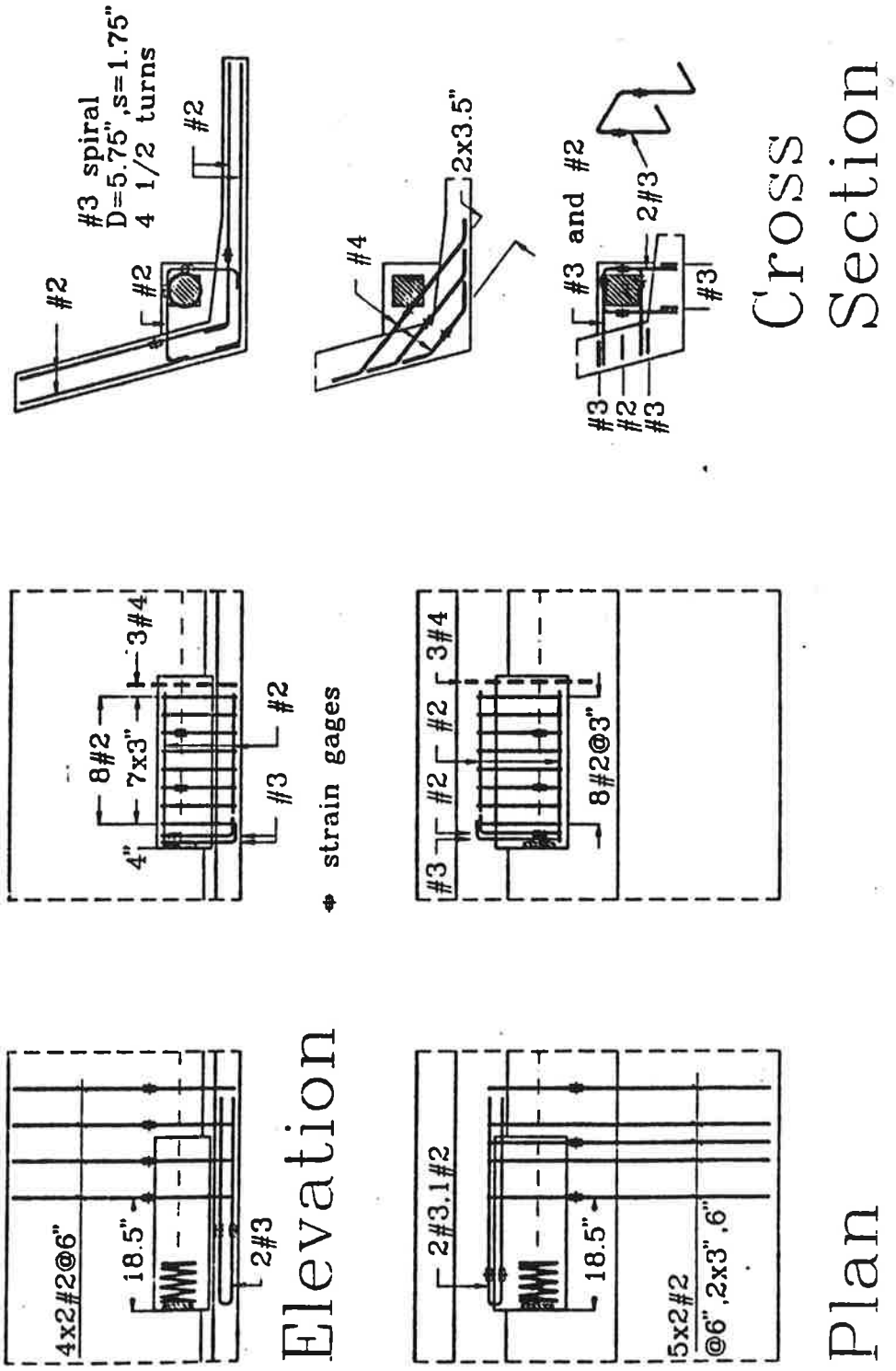

Figure C60 Details for Corner Blister Specimen Corner3

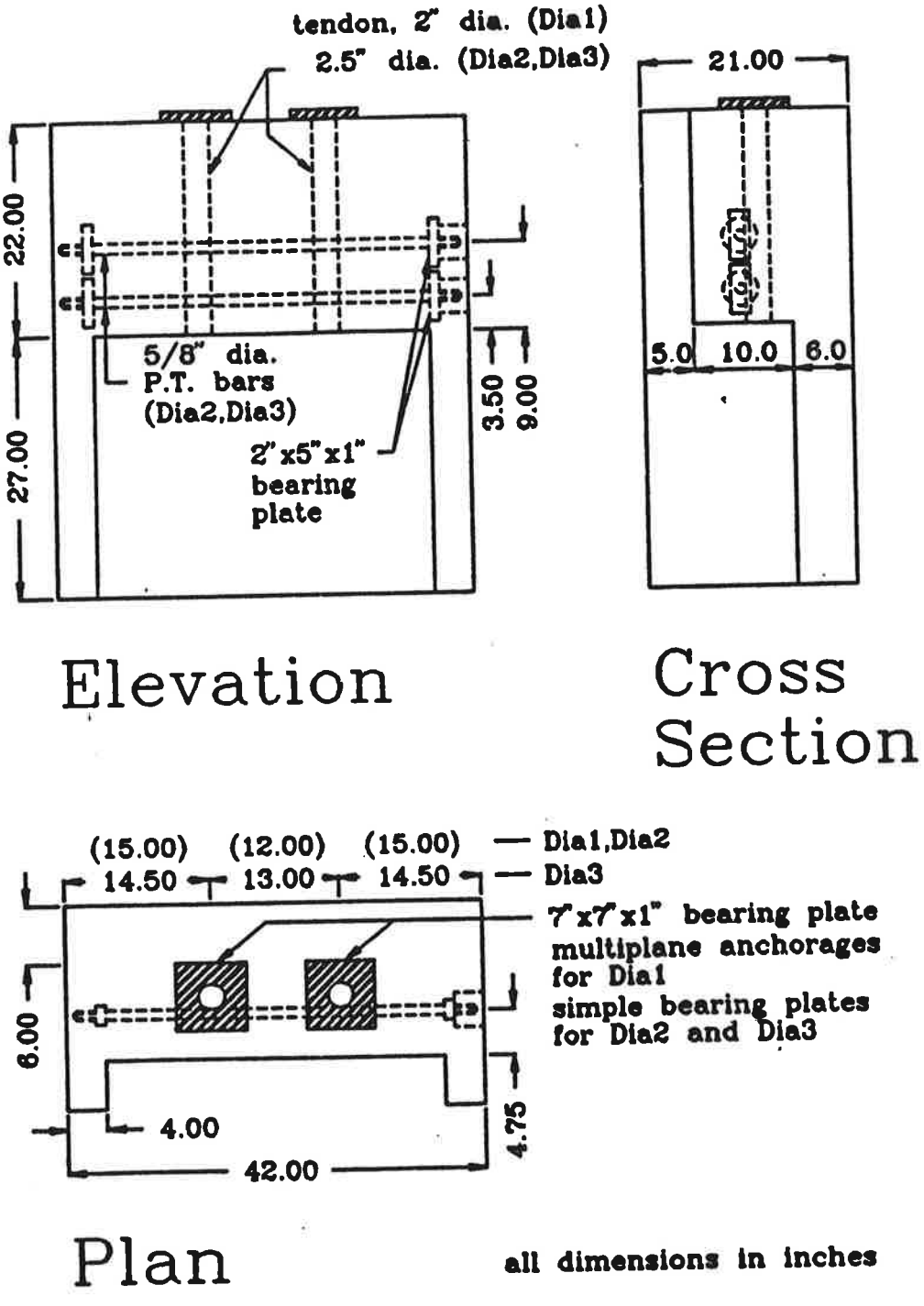

Figure C61 Geometry of Diaphragm Specimens

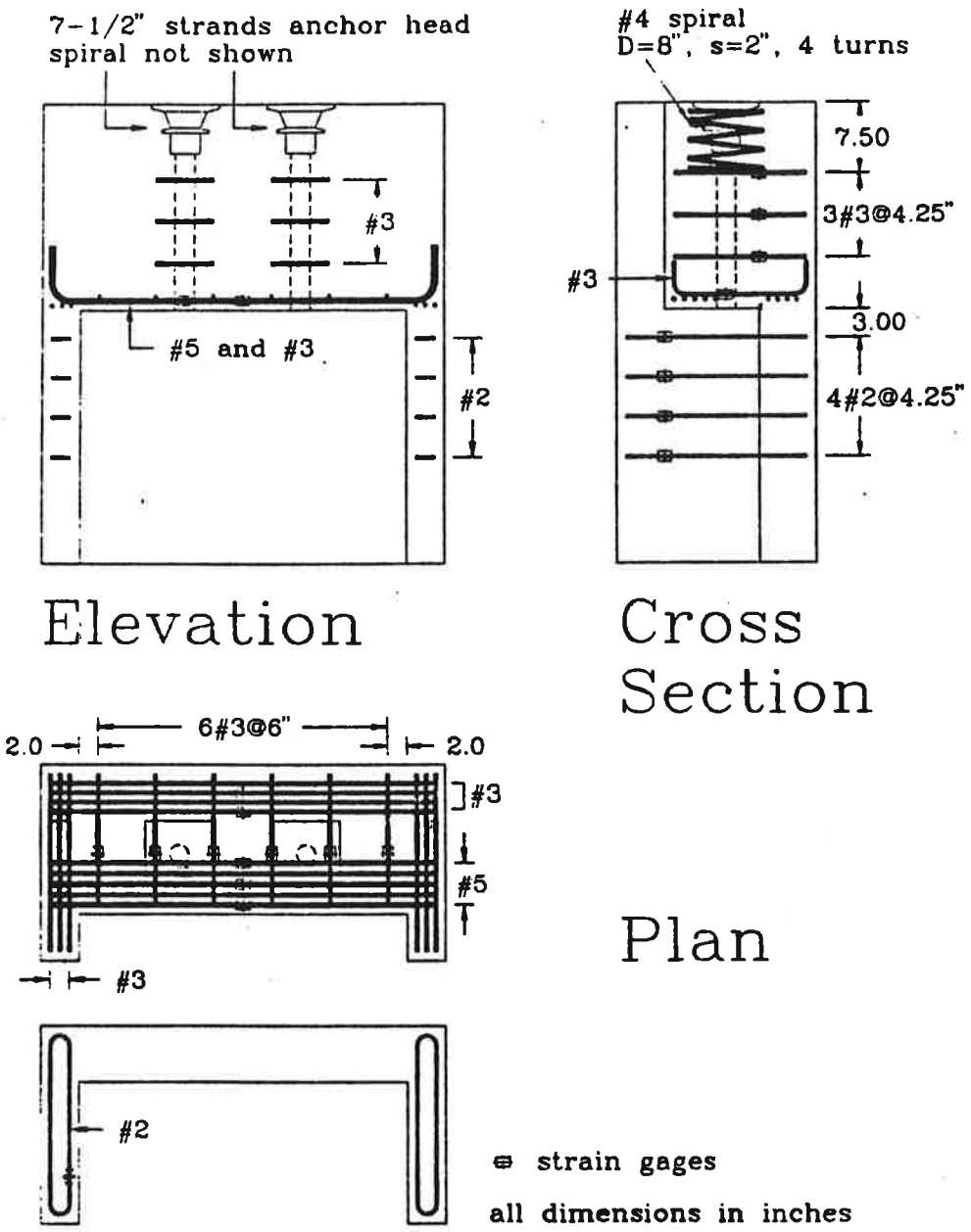

Figure C62 Details for Diaphragm Specimen Dia1

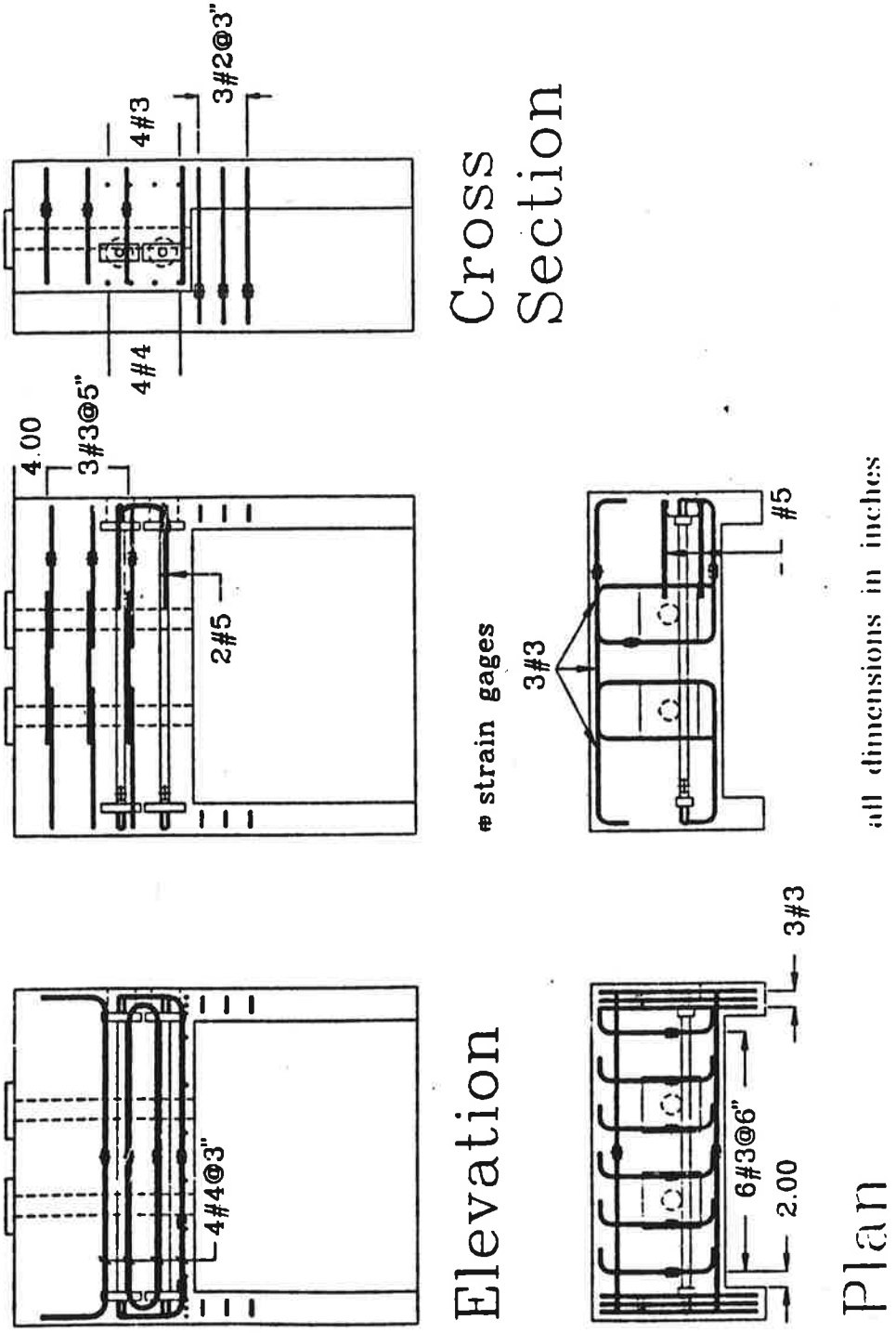

Figure C63 Details for Diaphragm Specimens Dia2

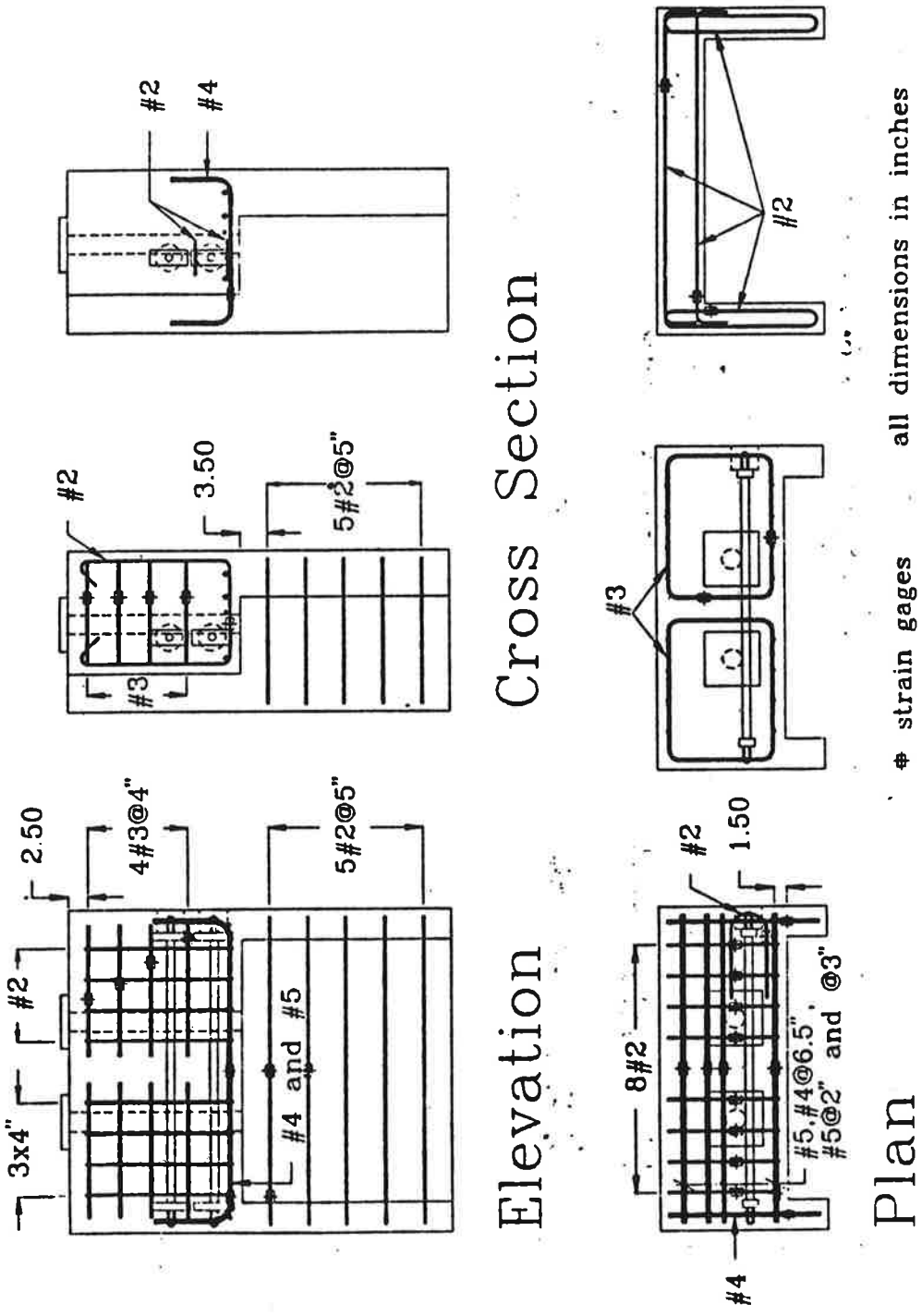

Figure C64 Details for Diaphragm Specimen Dia3